NOVEL POINT-OF-CARE DISPOSABLE DEVICE AND CELL CULTURE BIOPROCESSING TECHNIQUE

by

Kevin M. Okarski

A Dissertation Submitted to the Faculty of the

THE GRADUATE INTERDISCIPLINARY PROGRAM IN BIOMEDICAL ENGINEERING

In Partial Fulfillment of the Requirements

For the Degree of

DOCTOR OF PHILOSOPHY

In the Graduate College

THE UNIVERSITY OF ARIZONA

2016

THE UNIVERSITY OF ARIZONA
GRADUATE COLLEGE

As members of the Dissertation Committee, we certify that we have read the dissertation prepared by Kevin M. Okarski, titled "Novel Point-of-Care Disposable Device and Cell Culture Bioprocessing Technique" and recommend that it be accepted as fulfilling the dissertation requirement for the Degree of Doctor of Philosophy.

_____ Date: (04/28/2016)
Linda Powers

_____ Date: (04/28/2016)
Walther Ellis

_____ Date: (04/28/2016)
John Szivek

_____ Date: (04/28/2016)
Jonathan Vande Geest

Final approval and acceptance of this dissertation is contingent upon the candidate's submission of the final copies of the dissertation to the Graduate College.

I hereby certify that I have read this dissertation prepared under my direction and recommend that it be accepted as fulfilling the dissertation requirement.

_____ Date: (04/28/2016)
Dissertation Director: Linda Powers

STATEMENT BY AUTHOR

This dissertation has been submitted in partial fulfillment of the requirements for an advanced degree at the University of Arizona and is deposited in the University Library to be made available to borrowers under rules of the Library.

Brief quotations from this dissertation are allowable without special permission, provided that an accurate acknowledgement of the source is made. Requests for permission for extended quotation from or reproduction of this manuscript in whole or in part may be granted by the head of the major department or the Dean of the Graduate College when in his or her judgment the proposed use of the material is in the interests of scholarship. In all other instances, however, permission must be obtained from the author.

SIGNED: Kevin M. Okarski

ACKNOWLEDGEMENTS

I would like to thank my advisor, Dr. Linda Powers, for her unwavering commitment and high expectations that have driven both innovative research and design. Thank you for providing me with the opportunity to expand and hone my skills on a project that may soon combat the transmission of communicable disease. I would also like to thank Dr. John Szivek for his valuable insight and guidance throughout my academic career. I truly appreciate the time, effort, and resources you have dedicated to help develop a novel cell culture bioprocessing technique. I am also grateful to Dr. Walther Ellis and Dr. Jonathan Vande Geest for their mentorship and support. Without your help, these projects would not be where they are today. I would like to give a special thanks to Dr. Tim Secomb for his consultation and aid in the optimization of the diagnostic fluid dynamics. These elements were critical to the success of the diagnostic project and the potential for extending improved blood transfusion safety to resource-limited settings.

There were numerous other individuals that dedicated a significant amount of time and effort to this body of work. Without question, your assistance and contributions were essential to the success and quality of these projects. It was a pleasure to work alongside you and I look forward to seeing the impacts you will all make in the fields of science, medicine, and engineering. Thank you: Jerrie Fairbanks, Peter Hall, Matthew Bunting, Hannah Curtis, Nico Contreras, Matthew Nadolny, Radik Nasibulin, Niki Lajevardi-Khosh, Jonathan Wan, Malani Chauhan, Wei-Ren Ng, Min Liang, Miriam Eaton, Amanda Urbina, Kitsie Penick, and David Gonzales. I am also grateful to Patricia Stanley and Debby Howard – thank you for keeping me up-to-date and on track.

DEDICATION

I would like to dedicate this body of work to my mother.

Your strength and tenacity inspire me every day.

TABLE OF CONTENTS

LIST OF FIGURES 12

LIST OF TABLES 15

ABSTRACT 17

SECTION I: DEVELOPMENT OF RAPID DIAGNOSTIC DEVICE FOR INFECTIOUS AGENT DETECTION 19

CHAPTER 1: INTRODUCTION 20

Overview: Opportunities and Challenges in Blood Transfusion Therapy 21

Diagnostics for Detecting Infectious Agents 25

Conventional Screening Techniques 26

Rapid Diagnostic Tests 29

Rapid Diagnostics in Resource-Limited Settings 32

Project Framework 34

Specific Aims 35

Design Criteria 39

Application Design Requirements 39

Instrumentation Interface 40

Optimization of Diagnostic Performance 42

Initial Conditions: Base Diagnostic Platform 44

Assay Format 44

Sample Acquisition and Preparation for Processing 46

TABLE OF CONTENTS – *Continued*

Project Milestones 47

CHAPTER 2: FIRST GENERATION DIAGNOSTIC DEVICE 50

Phase I Objectives 51

Development of Sample Screening Protocol 55

Sample Collection and Transfer 56

Sample Preparation 59

Sample Processing 63

Blood Sample Screening Protocol 63

Development of the Diagnostic Platform 65

Sample Processing Channel 66

Methods and Materials 68

Computational Modeling 69

Flow Destabilization 72

Infectious Agent Capture 75

Results of Initial Testing 78

Flow Simulations 78

Turbulence 82

Optimal Infectious Agent Capture 83

Summary of the Pilot Study 84

Reagent Storage Network 85

TABLE OF CONTENTS - *Continued*

Device Housing 90

First Generation Rapid Diagnostic Device 95

Limited User Evaluation 97

Materials and Methods 97

Results 99

Summary of Limited User Evaluation 99

Conclusion 100

CHAPTER 3: SECOND GENERATION DIAGNOSTIC 102

Phase II Objectives 103

Diagnostic Device Design 103

Prototype Sample Processing Channel Configurations 104

Pump-Driven Slug Flow 105

Gravity-Driven Slug Flow 107

Prototype Device Platforms 110

Thumbwheel-Based Platform 111

Dial-Based Platform 116

Second Generation Diagnostic Device 118

Dial Subassembly 119

Reagent Storage Network 123

Device Housing 127

TABLE OF CONTENTS - *Continued*

Diagnostic Device Operation 128
Evaluation 130
Enhanced Limit of Detection: Pilot Particle Study 130
Materials and Methods 131
Results 132
Discussion and Conclusion 132
Environmental Resilience Evaluation 133
Offsite Testing 133
Results 135
Discussion and Conclusion 135
Summary 136
CHAPTER 4: THIRD GENERATION DIAGNOSTIC 138
Phase III Objectives 138
Diagnostic Device Design 139
Resolution of Design Weaknesses 140
Dial Subassembly 140
Device Housing and Captive Syringe Port 143
Design for Manufacture and Assembly 147
Evaluation 151
Material Compatibility.....152

TABLE OF CONTENTS - *Continued*

Injection Molding and Ultrasonic Welding Design 154

Summary 155

CHAPTER 5: CONCLUSION 157

Project Summary 157

Future Work 161

SECTION II: DEVELOPMENT OF A NOVEL BIOPROCESSING TECHNIQUE FOR ENRICHING ADIPOSE-DERIVED STEM CELLS WITH ENHANCED FUNCTIONAL CAPACITY 164

CHAPTER 6: INTRODUCTION 165

Overview 165

Articular Cartilage Structure and Function 168

Articular Cartilage Damage and Degeneration 171

Articular Cartilage Cellular Therapy 172

Therapeutic Potential of Adipose-Derived Stem Cells 175

Bioprocessing Extracted Cell Samples 177

Summary and Specific Aims 180

CHAPTER 7: A NOVEL BIOPROCESSING TECHNIQUE FOR ENHANCING CELL SAMPLE QUALITY 183

Introduction 183

Materials and Methods 186

TABLE OF CONTENTS - *Continued*

Cell Extraction and Culture Expansion.....186
Stress-Induced Cell Separation.....188
Metabolic Activity.....189
Induction of Multilineage Differentiation.....190
Data Analysis.....193
Results.....193
Bimodal Cellular Response to Nutrient Deprivation.....193
Metabolic Activity of SVF Subpopulations.....197
Capacity for Multilineage Differentiation.....199
Discussion.....202
CHAPTER 9: CONCLUSION.....206
Project Summary.....206
Future Work.....207
REFERENCES.....211

LIST OF FIGURES

Figure 2.1. First generation diagnostic device 51

Figure 2.2. Hemolysis experiments for sample preparation 62

Figure 2.3. Prototype flow channels for infectious agent capture 69

Figure 2.4. Baffle flow channel simulation with laminar flow 71

Figure 2.5. Demonstration of laminar flow within the miniature channel without flow obstructions 73

Figure 2.6. Converging inlet sample processing channel geometry 75

Figure 2.7. Turbulent flow simulations in channels with flow obstructions 80

Figure 2.8. Laminar flow computational simulation over roughed surfaces 81

Figure 2.9. Prototype flow channels with obstructions evaluated for mixing efficiency .83

Figure 2.10. Prototype flow channel infectious agent capture 84

Figure 2.11. First prototype reagent storage network 87

Figure 2.12. Pascal's law as a selector valve 89

Figure 2.13. Sample processing and reagent circulation within device.....90

Figure 2.14. Device housing and captive syringe port designs.....91

Figure 2.15. Sheath design for hypodermic syringe 93

Figure 2.16. Twist-lock design for hypodermic syringe 94

Figure 2.17. Locking tab design for hypodermic syringe 95

Figure 2.18. Functional prototype of first generation diagnostic 96

Figure 2.19. Boundary layer separation and vortex formation within the first generation rapid diagnostic device 97

LIST OF FIGURES – *Continued*

Figure 2.20. Assembly of first generation diagnostic devices for LUE 98

Figure 3.1. Second generation diagnostic device 102

Figure 3.2. Image of early slug flow system in operation 106

Figure 3.3. Second generation sample processing channel prototype 107

Figure 3.4. Validation of infectious agent capture using new channel geometry 109

Figure 3.5. Thumbwheel platform prototype CAD 112

Figure 3.6. Preliminary thumbwheel-based platform prototype 114

Figure 3.7. First and second generation reagent storage network components for thumbwheel-based platform 115

Figure 3.8. Second thumbwheel-based diagnostic prototype iteration 116

Figure 3.9. CAD rendering of preliminary dial-based platform prototype 117

Figure 3.10. First physical prototype of dial-based diagnostic platform 118

Figure 3.11. Second generation diagnostic device platform 119

Figure 3.12. Dial subassembly 120

Figure 3.13. Mold assembly for casting sample processing channel 122

Figure 3.14. Urethane reagent storage network 124

Figure 3.15. Cross-sectional illustration of the syringe port with compression collars..126

Figure 3.16. Mold assembly for reagent storage network 126

Figure 3.17. CAD rendering of diagnostic device illustrating device housing features 128

Figure 3.18. *S. aureus* capture with second generation diagnostic 130

LIST OF FIGURES – *Continued*

Figure 3.19. Visual confirmation of enhanced limit of detection 132

Figure 3.20. Small batch production of second generation diagnostic device 134

Figure 4.1. Third generation diagnostic device 139

Figure 4.2. Third generation platform semi-static gasket seal design 141

Figure 4.3. Cross section of dial subassembly illustrating sample processing channel integration 143

Figure 4.4. Exploded view and cross-sectional view of third generation diagnostic platform 144

Figure 4.5. Device housing enhancements 146

Figure 4.6. Images of platform ultrasonic weld joints 150

Figure 4.7. Platform design to prevent tacking (transverse cross-section).....151

Figure 4.8. Material compatibility testing 153

Figure 4.9. Image of FDM prototype used to confirm design accuracy 154

Figure 7.1. Images of a SVF cell culture progressing through stages of nutrient deprivation 194

Figure 7.2. Cell culture subpopulations 195

Figure 7.3. Characteristic SVF cell culture subpopulation morphologies 197

Figure 7.4. Metabolic activity of SVF cell culture subpopulations 198

Figure 7.5. Changes in metabolic activity and the rate of resazurin solution reduction .199

Figure 7.6. Adipogenic, chondrogenic, and osteogenic differentiation of treatment-sensitive cells 201

LIST OF TABLES

Table 1.1: Blood transfusion complications.....22

Table 1.2: Residual risk of major TTIAs in developed countries 23

Table 1.3: Transfusion-transmissible infectious agents 25

Table 1.4: Conventional diagnostic techniques 28

Table 1.5: Application-based design specifications 40

Table 1.6: Design specifications for instrumentation interface 42

Table 1.7: Design specifications for optimal diagnostic performance 43

Table 1.8: Overview of diagnostic device generations 49

Table 2.1: Primary objectives and criteria 52

Table 2.2: Secondary objectives and criteria 54

Table 2.3: Sample collection/transfer method and compliance with design objectives 59

Table 2.4: Cellular poration vs. lysis 61

Table 2.5: Preliminary blood screening protocol 64

Table 2.6: Feature requirements for diagnostic platform components 65

Table 2.7: First generation diagnostic device development summary 101

Table 3.1: Phase II objectives 103

Table 3.2: Platform operational requirements 104

Table 3.3. Infectious agents and surrogates captured with slug flow prototype channel 110

Table 3.4: Second generation diagnostic operation 129

Table 3.5: Second generation diagnostic device development summary 137

LIST OF TABLES – *Continued*

Table 4.1: Third generation diagnostic device development summary 156

ABSTRACT

This dissertation is composed of two projects dedicated to the development of techniques and technologies for improving the quality of life for patients in both clinical and resource-limited settings.

The purpose of the first project was to design a rapid diagnostic device to screen whole blood samples for the presence of infectious agents. Point-of-care (PoC) technologies are becoming increasingly important for the detection of infectious agents in resource-limited settings (RSLs) where state-of-the-art blood screening practices are not feasible for implementation. For this project, a rapid diagnostic device was developed to directly detect pathogen content within freshly drawn whole blood samples using a ligand-binding assay format. The assay is completely self-contained within a hermetically sealed device to minimize operational complexity and ensure operator safety. The diagnostic device is capable of processing complex sample matrices by selectively capturing, concentrating, and labeling infectious agents upon functionalized surfaces. Following sample processing, the assay is optically interrogated with a fluorescence-based reader to provide rapid feedback regarding sample purity. Designs of the rapid diagnostic platform evolved over several prototype generations corresponding to project milestones emphasizing ergonomic performance, military specification testing for environmental resilience, and manufacture to yield production-grade devices for future diagnostic performance data collection.

The goal of the regenerative therapy-based portion of this research was to develop a novel technique for the selective enrichment of cells demonstrating enhanced

regenerative capacity in tissue-extracted cell samples. Adherent cell cultures of stromal vascular fractions (SVFs) extracted from adipose tissues were exposed to nutrient deficient conditions – eliciting a bimodal cellular response between two dissimilar cell culture subpopulations. The regenerative capacity of these two distinct subpopulations was evaluated by assessing their characteristic morphology, metabolic activity, and ability to undergo multilineage differentiation. The SVF subpopulation which demonstrated sensitivity to the nutrient deficient conditions expressed typical morphological expression of adherent cell cultures, elevated metabolic activity, and the ability to differentiate along adipogenic, chondrogenic, and osteogenic lineages. The SVF subpopulation which demonstrated resistance to the nutrient deficient conditions, however, expressed atypical morphologies, impaired metabolic activity, and did not survive culture with differentiation growth media. Based on the data, the 'treatment-sensitive' SVF subpopulation demonstrated a greater regenerative capacity than the 'treatment-resistant' subpopulation. Furthermore, the treatment-resistant subpopulation of the SVF may be representative of the damaged, senescent, and otherwise less-functional cells that comprise a significant portion of tissue-extracted cell samples and pose a significant risk to therapeutic efficacy and reproducibility. Ultimately, this expedient and inexpensive bioprocessing technique may serve to improve cell-based regenerative therapies by eliminating undesirable cells from culture.

SECTION I

DEVELOPMENT OF RAPID DIAGNOSTIC DEVICE FOR INFECTIOUS AGENT DETECTION

CHAPTER 1: INTRODUCTION

Man is a shrewd inventor, and is ever taking the hint of a new machine from his own structure, adapting some secret of his own anatomy in iron, wood, and leather, to some required function in the work of the world [1]

– Ralph Waldo Emerson, *Wealth* (p. 857)

The first section of the dissertation identifies current unmet medical needs in the field of medical microbiology and describes the development process I followed to produce a rapid diagnostic device specifically designed to improve blood screening capabilities in resource-limited settings (RLSs). The first chapter within this section defines the context for the diagnostic research project and establishes the starting point from which designs proceeded. Subsequent chapters are dedicated to three main generations of the rapid diagnostic device where the research, development, and evaluation of the diagnostic device components/assemblies are described. The project required 3 years of work with deliverables due annually. With the time available, three rapid diagnostic device generations were produced to fulfill requirements for ergonomics/ease-of-use (Phase I), environmental resilience (Phase II), and manufacturability (Phase III). Future work on the project would ideally focus on data collection using production-grade diagnostic devices with the intent to receive clearance from the Food and Drug Administration (FDA) to deploy the devices for field use. The first section of the dissertation concludes with a review of the results and observations that were made over the course of the diagnostic research project and potential opportunities for future work on the diagnostic platform.

The purpose of this first chapter is to provide background information on transfusion-transmitted infections, detail the disparity in blood screening practices that

currently exist between developed countries and resource-limited settings, and present the project framework. The advantages and limitations of current rapid diagnostics are then reviewed with an emphasis on opportunities for improvement. The chapter concludes with a discussion of the diagnostic project specific aims, design criteria, infectious agent detection format, and sample acquisition and processing requirements that shaped three generations of diagnostic device designs. The generations of these designs are then described in the following chapters.

Overview: Opportunities and Challenges in Blood Transfusion Therapy

Transfusion therapy has undergone significant advances in both safety and efficacy since the inception of this medical practice in the mid-16th century [2, 3]. The earliest recorded human transfusion procedures involved animal-to-human blood transfusions where lambs served as the blood donors. The transfusion recipients complained of symptoms consistent with hemolytic reactions, but otherwise survived the procedure [4, 5]. With continued improvements, blood transfusions have become commonplace and used extensively for restoring or maintaining normal patient blood volume and component concentrations [5]. The utility and widespread acceptance of the procedure is evident with an annual collection of nearly 90 million units of blood worldwide for transfusion applications [6-8]. Despite being responsible for significantly enhancing the efficacy of numerous medical and emergency procedures, the blood transfusions are prone to a range of complications (Table 1.1) [8-11], including the risk of introducing infection. The scope of this research aims to reduce the risk of infectious complications with the development of a rapid diagnostic device designed to screen blood products for the presence of viruses,

bacteria, and parasites. The diagnostic device was specifically tailored for use in resource-limited settings where medical personnel do not have access to the necessary medical equipment, supplies, or laboratory facilities to adequately screen blood products prior to transfusion.

Table 1.1: Blood transfusion complications	
Non-infectious	Hemolytic reactions
	Febrile non-hemolytic reactions
	Allergic reactions to proteins
	Transfusion-related acute lung injury
	Circulatory overload
	Air embolism
	Thrombophlebitis
	Hyperkalemia
	Citrate and ammonia toxicity
	Hypothermia
	Coagulopathy
	Graft-vs-host disease
	Iron overload
	Post-transfusion purpura
	Immune sensitization
Infectious	Viral contamination
	Bacterial contamination
	Parasitic contamination
	Prion contamination

To provide perspective on the medical need for rapid blood screening diagnostics, one must consider that a single blood donation can be divided into three separate blood components which may then be transfused individually to different patients [11, 12]. Subsequently, a contaminated unit of blood derived from a single donor may pose an infectious risk to as many as three transfusion recipients if the contamination goes undetected. In the United States, hemorrhage resulting from traumatic injury accounts for 35% of prehospital deaths and over 40% of deaths within the first 24 hours following

hospital admission [13]. In order to perform emergency transfusions of blood components to resuscitate hemorrhaging patients, a healthcare facility must have an adequate supply of prescreened blood components available matching the patient's blood type. Even in developed countries, these resources are not always available in emergency situations and blood screening practices may be precluded to save an individual's life even though they may receive contaminated blood [14]. State-of-the-art blood screening assays require several hours before an initial result is produced [15]. After the preliminary screening process, initially positive (contaminated) blood components are screened a second time to confirm the results of the first test [16]. These assays have reduced the residual risk of transfusing contaminated blood products to the lowest level it has ever been (Table 1.2) but do not yield expedient results [17]. The situation is even worse in less-developed countries that lack the resources and infrastructure necessary to build or maintain a blood supply of pre-screened blood components [18-21]. Accordingly, there is a significant medical need for rapid diagnostic devices capable of screening blood for the presence of infectious agents.

Table 1.2: Residual risk of major TTIAs in developed countries

Infectious agent	Residual risk
HIV	1/1,446,671
HCV	1/1,148,628
HBV	1/292,561
HTLV	1/2,678,836
WNV	1/350,000
Bacteria	1/5,000 to 33,000 (platelet vs. red blood cell components)
Malaria	1/1,000,000 to 5,000,000

Developing diagnostics to screen blood products has not been a trivial process due to the broad spectrum of infectious agents that pose a substantial risk to blood transfusion safety. These agents include viruses, bacteria, parasites, and prions (Table 1.3) [22-26]. Based on the severity of diseases caused by viral pathogens, blood products contaminated with viruses were initially regarded as the primary infectious threat to the safety of blood supplies in developed countries [27]. Bacterial, parasitic, and prion contaminations were of lesser concern because they were considered easier to address, less frequent, and not as significant of a threat to transfusion recipients [28]. Many transfused blood products contaminated with bacteria do not lead to sepsis [29]. In fact, the incidence of transfused blood products with bacterial contaminants is presumed to be markedly underreported as these transfusion recipients develop minor, flu-like symptoms or no symptoms at all [30]. The situation was made apparent with improved bacterial screening diagnostics that detected a higher incidence of blood product contamination than reported bacterial infections following transfusions prior to the implementation of the new culture-based assays [31]. Further investigation found that the majority of bacterial contaminations originated from commensal bacteria (native to the skin); with improved blood collection practices the risk of bacterial contamination should be significantly reduced [32]. Due to the rarity of parasitic and prion infections in developed countries and their correlation with travel to foreign countries and hygienic food practices, donor screening questionnaires remain the primary means for mitigating the risk of collecting and transfusing blood products contaminated with these agents [33]. In resource-limited settings (RLSs), where the infrastructure does not support donor screening practices, all four classes of infectious agent pose a significant threat to transfusion safety. The long-term solution (outside the

scope of this research) would be to help build up the infrastructure for healthcare treatment facilities that may operate under regulatory agencies that institute and enforce effective blood screening practices. In the short-term, however, the most expedient path to improving blood transfusion safety under these circumstances is to produce a simple and effective diagnostic capable of withstanding field conditions.

Table 1.3: Transfusion-transmissible infectious agents	
Viruses	Hepatitis viruses (A-E)
	Human immunodeficiency viruses (1, 2)
	Human T-cell leukemia viruses (1, 2)
	Herpes viruses
	Parvovirus B19
	West Nile virus
Bacteria	*Treponema pallidum*
	Borrelia burgdorferi
	Brucella melitensis
	Yersinia enterocolitica
	Salmonella spp.
	Staphylococcus spp.
	Pseudomonas spp.
	Serratia spp.
Parasites	*Plasmodium* spp.
	Trypanosoma cruzi
	Babesia microti/divergens
	Leishmania spp.
Prions	Variant Creutzfeldt-Jakob disease

Diagnostics for Detecting Infectious Agents

While significant progress has been made in blood screening practices, it did not become a priority until 1943 when the first cases of transfusion-transmitted infection were documented [34]. The identified culprit was the hepatitis virus – spurring the development of blood screening diagnostics for viral pathogens in developed countries. The possibility

of transfusing other infectious agents was also recognized, but regarded as secondary concerns. This mentality, coupled with the invention of molecular diagnostics, resulted in the efficient reduction of residual risks for transfusion-transmitted infections from viral infectious agents. Transfusion-transmitted bacterial infections became the primary risk to blood transfusion safety and have since garnered the attention of numerous research laboratories seeking to improve diagnostic detection capabilities. The diversity of transfusion-transmittable infectious agents, historically, has presented a significant obstacle to the development and application of diagnostic technologies intended for broad spectrum infectious agent detection.

Conventional Screening Techniques

Diagnostics used to screen blood products must be amenable to high-throughput screening in order to procure and maintain an adequate supply of blood products in a timely manner. In the field of diagnostic medical microbiology, detection of infectious agents depends heavily upon specimen quality, effective sample processing, and the appropriate choice of diagnostic screening techniques [34]. This is especially true for screening blood products where high levels of diagnostic sensitivity and specificity are essential for ensuring the safety of the blood supply. Since conventional diagnostic technologies (Table 1.4) entail relatively lengthy screening processes, high-throughput screening is achieved by performing assays in parallel and pooling samples for analysis [35]. The screening methods include direct microscopy, culture-based assays, immunoassays, molecular diagnostics, and variants thereof [36]. In developed countries, immunoassays have traditionally been heavily relied upon to determine the purity of donated blood units and absence of viral pathogens [35]. It was not until relatively recently that molecular

diagnostics (i.e. PCR) became commonly used (by facilities with sufficient resources) to screen blood products for select viral pathogens of concern [35]. The use of molecular diagnostics has reduced the residual risk of transfusion-transmitted infection by viral infectious agents to such a degree that bacterial contaminations have become the greatest concern [35-40]. Culture-based assays are used to detect bacterial contaminations in donated blood products [35]. Direct microscopy is largely reserved for evaluating blood smears suspected of parasitic infection [35]. Regardless of pathogen, these state-of-the-art technologies cannot be feasibly employed in less developed countries or emergency situations that lack the requisite funding, infrastructure, training, reagents, and consumables for effective screening of donor blood [41].

Table 1.4: Conventional diagnostic techniques		
Technique	Advantages	Limitations
Microscopy	Inexpensive; simple-to-use; transportable; direct-detection; minimal training; rapid results; may be used to detect viruses, bacteria, and parasites with the aid of select reagents such as fluorescent labels	Limit of detection (under ideal conditions) around 10^5 organisms/mL [35]; microbes must be relatively large without select reagents to label pathogens; equipment maintenance
Culture-based assays	Inexpensive; simple-to-use; direct or indirect-detection; requires minimal training; limit of detection (under ideal conditions) around 10-10^3 organisms/mL [35]; best for bacteria but may be used for viruses	Delayed results (5-7 days) [35]; requires laboratory equipment and reagents; appropriate media must be selected for microbial growth; 20-40 mL samples; viable but not culturable false negatives; slow growing; tedious; no less than 18 hours (min) for results
Immunoassays	Rapid; limit of detection around 10^5-10^6 organisms/mL [35]; useful for detecting viruses, bacteria, and parasites; high-throughput; minimal window period sensitivity	Expensive; requires specialized laboratory equipment and reagents; requires trained personnel; sensitive to false-positive errors; 16-24 hours for results; seroconversion required for many platforms
Molecular assays	Rapid, ideal for viruses, most narrow window period, requires small sample volumes (often obtained after a preliminary target analyte concentration step)	Sensitive to contaminants, small sample volumes may miss infectious agents present in low concentrations, expensive reagents and equipment requiring cold storage, false negative errors due to infectious agent diversity, increased sample processing complexity, limit of detection around 10^4 copies of nucleic acid/µL [35], limited pre-analytic sample stability

Rapid Diagnostic Tests

Rapid diagnostic tests (RDTs) represent one solution for extending blood transfusion safety to resource-limited settings and emergency situations. Thus far, commercially available RDTs have demonstrated the ability to improve screening practices but their capabilities remain limited [42]. The diversity of the infectious agents and their affinity for change have posed significant obstacles to the development of a single rapid diagnostic assay capable of bearing the responsibility for all screening requirements [43].

The ability of an assay to rapidly process samples would be beneficial to both developed and less developed countries in emergency situations. The design of a rapid diagnostic device capable of extending blood transfusion safety to resource-limited environments may be based on a wide variety of different diagnostic technologies. Generally, the range of diagnostic technologies fall within a continuum with two extremes. At one end of the diagnostic continuum there are highly accurate, expensive, sensitive to variables, and time consuming techniques. At the opposite end there are less accurate, inexpensive, robust, and rapid diagnostic strategies. Accordingly, there are inevitable tradeoffs associated with performance, expense, resilience, and sample processing speed that occur in order to move a diagnostic assay from one end of the spectrum to the other [44]. Given the application of this research, the goal was to develop a rapid diagnostic and overcome the obstacles associated with limited diagnostic performance capabilities. Properties of rapid diagnostic tests that make them ideal for resource-limited settings include simple-to-use platforms, resilience to adverse environmental conditions, portability, cost-effectiveness, expedient sample processing, and self-sufficiency. With continued advances in microbiology, chemistry, materials science, and engineering,

innovative diagnostic design has elevated traditionally less accurate strategies to the point of being capable of achieving clinically relevant diagnostic performance characteristics [45-48]. Companies producing blood screening diagnostics for resource-limited settings have had to develop products governed by the diagnostic continuum-based tradeoffs and the resulting assays have inherent strengths and limitations [48].

Currently, there are a large number of rapid diagnostic kits available on the market designed to screen blood samples for the presence of infectious agents [49-52] in resource-limited settings. They have demonstrated the ability to detect HIV, HBV, HCV, syphilis, and malaria using immunoassay-based screening technologies [53]. Although these assays report high levels of sensitivity and specificity, they tend to be limited by three fundamental design-based weaknesses. The first weakness stems from the use of antibody-antigen binding detection schemes. Assays that rely upon the presence of antibodies (produced in response to the presence of an infectious agent) to produce a positive test result are sensitive to false-negative results. Once an individual is infected by a particular infectious agent, there is a lapse in time before seroconversion occurs and the immune system produces antibodies to the agent at detectable concentration levels. As a result, an infected individual may donate blood that is labeled as uncontaminated. Furthermore, the presence of pathogen-specific antibodies within the circulatory system does not mean that the individual donating blood is currently infected. Antibodies persist long after infections are resolved. Assays targeting these analytes are subsequently sensitive to false positives as well. This limitation could be dismissed as a safety precaution, but limited blood supplies cannot afford to turn away healthy donors. Immunoassays designed to detect the presence of target antigens within a blood sample using immobilized antibodies for capture are

subject to slightly different limitations. Antigen detection does not require seroconversion since the antigens are synthesized by the infectious agents or reside upon their surfaces. However, the antibodies used to capture the antigens are expensive, large proteins and sensitive to production variability [54]. Expense aside, the large proteins limit the total number of capture sites that may be immobilized upon a given surface – reducing the probability of capturing target analytes present in low concentrations and producing a meaningful signal beyond the background noise of the system. The production variability of antibodies also limits the reliability and reproducibility of the assay's diagnostic performance characteristics (i.e. sensitivity and specificity). The second fundamental weakness of these assays is that they process small sample volumes. The limited sample volumes are generally regarded as a selling point for the diagnostics but it severely reduces the probability of collecting a contaminated specimen from an infected donor – especially if the infectious agent is present at low concentrations. The first two weaknesses pertained to reagent and sample processing limitations. The third weakness is inherent in the detection system employed by the diagnostic platforms. The vast majority of commercially available diagnostics used to screen blood samples for infectious agents utilize colorimetric indicators to identify samples as positive or negative for the presence of infectious agents. Colorimetric assays require high concentrations of target analytes to be present within screened samples in order to produce discernable results – which are subject to operator interpretation. This design feature impairs the diagnostic's limit of detection and predisposes the assay to false-negative results. Operator error may contribute to false-positive or false-negative results depending on the ambiguity of the diagnostic's result.

While certain design features limit the overall efficacy of the device, these assays also exhibit limited utility.

Many rapid diagnostic tests are limited in their capacity to detect only a single strain or class of infectious agent [55-60]. As mentioned previously, there are a wide variety of viruses, bacteria, and parasites that pose a risk to blood transfusion safety. As a result, assays that are capable of detecting a single infectious agent are insufficient for determining whether a donated unit of blood is suitable for transfusion and are constrained to diagnosis-based applications. It is possible to use multiples of the specialized rapid diagnostics in parallel to screen an individual to determine suitability for blood donation, but the process becomes tedious and expensive. In addition, to our knowledge, a rapid diagnostic device capable of screening blood samples for bacterial agents in resource-limited settings has yet to be produced. Accordingly, one of the primary sources of transfusion-transmitted infections would be missed by this hypothetical screening process. Furthermore, when considering point-of-care (POC) applications, many immunoassays require short term storage at 4°C and long term storage at -20°C. This is not always possible in resource-limited settings and the assays are therefore constrained in their ability to diagnose individuals in remote locations.

Rapid Diagnostics in Resource-Limited Settings

In the context of this research, resource-limited settings include regions that lack formal laboratory facilities, pre-screened blood products, diagnostic equipment, trained staff, or the healthcare service infrastructure necessary to support recommended donor and blood product screening practices. Resource-limited settings are not constrained to less developed countries and may spontaneously arise in the event of emergency situations

where otherwise adequate resources become temporarily unavailable. Developed countries are mandated by regulatory agencies to collect blood samples and screen donors for the presence of infectious agents [61, 62]. This has made it possible for the diagnostic screening technologies to effectively reduce the residual risk of transfusion-transmitted infections to nearly negligible levels with the exception of bacterial-related contaminations. This, in part, is why there is such a disparity in transfusion safety between developed countries and resource-limited settings associated with less developed countries.

Major factors that contribute to the increased risk of transfusing infected blood components in resource-limited settings include an elevated prevalence and incidence of infectious disease within the donor population; insufficient screening of donated blood products; unsanitary conditions in which the blood products are collected and transfused; and mishandling of donated blood products during collection, processing, and/or storage [63]. An increased prevalence of infectious agents within the donor population correlates with a greater probability of blood product screening measures incorrectly indicating infected blood products as uncontaminated [63]. A higher incidence of viral, bacteria, and parasitic infections within the donor population increases the probability that an infected individual may donate blood during the window period of infection – an interval of time during which the concentration of infectious agents within the sample are below the limit of detection for the diagnostic technique used to screen the sample. Unsanitary conditions, attributable to the absence of formal laboratory facilities and supplies (especially out in the field), increase the likelihood that blood samples may become contaminated during the collection or transfusion processes. This particular issue may be exacerbated by untrained personnel who fail to apply appropriate aseptic techniques during blood collection,

handling, and storage. Under these conditions, the development and implementation of high-quality, rapid diagnostic tests for blood screening may substantially mitigate the risks associated with these factors associated with less developed countries or field use. Even though a well-designed rapid diagnostic may eliminate the need for laboratory equipment and trained staff, its application must be regulated and enforced. It is recognized that the implementation of regulatory policies and identification of low infection prevalence and incidence populations is critical for ensuring safe blood transfusion practices but do not fall within the scope of this research.

Based on these considerations, a rapid diagnostic device capable of detecting viruses, bacteria, and parasites *en masse* is critical for screening blood components in resource-limited settings. In the following section, the project framework for this research is described along with the project's specific aims, design specifications, and initial conditions.

Project Framework

The goal of this project was to produce a rapid, disposable, handheld diagnostic device capable of screening whole blood samples for the presence of viral, bacterial, and parasitic infectious agents in resource-limited settings. In order to achieve this goal, the diagnostic device was required to be more than just safe and effective. Competitive market conditions required: 1) the diagnostic device to fulfill a currently unmet medical need, 2) inexpensive manufacture and assembly of the product, and 3) a modular product platform capable of adapting to alternative applications and emerging infectious diseases. As a result, a holistic approach was taken toward the product development process to account

for these requirements whereby integrated product development and parallel path engineering were critical elements for success.

There are a wide array of rapid diagnostic tests currently available on the market designed to screen blood samples for select infectious agents. However, while these assays might be field-deployable, their primary purpose is to diagnose or monitor suspected infections in point-of-care (POC) settings. There is a medical need for a rapid diagnostic device capable of screening blood samples for a broad spectrum of infectious agents for the purpose of performing emergency transfusions. In order to produce such a device, this project established specific aims and design specifications emphasizing expedient prototype development to bring the product to market and out to resource-limited settings as soon as possible.

This project is a continuation of previous research performed by Dr. Powers' laboratory whereby fluorescence-based instrumentation and functionalized surfaces were developed for the detection and capture of microbial agents [64-68]. The previous work helped determine the design specifications for the development of the rapid diagnostic device for this project and established the initial conditions for the design process. Product development and evaluation was divided into three separate phases that emphasized the augmentation of device characteristics associated with ease-of-use, environmental resilience, and manufacturability.

Specific Aims

There were five specific aims for the rapid diagnostic project that defined: 1) the desired scope of screening capabilities; 2) operational safety; 3) durability; 4) diagnostic performance; and 5) production of a rapid diagnostic device with optimal diagnostic

performance characteristics. While some of the aims were explicit goals, others were based on device optimization. In this section, each aim is independently presented and described in the context of the project.

> **Specific Aim 1:** To produce a disposable rapid diagnostic device capable of detecting viruses, bacteria, and parasites present within whole blood samples at clinically relevant concentrations when interfaced with fluorescence-based instrumentation.

For the first specific aim, the diagnostic device was required to demonstrate the ability to detect a broad spectrum of infectious agents including viruses, bacteria, and parasites. These transfusion-transmittable infectious agents pose a significant threat to blood transfusion safety in the field. Prions were excluded from the list of agents due to the low incidence of transfusion-transmitted infections associated with prions and difficulty in obtaining samples of the infectious agent for testing. The diagnostic device was intended to yield a positive (infectious agents present) or negative (infectious agents absent) test result after optical interrogation by a fluorescence-based reader. This would provide the operator with 'GO/NO-GO' feedback indicating whether or not blood obtained from a donor or blood product may be used safely for transfusion.

> **Specific Aim 2:** To ensure operational safety while processing biohazardous materials potentially contaminated with infectious agents in resource-limited settings.

The second specific aim defines the goal for developing a diagnostic device that ensures operator safety while processing whole blood samples under dynamic conditions. Protocols for good laboratory practices (GLPs) are generally sufficient for protecting

laboratory personnel from inadvertent contact with hazardous materials. In the field, however, circumstances may make it difficult (if not impossible) to adhere to GLPs. Accordingly, special precautions must be taken into consideration when developing a diagnostic device for use in resource-limited settings. The device must be designed to mitigate the risk of operators making direct contact with samples collected for processing. Safety must be ensured during sample acquisition, transfer to the diagnostic device, processing, and disposal of the device. Most importantly, the hermetic seals of the device must maintain their integrity over a wide range of field conditions – giving rise to the third specific aim.

> **Specific Aim 3:** To develop a robust and reliable platform demonstrating resilience to adverse environmental conditions.

The third specific aim describes the goal of developing a durable diagnostic platform for use in resource-limited settings. The durability of the device is critical for both operator safety and diagnostic efficacy because the device must survive transport in the field, operate under potentially harsh environmental conditions, and yield reproducible, clinically-relevant results without compromising operator safety. Harsh environmental conditions include temperature fluctuations (-26 - 60°C); variable altitudes (0 – 18,000 ft.); humidity; and weather conditions such as blowing dust, sand, and rain. The device must also survive impacts and vibrations associated with handling and vehicle/aircraft transport.

> **Specific Aim 4:** To incorporate design features into the diagnostic platform that optimize diagnostic performance by enhancing the efficacy and reproducibility of sample processing.

The fourth specific aim details the goal of constructing a rapid diagnostic device with optimal diagnostic performance characteristics. The ability of the rapid diagnostic device to effectively screen samples for infectious agents directly determines the utility of the diagnostic assay. Special consideration must be given to the design of the fluid mechanics within the device and the sample processing protocol to enhance infectious agent capture and labeling. Many of the design criteria, described in the following section, directly conflict with the optimization of target analyte capture. Therefore, the design of the diagnostic platform components must be carefully considered in order to strike a balance between the conflicting goals.

> **Specific Aim 5:** To integrate the components of the diagnostic platform into a configuration that maximizes ease-of-use, portability, and cost-effective manufacture.

The fifth, and final, specific aim instantiates the project objective for the production of a rapid diagnostic device capable of translating from the laboratory to the field setting. The requirements for developing a simple, ergonomic, and inexpensive platform were intended to aid in the production of a device that was cost-effective for manufacture, easy-to-use, and safely disposable. These properties are essential for a field-deployable device in resource-limited settings. A simple and ergonomic design aids in rapid sample processing while also mitigating the risk of operator error. Device complexity has a direct impact upon usability, production costs, and device reliability.

To help guide the development of a rapid diagnostic device capable of achieving and optimizing the specific aims for this project, a list of design specifications was generated. The design specifications were the product of requirements derived from

practical considerations associated with device operation, optical interrogation, and desired diagnostic performance characteristics. The specifications effectively provided boundary conditions to guide product development but also presented unique obstacles that had to be overcome while balancing the properties of the device. The end product of this research project was a novel rapid diagnostic device (patent pending) with the ability to detect viruses, bacteria, and parasites present within freshly drawn whole blood sample in less than 10 minutes (from sample collection to diagnostic report).

Design Criteria

To develop a rapid diagnostic device capable of extending blood transfusion safety and efficacy to resource-limited settings, a list of design specifications was produced at the beginning of the project to guide device development. These specifications were adapted over the course of the project to account for technical and design obstacles. Based on the requirements of the project, the design specifications were divided into three subcategories associated with 1) application, 2) instrumentation interface, and 3) optimal diagnostic performance, which are discussed next.

Application Design Requirements

The application-based design criteria (Table 1.5) evolved over the course of the project with a limited user evaluation during the first phase of device development and military-specification testing during the second stage. The primary application-based device design requirements were: 1) operational safety, and 2) effective screening of whole blood samples for viruses, bacteria, and parasites. A device that cannot safely or effectively screen blood products would have no utility. Additional design criteria included yielding

results within 10 minutes of sample acquisition, developing a portable platform for the assay, designing the device to withstand harsh environmental/handling/transport conditions, minimizing operational complexity, incorporating the device components into a disposable platform, and limiting manufacturing costs. Design challenges associated with these criteria included: minimizing the dimensions of the handheld device while maximizing reagent storage capacity; developing a hermetically sealed and completely self-contained diagnostic platform without compromising ease-of-use; designing a reagent storage network for circulating fluids within the device that optimized rapid and effective sample processing; and producing a robust diagnostic device without becoming prohibitively expensive to manufacture.

Table 1.5: Application-based design criteria	
1	Safe-to-operate
2	Effectively detect viruses, bacteria, and parasites
3	Process freshly drawn whole blood
4	Provide results ≤ 10 minutes
5	Portable, handheld device
6	Resilient to adverse conditions
7	Easy-to-use
8	Incorporate completely self-contained reagents
9	Disposable assay
10	Inexpensive to manufacture design

Instrumentation Interface

Design criteria for establishing an effective interface between the fluorescence-based reader and the rapid diagnostic device for optical interrogation (Table 1.6) were essential for ensuring sensitive, reproducible test results. Requirements included using two

quartz windows for ligand coatings and infectious agent capture, minimizing the gap distance between the quartz surfaces to improve signal, maintaining optimal position and depth of the device's optical region of interrogation (ROI) relative to the instrument, maximizing the ROI without compromising ergonomics or other design features, and choosing appropriate materials that satisfied durability requirements without compromising optical interrogation or inexpensive manufacturability. The windows were essential for providing an optical path into the sample processing channel of the diagnostic device. Quartz was specifically selected for durability, low background noise during fluorescent interrogation, and compatibility with surface functionalization/ligand conjugation techniques. The use of two quartz windows with a minimal gap distance within the diagnostic device was intended to double the surface area for infectious agent capture without compromising the fluorescent signal produced by the bound and labeled infectious agents on the distal quartz surface. With too large of a gap between the windows, the contribution of the fluorescent emissions to the overall signal from the distal window's surface would be lost. The position and depth of the device's ROI were critical features that directly determined how well the diagnostic device interfaced with the fluorescence-based reader. The ROI was required to be recessed from the diagnostic device's surface by 7 mm to align appropriately with the instrument's light emitting diodes (LEDs) and photomultiplier tube (PMT). The surface area of the ROI was required to be at least 300 mm^2 to sufficiently offset the perimeter of the window mount from the light path – minimizing the contribution of the device's surface to light scattering and background noise. Additionally, the materials that were selected for the production of the exterior diagnostic device components were required to exhibit low background fluorescence when

exposed to excitation and emission wavelengths during optical interrogation. The materials that composed the reagent storage network of the diagnostic device were required to demonstrate reagent compatibility during storage. The requirement to keep material obstructions outside of the sample processing channel eliminated options for using wicking materials or packed-bed designs for infectious agent capture. Design challenges associated with this list of design criteria included: minimizing the gap distance between the quartz windows without compromising fluid circulation; maximizing the device's ROI surface area without compromising operation, ergonomics, or safety; and configuring the layout of the device platform so that the position and depth of the device's ROI aligned appropriately with the instrumentation without negatively impacting the other design criteria (ergonomics, portability, durability, etc.).

Table 1.6: Design specifications for instrumentation interface*	
1	Use ligand-coated quartz windows
2	Minimize gap distance between windows
3	Recess interior surface of proximal quartz window 7mm
4	Region of interrogation at least 300^2 mm
5	Material-reagent compatibility
6	Minimize background signal
7	No material obstructions in the sample processing channel

*These design criteria pertain to the finalized fluorescence-based instrumentation design

Optimization of Diagnostic Performance

The design criteria for optimizing the diagnostic performance characteristics (Table 1.7) were derived from a combination of theoretical and practical considerations. The requirements included optimizing sample exposure to the ligand-coated surfaces, minimizing wall shear stress during sample processing, developing a protocol for sample

processing and diagnostic platform that minimized operational variability and sensitivity to external factors, and creating a reagent storage network within the device capable of processing relatively large sample volumes (1-3mL) in order to improve the probability of detecting infectious agents present in low concentrations. Wicking material and packed-bed sample processing channel designs were not compatible with optical interrogation requirements. This constraint provided opportunities for enhanced sample presentation to ligand-coated surfaces using alternative means. These alternative techniques included flow destabilization within the sample processing channel, multiple passage sample processing, and incorporating features or techniques that increased effective target analyte concentrations relative to the ligand-coated capture surfaces. Design challenges associated with this list of design criteria included: optimizing mass transport and pathogen capture within the ROI without inadvertently washing away bound pathogens during sample processing steps intended to remove unbound sample and reagent residues from the sample processing channel; developing an internal fluid network that provides multiple pass sample processing; minimizing wall shear stresses produced by circulating fluids without impairing mixing with the sample processing channel; and maximizing the sample volume processing capacity of the device without detracting from the ergonomics or portability of the diagnostic device.

Table 1.7: Design specifications for optimal diagnostic performance	
1	Optimize sample presentation to functional surfaces
2	Minimize wall shear stresses during sample processing
3	Minimize sensitivity to operational variability
4	Process relatively large specimen volumes (1-3mL)

Initial Conditions: Base Diagnostic Platform

Previous research performed by Dr. Powers' laboratory team on the functionalization of substrate surfaces with capture ligand coatings and fluorescence-based optical detection of pathogens provided the basis for the rapid diagnostic platform [64-68]. These required design features comprised a portion of the initial conditions for the development of the rapid diagnostic device. The remaining conditions were derived from requirements for versatile field use and efficient sample processing. The following subsections describe the basic assay format that was employed by the rapid diagnostic device and requirements for sample acquisition, transfer, and preparation for processing.

Assay Format

The selection of an optimal diagnostic format for a handheld assay was dependent on several factors. These factors included the specific application, the environment of intended use, and the desired method of detection for the assay. As mentioned previously, this diagnostic device was intended to detect infectious agents present within freshly drawn whole blood samples collected in resource-limited settings (RLSs). For this project, the most sensitive method of detection was fluorescence-based and the self-contained handheld diagnostic was intended to interface with an optical sensor in the form of a portable fluorescence-based reader. As a result, a sandwich-style ligand-binding diagnostic format was selected for use in the handheld diagnostic device.

The ligand-binding assay is well-suited for interfacing with fluorescence-based instrumentation as the ligands are easily conjugated to fluorescent dyes without compromising form or function. Additionally, conventional sample processing used for sandwich-style assays aids in stripping target agents from complex sample matrices. This

addresses the problem in which residual sample matrix components are left behind by inefficient sample processing, which otherwise would elevate background noise and compromise limits of detection. The technique is also suitable for use with macro- or microfluidics while maintaining optical requirements for optimal sample interrogation. Furthermore, this diagnostic format directly detects the presence of infectious agents and thereby mitigates risk associated with the window period of infection and the probability of false positives attributed to individuals who may have antibodies against an infectious agent of interest but not the agent itself (previous infection/exposure).

The advantages of the ligand-binding assay over more conventional diagnostic techniques include enhanced sensitivity, specificity, and reproducibility. The fluorescent dyes improve diagnostic sensitivity as they amplify detection signals several orders of magnitude above background noise. The ligands used in the assay may also be conjugated to several different dyes, individually, for multiplexed assays. The ligands themselves are more specific and less variable than antibodies by virtue of the processes involved in their isolation and/or synthesis. The ligands are also less expensive and significantly smaller than antibodies, providing the opportunity to increase the density of binding sites (and subsequently the sensitivity) on ligand-coated surfaces. Furthermore, ligands are not subject to the batch-to-batch variability that is expected from antibodies which rely upon the immune response of an animal model for synthesis.

Potential limitations of the technique include the upfront commitment of resources necessary to accurately determine functional peptide sequences to synthesize ligands with appropriate binding affinities for separate target agents, the process requires several processing steps to strip and label target agents from screened samples, and emerging or

continually evolving/mutating infectious diseases may render select ligands within the assay obsolete or ineffective. However, with careful choice of the unique surface antigen of the pathogenic microbe, this problem is avoided.

The modularity of the ligand-binding assay helps prevent the diagnostic from becoming obsolete with emerging infectious diseases or alternative applications. The ligands may be readily updated to meet the screening demands for emerging infectious diseases or changed altogether to screen other fluids (such as saliva and urine) for alternative target agents. Furthermore, meeting the design requirements for successfully implementing the ligand-binding assay format would also allow the handheld diagnostic to be readily modified for alternative applications and sensing schemes (colorimetric, electrochemical, chemiluminescence, etc.).

Sample Acquisition and Preparation for Processing

Two important procedural considerations that have significant impacts upon the efficacy of an assay include the methods of sample acquisition and preparation for processing. Prior to beginning the development of the rapid diagnostic device for this project, these methods required investigation and definition. The process of investigating and defining a protocol for sample collection entailed determining what supplies were available for use and which of the available supplies were most compatible with the design specifications for the project. The process of defining a protocol for sample preparation required familiarization with the properties of whole blood and the potential obstacles associated with screening the complex sample matrix. Ultimately, the protocols used for collecting and preparing samples would form the foundation upon which the diagnostic platform would be constructed.

Samples must be collected using equipment readily available in the field, or supplied alongside the diagnostic device in the form of a kit. In either case, the device must then interface with the sample collection vessel in a manner consistent with the design specifications for the project and mitigates the risk of sample contamination during handling. The risk factors that could compromise the quality of collected samples included inadvertent specimen contamination or specimen collection during a donor's window period of infection. Optional implements for sample acquisition and transfer to the diagnostic device included vacutainers containing sodium citrate, 3 mL hypodermic syringes, or a combination of the two. Both vacutainers and hypodermic syringes were readily available for use in the field, but they had distinct advantages and limitations.

Accordingly, the rapid diagnostic device was required to directly interface with a 3 mL hypodermic syringe for sample transfer and prime the sample for processing by adjusting sample viscosity and impairing the integrity of cell membranes. These requirements dictated a starting point for the design and development of the rapid diagnostic housing and reagent storage network components. From this starting point, the production, evaluation, and assembly of device components was possible. The end product was a full rapid diagnostic device assembly composed of 1) a sample processing channel, 2) a reagent storage network, and 3) the device housing with captive syringe port in a fully integrated system.

Project Milestones

This research project was divided into three phases of development. The following three chapters detail each phase of development individually with an emphasis on the evolution and evaluation of each rapid diagnostic device generation. Table 1.8 provides an

overview of the primary rapid diagnostic device designs along with a summary of their respective advantages, limitations, and required revisions. While significant modifications were made to the diagnostic device over the course of the project, each platform was composed of a sample processing channel, reagent storage network, and device housing with captive syringe port. The modular structure of the diagnostic devices and compartmentalized approach to development made it possible to preserve advantageous design features throughout prototype iterations.

Table 1.8: Overview of diagnostic device generations				
Diagnostic Generation	Primary Goals	Advantages	Limitations	Revisions
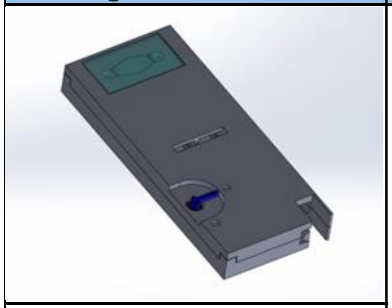 Generation 1	Establish a starting point; incorporate design elements into a handheld device; rapidly screen samples in a simple-to-use platform	Mutlipurpose reagent reservoirs store reagents, collect waste, and manipulate fluid circulation; achieve vortex mixing in microchannel; valid locking mechanism	Complex internal fluid network; complex operational procedure; weak syringe port arm; loose tolerances resulted in complications related to fit/alignment	Reduce part/assembly complexity; reduce operational complexity; reinforce syringe port arm; fortify internal fluid network to prevent leaks; tighten tolerances
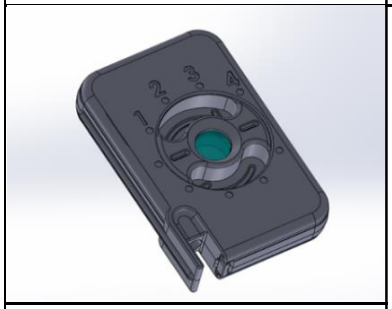 Generation 2	Revise platform to meet design specifications for size, simplicity (production and operation), and function; fortify design to withstand harsh environments	Significantly simplified design relies on a passive form of mass transport to process samples; enhanced design guards against harsh environmental and handling conditions	Critical design features are sensitive to part production and assembly variations due to size and configuration; dye reagents incompatible with inlay material	Convert designs into injection moldable parts; add ultrasonic weld joints for assembly; select new material compatible with dye reagents; mitigate sensitivities
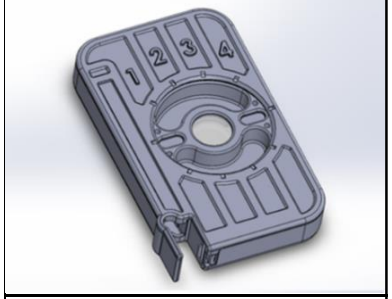 Generation 3	Begin manufacture and assembly of diagnostic devices; Begin process of diagnostic performance characteristic optimization	Robust, durable, ergonomic, rapid, easy-to-use diagnostic device; modular design for easy manipulation of variables during optimization; uses compatible materials	Platform configuration too expensive to manufacture and assemble domestically; revisions either add complexity to the device or tooling for production	Reconfigure the design for inexpensive manufacture and assembly - maintain previously validated, advantageous design features

CHAPTER 2: FIRST GENERATION DIAGNOSTIC DEVICE

This chapter presents the development process that was followed to create a rapid diagnostic device in accordance with project design criteria. In the first section of the chapter, I describe the Phase I project objectives and their significance for preparing the rapid diagnostic device for use in resource-limited settings (RLSs). The subsequent sections specifically address the methodology that was used to design, develop, and produce the first generation functional prototypes (Figure 2.1) of the disposable device. After the first full diagnostic assembly was designed, a small batch of functional prototypes were produced for a limited user evaluation (LUE) intended to gather feedback on platform ergonomics and ease-of-use. The chapter concludes with a summary of the advantages and limitations of the first generation prototype along with the requirements for preparing the device for the second phase of development.

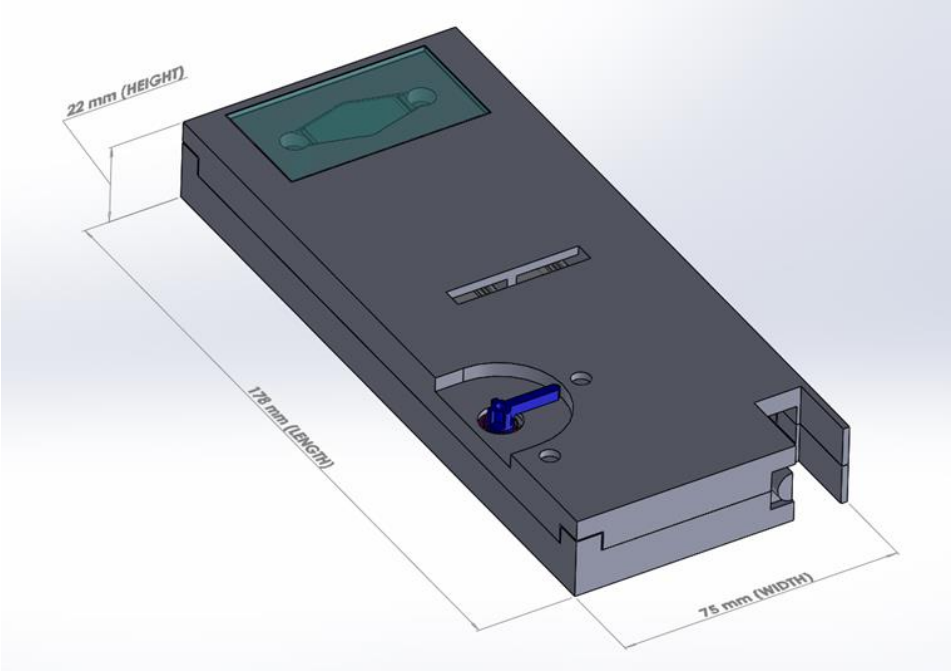

Figure 2.1. First generation diagnostic device. Computer aided design (CAD) of the first generation diagnostic device. The dimensions of the device were 176 mm X 75 mm X 22 mm (length X width X height).

Phase I Objectives

The primary objectives (Table 2.1) for the first phase of diagnostic development were to produce a safe, portable, and easy-to-use disposable diagnostic device capable of rapidly detecting infectious agents. These objectives led the development of the design requirements early in the design process for several reasons relating to efficient product development and utility of the diagnostic platform in RLSs. Operational safety was of paramount importance since the device was intended to process biohazardous materials potentially contaminated with infectious agents. A diagnostic device that spread disease, rather than diagnose, would be worse than no diagnostic at all. The operational safety requirements dictated that the diagnostic platform was hermetically sealed and resistant to leak formation. The portability objective was important for translating the assay from the laboratory to RLSs but also represented a dimensional constraint that affected the design

and configuration of all internal device components. Concrete dimensional requirements were not specified in order to provide design flexibility during the development and integration of design components; however, the device was required to be handheld. Device ease-of-use was critical for the efficacy of the assay and operation under dynamic field conditions. Operator error has the potential to adversely impact the performance of assays with high levels of sensitivity and specificity. In RLSs, the risk of operator error may be assumed much greater than in clinical or laboratory settings due to lack of training, duress, distraction by dynamic environmental conditions, rushing to screen samples in an emergency, or a lack of familiarity with the diagnostic. As a result, the diagnostic device was required to automate sample processing as much as possible (minimizing the number of actuating components) and utilize an intuitive sample processing protocol. These primary objectives provided boundary conditions for the development field-deployable rapid diagnostic device.

Table 2.1: Primary objectives and criteria

Objective	Corresponding criteria
Operational safety	Self-contained reagents, hermetic seal, permanent retainment of sample collection/transfer vessel, resilient in RLS situations
Portability	Handheld device dimensions
Ease-of-use	Minimal actuating components, intuitive operation, limited number of steps, configured for right-handed users (yet facilitate ambidextrous operation)

While safety, portability, and ease-of-use were the primary objectives, the interrelated nature of both the design criteria and diagnostic platform components made it necessary to establish secondary objectives to meet requirements and avoid inadvertently

compromising or limiting other essential design characteristics. The secondary objectives (Table 2.2) for the first phase of development were to optimize conditions for infectious agent capture within the diagnostic device, maximize sample processing speed, and minimize platform complexity. Although these objectives were conferred a lower level of priority relative to the primary objectives, they were critical for establishing diagnostic efficacy and utility. Implementing two tiers of objectives was intended to improve the likelihood that the first generation prototypes would meet the requirements for ergonomics and ease-of-use during the limited user evaluation without compromising diagnostic performance or other design criteria. The two-tiered system provided a mechanism for balancing tradeoffs when technical or design obstacles were encountered that placed primary and secondary objectives in direct conflict. In such cases, decisions were made to preserve or optimize component designs in favor of the primary objectives while attempting to limit or circumvent the impact on the secondary objectives.

Table 2.2: Secondary objectives and criteria	
Objective	Corresponding criteria
Rapid sample processing	Provide results ≤ 10 minutes
Optimal conditions for infectious agent capture and detection	Effectively detect infectious agents (viruses, bacteria, parasites), use ligand-coated quartz windows, minimal gap distance between windows, proximal window flush with device body (to mate with the first generation design of the instrumentation), region of interrogation (ROI) at least 300^2 mm, material-reagent compatibility, minimal material background signal, evacuate all air from ROI before analysis, optimize sample presentation to capture substrates, efficiently clear ROI of unbound residues, minimize wall shear stresses during processing, minimize sensitivity to operational variability, process specimen volumes (1-3mL)
Minimal design complexity	Inexpensive platform to manufacture, disposable

In order to efficiently manage the design process and mitigate potential conflicts between the primary and secondary objectives, development of the diagnostic platform was divided into two sequential stages. The first stage, heavily governed by the primary objectives, was to define the sample screening protocol for the diagnostic platform. The requirements for sample collection, handling, transfer, preparation, and processing would dictate platform configuration and dimensions. After determining a preliminary screening procedure, the second stage was to design and integrate the diagnostic platform components into the first generation functional prototype. The diagnostic platform was divided into three main components based on function and developed in parallel according

to the secondary objectives. This strategy made it possible to maneuver around technical and design obstacles while striving to satisfy the project design criteria.

Development of Sample Screening Protocol

The basic biosensor configuration is composed of a biological receptor, a transducer, and a detection system [3]. First, the biological receptor selectively binds target analytes – separating the targets from a sample matrix and concentrating them for further processing. Next, the transducer converts the recognition/capture event into a physical signal. Lastly, the detection system collects, processes, and analyzes the physical signal to yield a result. The biological receptors of the rapid diagnostic device developed for this project were created by covalently bonding heparan sulfate or lignosulfonic acid to quartz windows embedded within the device. The transducer employed within this system was a fluorophore-conjugated ligand (heparan sulfate or lignosulfonic acid) which would label captured target analytes with a fluorescent marker that the detection system could excite to produce an emission spectrum for data collection and analysis. The detector was an updated version of fluorescence-based instrumentation configured to optically interrogate the diagnostic device.

Based on this biosensor configuration, the diagnostic design process was separated into two tasks. The first task was to develop a sample screening protocol that facilitated infectious agent capture by the biological receptors, labeling of bound targets, and removal of unbound sample and reagent residues prior to optical interrogation. Techniques for performing the sample screening protocol were investigated and assessed for compliance with the design criteria for the project. The end result was a conceptual sample screening

protocol that provided the framework for the second task – designing the physical elements of the diagnostic device.

To develop an optimized sample screening protocol, the procedure was divided into three fundamental steps: sample collection and transfer to the device, sample preparation for processing, and sample processing. Each step was subject to a unique set of variables that could be managed or manipulated to enhance diagnostic safety, ease-of-use, portability, and performance. After satisfactory methods for performing each step were determined, a preliminary sample screening protocol was established that would provide the framework for the development and integration of the diagnostic platform components.

For development, the diagnostic platform was divided into three main components: the sample processing channel, the reagent storage network, and the device housing. This made it possible to formulate a variety of design concepts for each element that could be easily assessed for compatibility with platform integration and compliance with design specifications. The diagnostic device component designs that best supported the design criteria and Phase I objectives were integrated together to produce the first generation diagnostic device.

Sample Collection and Transfer

The sample collection and transfer step of the screening procedure potentially posed a significant risk to sample quality, operator safety, and diagnostic performance. In RLSs, the risks become more severe with unsanitary conditions, limited supplies, untrained staff, and potentially no immediate access to biohazardous waste disposal systems. Aside from utilizing aseptic techniques, the most practical solution for addressing these risks was to select an appropriate sample collection vessel that would support the design criteria for the

project. Samples must be collected using equipment readily available in the field, or supplied alongside the diagnostic device in the form of a kit. Optional implements for sample acquisition and transfer to the diagnostic device included either an evacuated tube or hypodermic syringe. Both vessels were readily available for use in the field, but they had distinct advantages and limitations.

Advantages associated with the use of an evacuated tube for sample collection included improved operator safety, immediate specimen exposure to anticoagulants, compact dimensions, and a barrier to prevent inadvertent contamination during handling. However, the utility of the evacuated tube was limited due to an inability to directly measure and meter the volume of whole blood collected and transferred to the diagnostic device. Additional drawbacks included an elevated expense (relative to hypodermic syringe), the glass composition of the vessel that may fracture under adverse conditions (operator safety), the rubber stopper which may elute substances that interfere with assay performance (material incompatibility), and sensitivity to dynamic environmental conditions (unreliable performance) [4]. If an evacuated tube was used to collect and transfer samples, the diagnostic device would have to be adapted to extract the sample from the vessel – increasing design complexity, cost, and operational difficulty.

Advantages associated with use of a hypodermic syringe for the collection and transfer of samples to the diagnostic device included the ability to accurately collect and transfer specified sample volumes, no need for additional equipment or an augmented diagnostic device design, and a polypropylene composition that is inherently more resistant to impacts. Designing the diagnostic device to accommodate a hypodermic syringe also increased the modularity of the platform and extended screening capabilities to fluids

beyond blood. The limitations associated with using the hypodermic syringe for sample collection and transfer included the exposed hypodermic needle during transfer (operator safety), the overall length of the hypodermic syringe (device portability), and an absence of anticoagulant within the vessel (sample processing efficacy).

Based on the advantages and limitations of each sample collection vessel, the hypodermic syringe was better suited for accomplishing the Phase I objectives. Although the exposed hypodermic needle did pose a risk to operator safety, the majority of inadvertent needle sticks occur when people attempt to recap the syringe [5]. This risk can be mitigated with an appropriate device configuration that distanced the operator's hand from the needle tip during the sample transfer process. The two factors that played the most significant roles in determining the best-suited sample collection vessel were 1) the ability of the hypodermic syringe to perform all required duties, and 2) the sensitivity of the evacuated tube to fluctuations in environmental conditions – altering the volumes of samples collected and transferred. The diagnostic platform was now required to provide a hypodermic septum for sample transfer and permanently retain the hypodermic syringe following sample transfer. The issue of coagulation suppression is addressed in the following section with sample preparation.

Table 2.3: Sample collection/transfer method and compliance with design objectives		
Design objectives	Hypodermic syringe	Evacuated tube
Safety	(M): Risk of needle stick	(H): Glass tube fracture
Portability	(H): Small dimensions	(H): Small dimensions
Ease-of-use	(H): Direct collection and transfer	(L): Easy to collect sample, difficult to transfer. Would require increased device complexity
Assay efficacy	(H): Accurate and reproducible sample collection and transfer	(L): Sensitivity to environmental conditions and leaching substances that may interfere with binding kinetics
Sample processing speed	(H): Direct collection and transfer. Transfer aids in hemolysis	(M): Requires extraction step or integrated extraction mechanism within device. Increases complexity
Low production cost	(H): Vessel is inexpensive and reduces complexity of diagnostic device.	(L): Vessel is relatively expensive and increases complexity of device

*(H): high compliance; (M): medium compliance; (L): low compliance

Sample Preparation

Freshly drawn whole blood is a complex sample matrix with physical properties that present potential obstacles to efficient and accurate screening [6]. Whole blood exhibits relatively high apparent viscosity under low flow conditions and is prone to coagulation unless supplemented with anticoagulants. Additionally, significant concentrations of select infectious agents may reside within the intracellular space of the blood sample. These infectious agents would go undetected unless liberated from the red blood cells. Options for addressing these issues included supplementing samples with

anticoagulants upon transfer to the device, reducing blood sample viscosity through dilution, and extraction of intracellular infectious agents through cell lysis or poration.

The advantages associated with inducing hemolysis included a wide range of available techniques, rapid sample treatment, reduced sample variability, minimal screening complexity, and an insensitivity to fluctuating environmental and donor conditions. The most significant limitation correlated with hemolysis was the release of proteolytic agents into the diagnostic environment. These enzymes indiscriminately cleave peptide chains – potentially compromising the binding efficacy between targeted pathogen surface antigens and the capture ligands. Screening efficacy may be more sensitive to proteolytic agents when infectious agents are present in low concentrations, but the rate of degradation is not well characterized and rapid sample processing may be adequate for addressing the issue.

The advantage of cellular poration is that infectious agents may be extracted from the red blood cells without releasing proteolytic agents [7, 8]. There are a variety of techniques available (i.e. sonoporation, photoporation, electroporation, etc.) for inducing cellular poration with the capabilities to selectively target specific membranes (extracellular versus intracellular) and adjust pore sizes. The disadvantage, however, would be a substantial increase in design complexity, sensitivity to sample variations (i.e. volume, hematocrit, etc.), and (depending on the technique) sensitivity to fluctuating temperatures associated with the outside environment. Based on the advantages and limitations of both procedures (Table 2.4), it was decided that hemolysis could significantly improve detection capabilities with minimal complexity.

Table 2.4: Cellular poration vs. lysis		
Strategy	Advantages	Limitations
Cell poration	Increased effective target concentration	Methods for achieving cellular poration are nontrivial and add complexity to the sample processing strategy
	Intracellular components that may confound target capture efficiency are retained within the cell	Added complexity may result in increased sample processing time, unit cost, risk of variability, and add potential modes of failure to the system
	Intact cell bodies may enhance mass transport and target capture within the target capture zone of the diagnostic device	
Cell lysis	Increased effective target concentration	Intracellular components may compromise target binding affinity during sample processing
	Opportunity to dilute sample and mitigate viscosity related complications	
	Simple, inexpensive, and rapid	

Methods investigated for achieving effective cellular lysis of the freshly drawn whole blood samples included direct application of electrical current, exposure to rapid pressure fluctuations, enzymatic digestion, and osmotic shock. Each technique was evaluated using bovine whole blood supplemented with EDTA. Osmotic shock demonstrated the most effective results and was in compliance with the project design criteria (Figure 2.2). Lysing the cells by exposing them to deionized water had an additional benefit as well. The deionized water diluted the blood sample and reduced the sample viscosity. The lower sample viscosity was beneficial because sample processing would be less sensitive to ambient temperature fluctuations, mitigate the risk of plugging the lumen of the reagent storage network and sample processing channel, improve flow destabilization and boundary layer separation under laminar flow conditions, aid in the

removal of residues from the optical region of interrogation, and enhance infectious agent separation from complex sample matrices. The impact of releasing proteases into the diagnostic environment was not known.

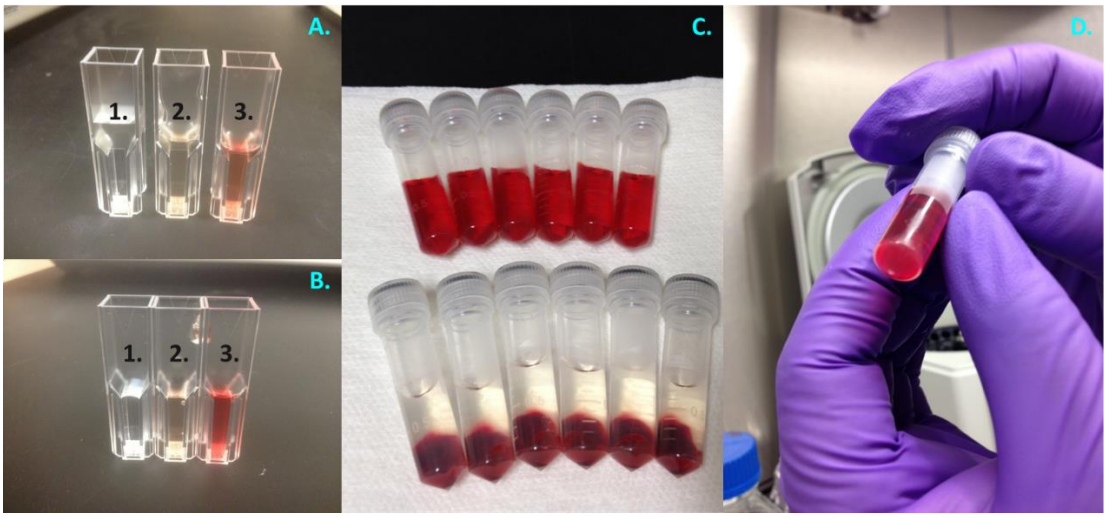

Figure 2.2. Hemolysis experiments for sample preparation. (A) Blood samples that were exposed to rapid pressure fluctuations (A.3) exhibited increased cell lysis compared to control sample (A.2). (B) Blood samples exposed to direct electrical current (B.3) demonstrated greater cell lysis than control sample (A.2, B.2) and samples exposed to fluctuating pressures (A.3). (C) Osmotic shock produced greatest cell lysis – top row of centrifuge tubes. (D) Osmotic shock was so thorough that 'ghost pellets' were readily visible following centrifugation.

Osmotic shock could be easily integrated with the other sample preparation requirements into a single step which supported diagnostic ease-of-use. If the proteolytic agents were found to be problematic in later stages of the diagnostic evaluation process, the deionized water could be replaced with phosphate buffered saline (PBS) and the diagnostic platform would not require physical modification. Based on the Phase I objectives and corresponding design criteria, incorporation of a sample preparation reservoir into the reagent storage network would be beneficial to both sample processing and diagnostic efficacy.

Sample Processing

Sample processing, in the context of the sample screening procedure, refers to the method by which infectious agents were separated from the sample matrix, labeled with fluorescent markers, and prepared for optical interrogation. For the purpose of defining a practical screening protocol, the primary concerns associated with the implementation of a rapid and effective method for sample processing applied to 1) the duration of sample exposure to capture substrates, 2) the removal of unbound sample and reagent residues from the sample processing channel prior to optical interrogation, and 3) a method for circulating and exchanging reagents within the hermetically sealed device. Compared to immunoassays that used wicking materials or packed-bed configurations, the parallel plate design utilized by this assay had significantly less surface area for capturing target pathogens and fewer diffusion-based obstacles associated with the samples flowing over, rather than through, the capture substrate material. Methods for addressing these concerns included the incorporation of a multiple passage sample processing system within the device, a wash reservoir for removing unbound residues from the region of optical interrogation, and a pump system to circulate flow through an interconnected reagent storage network.

Blood Sample Screening Protocol

In theory, the protocol for screening samples represents a best-case-scenario for effectively capturing, labeling, and detecting infectious agents in contaminated whole blood samples. From the evaluation process, a basic formulation of the blood sample

screening protocol was derived that the diagnostic device would be designed to implement and optimize (Table 2.5).

Table 2.5: Preliminary blood screening protocol

Stage	Step	Process
1 Hemolysis and target capture	1	Sample is transferred to device where it is immediately mixed with deionized water to induce hemolysis. *Water could be supplemented with EDTA if hypodermic syringe is used to collect and transfer sample alone.
	2	The lysed and diluted sample is recirculated through the sample processing channel (25x) for optimal target capture.
2 Labeling of bound targets	3	The processed blood sample is emptied from the sample processing channel into a self-contained waste reservoir.
	4	After the waste has been removed from the sample processing channel, the lysed and diluted sample is replaced (in the sample processing channel) with the dye-conjugate solution from the second stage reservoir.
	5	After volumes are exchanged, the dye-conjugate solution within the sample processing channel is recirculated through the channel (25x).
3 Washing sample processing channel for optical interrogation	6	The processed dye-conjugate solution is emptied from the sample processing channel into a self-contained waste reservoir.
	7	After the waste has been removed from the sample processing channel, the dye-conjugate reagent is replaced (in the sample processing channel) with the PBS rinse solution. An excess rinse solution is incorporated with the device so that the extra solution removes residual reagents as it passes through the sample processing channel.
	8	After volumes have been exchanged, the diagnostic device is interfaced with the fluorescence-based reader.

Based on the preliminary blood screening protocol, estimates could be made to predict the total amount of time that would be required to collect a blood sample, screen the sample with the diagnostic device, and produce a result. If sample collection required 2 minutes, each step of the screening procedure required 0.5 minutes (4 minutes), and optical interrogation require another 2 minutes to complete, the total time required would be roughly 8 minutes. This approximation would satisfy the rapid sample screening design

criteria that required the diagnostic device to provide a result in less than 10 minutes after sample collection. More importantly, the preliminary blood screening protocol illuminated the constraints for developing the diagnostic platform components to facilitate the screening protocol. The protocol also suggested where there were design opportunities that could be used to balance diagnostic performance characteristics. The next step was to begin the design and production of the first generation diagnostic device components based on the preliminary blood screening protocol. Based on the analysis, the diagnostic platform required a few basic features to comply with the screening procedure (Table 2.6).

Table 2.6: Feature requirements for diagnostic platform components

Screening element	Component	Feature
Sample collection and transfer	Reagent storage network	Hypodermic needle septum
	Device housing	Captive syringe port
Sample preparation	Reagent storage network	Hemolysis reservoir filled with deionized water*
Sample processing	Reagent storage network	Reservoirs for dye reagent and wash solutions
		Pump buttons for reagent circulation
		Multiple passage configuration

*water could be supplemented with sodium citrate if hypodermic syringe was used alone

Development of the Diagnostic Platform

The second stage of the development process was predominantly governed by the secondary objectives for Phase I of the rapid diagnostic project which were intended to augment the efficacy and speed of the assay as the designs transitioned from concept to the first functional prototype. Although the optimization of speed and efficacy were important, designs were moderated by the secondary objective for maintaining platform simplicity and the primary objectives for safety, ease-of-use, and portability. The diagnostic platform

was divided into three components that were developed in parallel to maintain design flexibility and accommodate design modifications as design challenges were encountered. These components included the sample processing channel, the reagent storage network, and device housing based on functional requirements. Sample screening efficacy was dependent on the ability of the sample processing channel to facilitate infectious agent capture, labeling, and presentation for optical interrogation. Diagnostic safety, resilience to adverse conditions, ease-of-use, and sample screening speed were dictated by the configuration of the reagent storage network. The diagnostic housing primarily functioned as the user interface for the diagnostic platform but also retained the sample transfer vessel and conferred environmental resilience.

Sample Processing Channel

Three methods of improving sample processing were designed into the sample processing channel: use of multipass sample processing, a miniature channel configuration, and turbulent flow. Due the large volume sample processing requirement for this project, designs utilizing wicking materials or packed-bed configurations were immediately eliminated from consideration due to their limitations.

Minimal channel dimensions and multi-pass sample processing presented simple methods for easily enhancing infectious agent capture within the target capture zone of the diagnostic device. Generally, a decrease in channel dimensions results in a correlated drop in boundary layer thickness and an increase in capture surface area to sample volume ratio. The thinner the laminar boundary layer, the shorter the path of diffusion to reach the ligand-coated channel surface. It would appear to be obvious that flow channels within

diagnostics should be made as small as possible based on these relations. This was not feasible, however, when the diagnostic application called for processing large volumes (1-3 mL) of complex sample matrices in resource-limited settings and the ambient conditions were not controllable. The miniature channels must be made large enough that capillary action does not drive flow, and samples may pass through the sample processing channel passively or by an applied force. While boundary layer thickness increases and surface area/sample volume decreases under these conditions, their impact may be mitigated with multipass sample processing and turbulent flow.

The methodology and duration of sample exposure to target-binding, ligand-coated substrates has a direct impact on assay sensitivity. Accordingly, the fluid dynamic flow regime within the sample processing channel played a significant role determining the efficacy of the diagnostic device. For example, microfluidic channels tend to exhibit laminar flow behavior due to their characteristically low Reynolds numbers. As a result, the majority of the sample volume passing through the sample processing channel would have limited opportunity to interact with the ligand-coated quartz windows within the optical region of interrogation (especially true for short channels and high volumetric flow rates). Infectious agents must be entrained in laminar sheets within close proximity to the channel walls so the agents may readily bind with complimentary ligands through diffusion (enhanced by turbophoresis). Under turbulent conditions, the fluid sheets characteristic of laminar flow are destabilized and replaced by fluctuating eddies that bring a greater proportion of target agents within proximity of capture ligands. Not only is a greater proportion of the sample exposed to the boundaries of the channel (specifically the capture substrates), laminar flow is significantly reduced and constrained to a laminar sublayer

located at the surfaces of the channel walls. The disadvantage of turbulent flow was that the high volumetric flow rates required to destabilize flow result in reduced duration of exposure and high wall shear stresses. As a result, the sample processing protocol required considerable modeling and testing to yield clinically relevant performance characteristics.

Methods and Materials

There are a variety of techniques that may be utilized within the sample processing channel to improve infectious agent capture, labeling, and presentation for optical interrogation. Experiments performed for this study sought to identify an optimal method for enhancing sample screening within the diagnostic platform. The ideal technique would be easy to implement, robust, effective, and compliant with the design criteria for the project. Techniques for flow destabilization that were investigated included surface roughening, inline flow obstacles (Figure 2.3), a baffled channel, and converging flows.

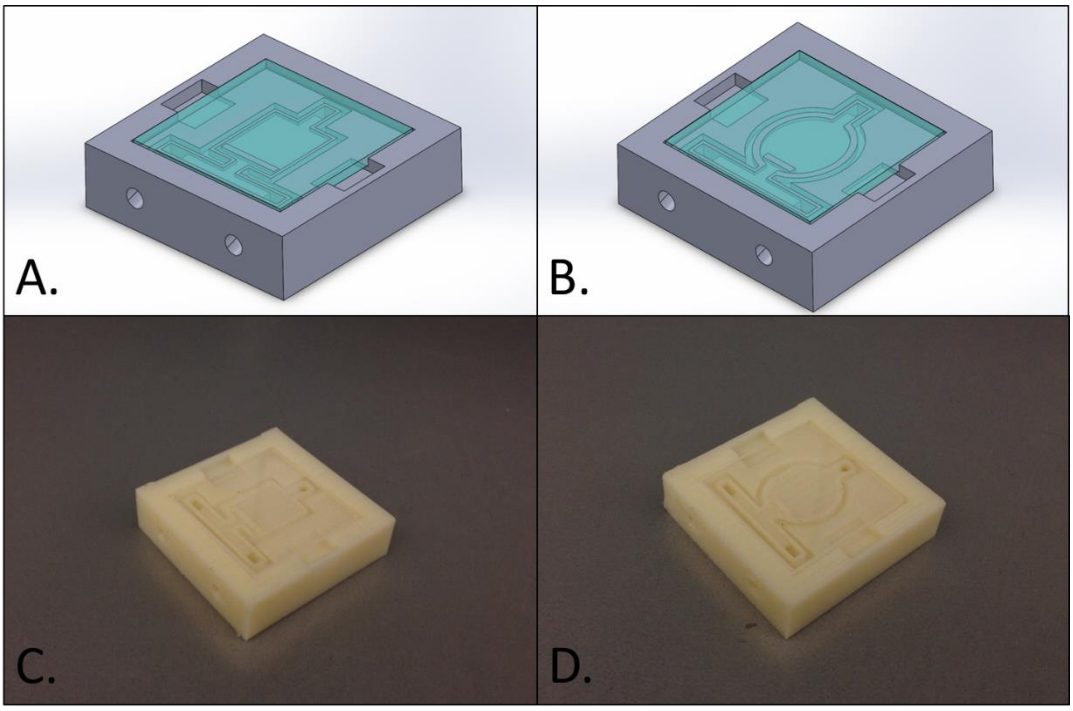

Figure 2.3. Prototype flow channels for infectious agent capture. (A) Computer aided design (CAD) of rectangular flow channel with flow obstruction to destabilize flow. (B) Computer aided design (CAD) of elliptical flow channel with flow obstruction to destabilize flow. (C and D) functional sample processing channel prototypes produced in ABS plastic by fused deposition modeling. The overall dimensions of the prototypes were 35 mm X 35 mm X 8 mm (length X width X height).

Computational Modeling

The methodology used to enhance mass transport and infectious agent capture in the first generation diagnostic device involved adding flow obstructions within ligand-coated miniature channels to destabilize flow and induce boundary layer separation. In order to assess the feasibility of destabilizing flow and inducing vortex formation, computational modeling of fluid dynamics was performed using ANSYS software. Based on the simulations, the impact of channel and obstacle geometries on vortex formation were investigated.

The methodology used to enhance mass transport and infectious agent capture in the first generation diagnostic device involved adding flow obstructions within ligand-

coated miniature channels to destabilize flow and induce boundary layer separation. In order to assess the feasibility of destabilizing flow and inducing vortex formation, computational modeling of fluid dynamics was performed using ANSYS software.

Irregular flow channel configurations considered for improving sample processing and infectious agent capture were intended to induce boundary layer separation under laminar flow conditions. Possible options included adding baffles to the flow channel, suspending mid-planar flow obstacles throughout the channel, and/or flow obstacle projections positioned near the inlet and outlet of the sample processing channel. While the system demonstrated the necessary properties to achieve enhanced sample mixing, the baffles would also make clearing unbound sample and reagent residues from the region of interrogation more difficult and impair the diagnostic detection limit (Figure 2.4). Additionally, the baffles themselves would obstruct portions of the optical region of interrogation. Mid-planar flow obstructions were briefly investigated as well. 100 μm diameter strings were suspended within 300 μm channels in an attempt to induce vortex shedding. The channels demonstrated limited success and a significant amount of variability – leading to the formulation of a compromise between the two techniques (baffles and mid-planar flow obstructions).

The compromise was to implement flow obstacle projections near the inlet and outlet of the sample processing channel interior. The surface projection flow obstacles were a good fit with the requirements of the project because they were simple to produce with limited variability, did not obstruct the channel optical region of interrogation, and could accommodate a variety of channel configurations. Interestingly, they nearly function

as the inlet/outlet modifications described previously but excel in achieving more diffuse mixing without the limitations.

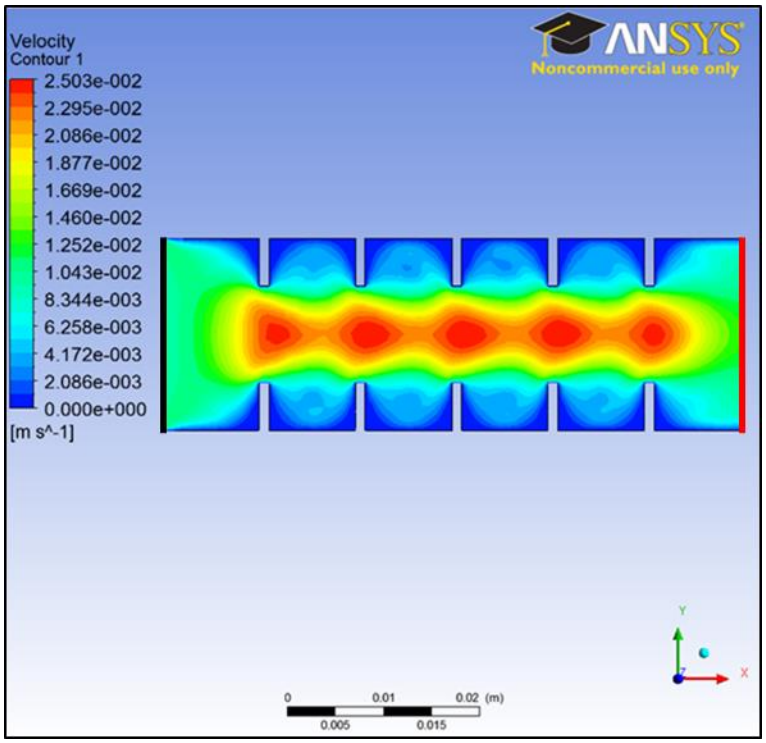

Figure 2.4. Baffle flow channel simulation with laminar flow. The baffles within the flow channel (5 mm in height) form flow restrictions that generate regions of high fluid velocity near stagnant pockets of fluid. This situation readily induces boundary layer separation and mixing between baffles. The projections also result in boundary layer compression (reduced diffusion path length) which would be beneficial for infectious agent capture except for the elevated wall shear stresses. There may be an optimal projection height that compresses boundary layer thickness without resulting in exceptionally high wall shear stresses. If the baffles were converted into a single narrow flow restriction (e.g. two quartz windows), boundary layer compression may be advantageous. No-slip boundary conditions were set for the walls of the channel, while the inlet (black) was assigned a volumetric flow rate of 1 mL/s and the outlet (red) was assigned a gauge pressure of 0 mmHg. The material properties of the fluid were defined by density (1060 kg/m^3) and viscosity (3 cP). The fluid was assumed to be Newtonian and incompressible while the flow was unsteady. Blood is a non-Newtonian fluid, but may behave similar to Newtonian fluids under the appropriate flow conditions. Since the blood would be diluted for testing, the Newtonian assumption was reasonable. Material properties for the blood were not altered to account for dilution in order to provide a worst-case scenario. The simulation implemented a quadrilateral mesh with 16246 nodes that was refined via a mesh study until results varied less than 1%.

Surface modification strategies considered for optimizing infectious agent capture within the target capture zone of the diagnostic device were constrained to the quartz

windows. These strategies primarily focused on surface roughening/etching techniques and ligand-coating modifications. Surface roughening of the quartz windows could be beneficial by: 1) increasing surface area for capturing infectious agents, 2) compressing boundary layer thicknesses over surface projections, and 3) aiding in transition between laminar and turbulent flow regimes. An investigation of these potential benefits was explored using ANSYS software to perform computational simulations of fluid dynamics over roughened surfaces.

Flow Destabilization

Before designing multiple different sample processing channels, it was important to confirm that laminar flow did occur within the miniature channels configured with the dimensions intended for use. A prototype flow channel was designed in SolidWorks and produced using an additive manufacturing process referred to as fused deposition modeling. The prototype channel was rectangular, included two inlets and one outlet, and was void of flow obstructions. The dual inlets made it possible to inject two dyes simultaneously through the channel. Even though the sample processing channel of the diagnostic device was intended to facilitate bidirectional flow, the prototype channel was configured for unidirectional flow based on symmetry.

With confirmation of the laminar flow behavior within the miniature channels (Figure 2.5), production of the miniature channels with flow obstacles ensued. A variety of different miniature channel configurations were produced and evaluated for both mixing and infectious agent capture. The sample processing channels were configured with a prototype channel base with a framed depression to accommodate a ligand coated quartz window. Mixing evaluations were performed by simultaneously injecting two different

dyes through the dual inlets of the prototype channel and visually monitoring mixing downstream of the flow obstacle. The evaluation of infectious agent capture was performed using S*taphylococcus aureus* (*S. aureus*) as the target analyte. This infectious agent was an ideal model because the bacterium exhibits intermediate dimensions relative to viruses and parasites. 3 mL samples would be collected from overnight cultures (approximate concentration: $10^{8\text{-}9}$ CFU/mL) and passed through prototype miniature channels (single pass) at volumetric flow rates approximately equivalent to 1 mL/s. Preliminary tests revealed design weaknesses requiring channel modification.

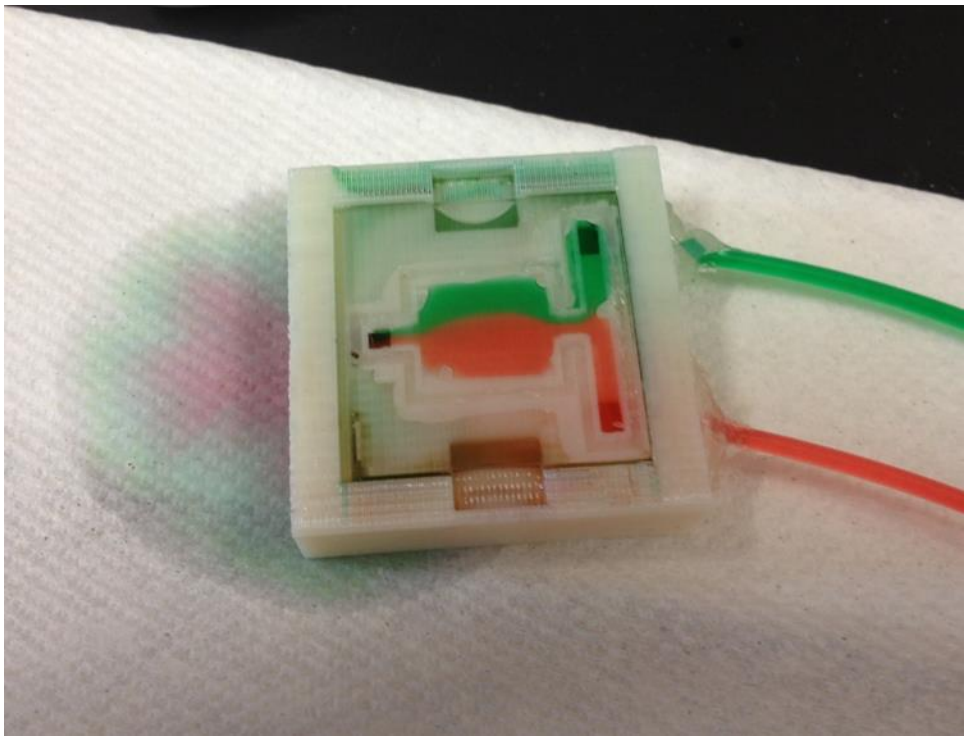

Figure 2.5. Demonstration of laminar flow within the miniature channel without flow obstructions. Laminar flow within the sample processing channel confirmed the need to use specialized channel geometries to optimize sample exposure to ligand-coated substrate surfaces. Additionally, the sharp corners of the rectangular channel appear to readily collect bubbles – potentially as issue during optical interrogation.

An additional method for improved infectious agent capture involved the incorporation of specialized inlet/outlet designs for the sample processing channel of the

diagnostic device. These designs included converging flow channels leading to the inlet of the sample processing channel, orifice plates, and flapper valves. Converging flow channels were tested for mixing efficiency and performed well (Figure 2.6). The designs were deemed too complex for production, however, because they would complicate the reagent storage network designed to circulate reagents within the diagnostic device. The use of orifice plates was considered because they could be used to generate vortices. The narrow orifice of the plate produces a high velocity stream of fluid with stagnant or low velocity pockets of fluid immediately adjacent – resulting in flow destabilization. Potential limitations of this design included a narrow stream of turbulent flow, flow resistance impairing speed and ease of sample processing, and diminished efficiency given the channel dimensions and geometry required to accommodate the plates and achieve the desired flow dynamics. The flapper valve design could also work but it was subject to the same limitations as the orifice plates except with a heightened level of complexity as the valves only allow unidirectional flow – requiring an extra set of valves to allow fluid circulation.

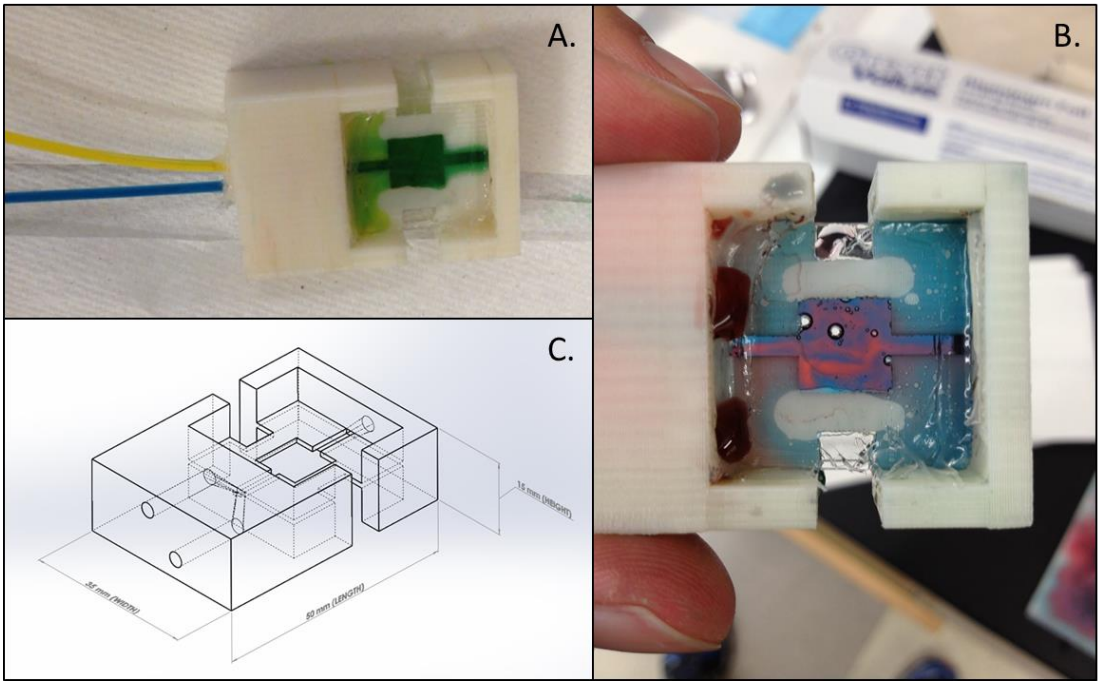

Figure 2.6. Converging inlet sample processing channel geometry. (A) Yellow and blue dyes were simultaneously injected into the prototype flow channel to evaluate mixing – indicated by the green coloration of the fluid within the optical region of interrogation. (B) Slower volumetric flow rates diminish mixing efficacy as illustrated by the separate blue and red streaks within the channel. (C) Computer aided design (CAD) of the sample processing channel. Dimensions are 50 mm X 35 mm X 15 mm (length X width X height).

Infectious Agent Capture

A variety of miniature channel configurations were created to evaluate infectious agent capture and assess potential configuration-based capture efficiency correlations. Four designs were produced for the pilot study to evaluate two channel geometries with and without obstacles. Based on these results[1], one preliminary design configuration performed the better than the others and was selected for continued development.

The pilot studies evaluating prototype channel infectious agent capture used custom miniature channels combined with ligand-coated quartz windows to simulate the sample

[1] Quartz window functionalization, infectious agent culture, and capture evaluation protocol execution were performed with the aid of Malani Chauhan, Jonathan Wan, and Hannah Curtis.

processing channel of the first generation diagnostic device. To minimize the influence of variables on the results, samples were screened by passing them through the miniature channel with only a single pass. While the goal was to determine the best configuration/features, it would also would help approximate the number of infectious agents capture per pass. After screening contaminated samples, the quartz windows were removed from the prototype channels and stained for histological evaluation using brightfield microscopy. Tests were performed in triplicate for each miniature channel configuration.

Freshly dawn bovine whole blood was spiked with *S. aureus* as a model infectious agent for capture. *S. aureus* was chosen because it is easily cultured, visible under the microscope, and exhibits intermediate infectious agent dimensions. To prepare the spiked samples, *S. aureus* was inoculated into 25 mL of Luria-Bertani (LB) medium and cultured overnight at 37°C with continual aeration and gentle agitation. The final concentration was estimated to be approximately 10^8 cells/mL. A 12 mL sample of the *S. aureus* culture was centrifuged (5,000 x g for 5 minutes) to form a cell pellet and exchange the LB medium supernatant with PBS. The cells were resuspended and transferred to the whole blood sample at a 1:2 ratio (v/v) – for a total sample volume of 3 mL/test. The resulting blood samples were subsequently contaminated with approximately 8.52 x 10^9 cells/mL of *S. aureus.*

The quartz windows were functionalized with a ligand-coating of heparan sulfate adapted from a previously described protocol [9]. In order to apply the coating to the quartz surface, the slides were first cleaned using a mixture of 80% fuming sulfuric acid and 20% hydrogen peroxide (30%) for 30 minutes. After this ‘piranha etch’ solution cleaned the

slides for 30 minutes, the slides were rinsed with copious amounts of deionized water and baked in a glassware drying oven overnight. To conjugate heparan sulfate to the quartz surfaces, the slides had to be silanized. The clean quartz slides were reacted with 3-glycidoxypropyltrimethoxysilane (2% v/v in 95% ethanol) for six hours in Coplin jars agitated by gentle shaking. Following this procedure, the quartz slides were washed with ethanol and dried at 135°C for an hour. The surfaces were then reacted with heparan sulfate in 0.01M sodium hydroxide for 10 hours.

The miniature flow channels for the pilot study were designed using SolidWorks and produced using an additive manufacturing process known as fused deposition modeling (FDM). The channels were produced in white ABSplus plastic (uPrint SE 3D printer) and external surfaces were sealed using a 15 second bath in methyl ethyl ketone. After the bath, the miniature chips dried for 5 hours within a chemical fume hood. Once dried, the miniature channels were rinsed with ethanol and allowed to air-dry. Teflon tubing segments were attached to the inlet and outlet of each channel and ligand-coated slides were sealed to the surfaces each channel using silicone. Spiked samples were transferred to and through these channels using 3 mL BD luer-lock syringes fitted with barbed luer-to-tubing adaptors. Four channel configurations were tested, three times each. Between tests, channels were soaked in bleach and rinsed with ethanol before being dried at 50°C. Prototypes were cooled to room temperature before reuse.

Histological evaluation of pathogen capture efficiency was performed after removing the quartz slides from the miniature channels. Once freed from the channel, each slide was rinsed with PBS to remove residual sample from the surface. Each quartz slide would then be rinsed with crystal violet to stain any bound pathogens residing on the quartz

surfaces. When the quartz slides were removed from the channels, the silicone adhesive would remain adhered to the quartz surface. The gasket was left on the surface to help contain reagents during staining and rinsing processes, but removed with a scalpel afterward. Crystal violet solution was allowed to remain in contact with the surface of the slide for approximately 1 minute before being washed away with a second PBS rinse.

After thoroughly removing the histological stain from the slide and residual silicone adhesive, a coverslip was placed over the capture surface of each slide before being viewed using bright field microscopy (1,000x, oil-immersion objective). The quartz slide was centered under the objective to obtain count estimates the infectious agents captured within the approximate optical region of interrogation. Three central optical fields of view were used to count captured pathogens on each slide to estimate infectious agent capture efficiency among the different miniature channel configurations. The fields of view that were selected for counting were representative of the quartz slide capture surface. Counts were tallied and cumulative totals (sum for all three regions) were averaged over the triplicated experiments due to sparse pathogen capture.

Results of Initial Testing

Flow Simulations

Computational simulations suggested that obstacles blocking a greater percentage of the channel width more readily destabilized flow (Figure 2.7). This was consistent with observations found in literature and the governing theory behind flow destabilization [10]. Larger flow obstructions minimize the gap distance between the obstruction and the

adjacent channel wall – thereby significantly increasing fluid velocity through the two flow restrictions. When regions of high fluid velocity occur immediately adjacent to regions of low fluid velocity (or even stagnant fluid), destabilization readily occurs because inertial forces overcome viscous forces. Potential obstacles associated with the induction of mixing by this method included cavitation and bubble entrapment behind the obstacle. The implosion of bubbles during cavitation may occur within the optical region of interrogation (rapid channel expansion results in increased pressure) and the resultant shockwaves may dislodge bound infectious agents. Bubble entrapment behind the obstacle could impair boundary layer separation and optical measurements.

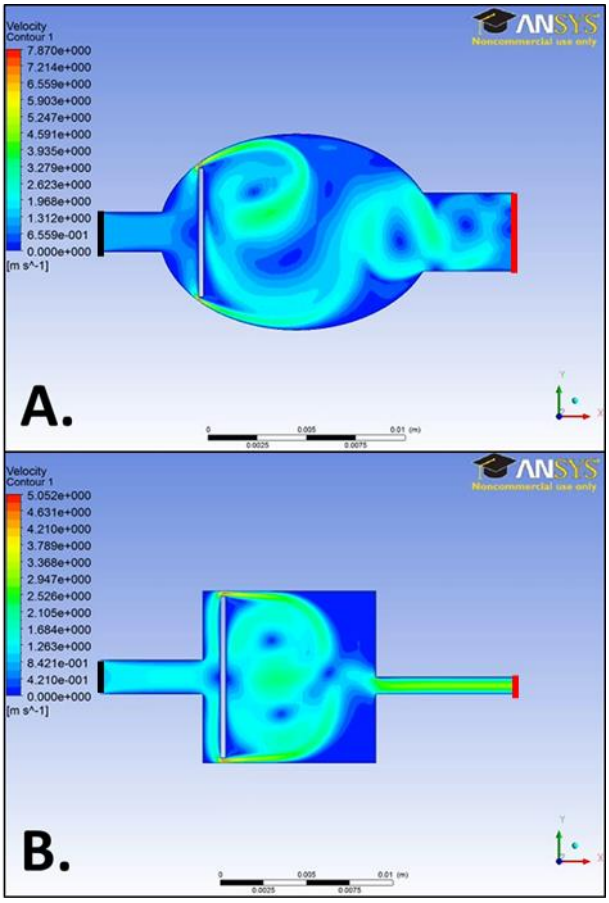

Figure 2.7. **Turbulent flow simulations in channels with flow obstructions.** (A) An elliptical channel geometry designed to improve dispersion of mixing within the flow channel by eliminating dead zones of stagnant fluid. (B) A rectangular channel with two significant dead zones of stagnant fluid located in the distal corners of the channel just before the outlet. No-slip boundary conditions were set for the walls of the channel, while the inlet (black) was assigned a volumetric flow rate of 1 mL/s and the outlet (red) was assigned a gauge pressure of 0 mmHg. The material properties of the fluid were defined by density (1060 kg/m^3) and viscosity (3 cP). The fluid was assumed to be Newtonian and incompressible while the flow was unsteady. Blood is a non-Newtonian fluid, but may behave similar to Newtonian fluids under the appropriate flow conditions. Since the blood would be diluted for testing, the Newtonian assumption was reasonable. Material properties for the blood were not altered to account for dilution in order to provide a worst-case scenario. The simulations implemented quadrilateral meshes with 18690 (A) and 17322 (B) nodes that were refined via a mesh study until results varied less than 1%.

While the simulated flows over roughened surfaces may support the hypothesis concerning boundary layer compression (Figure 2.8), a literature review on the subject raised more concerns than advertised benefits [11]. These concerns eliminated surface roughening as a reasonable consideration for enhancing target capture for this project and timeline.

The modification of ligand-coatings, however, was a much more reasonable option. Tethers could be conjugated to the quartz surfaces to extend capture ligands further toward the center of the sample processing channel – mitigating boundary layer effects. Additionally, branched (i.e. multidentate) tethers may be used to increase the total number of binding sites available for capturing target analytes within the sample. The use of custom ligand-coating strategies could be beneficial but they also increase production complexity, cost, and risk for increased variability. As a result, they would only be considered for use if more simplified strategies were unsuccessful [68].

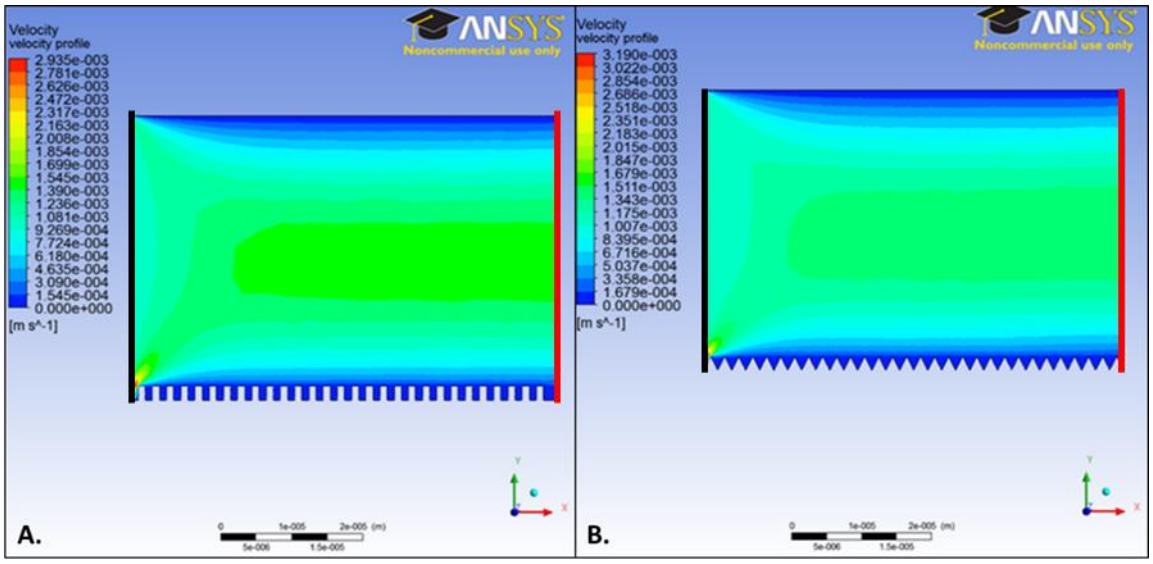

Figure 2.8. Laminar flow computational simulation over roughed surfaces. (A) Laminar flow through a channel with a rectangular roughened surface geometry. (B) Laminar flow through a channel with a triangular roughened surface geometry. The simulations were conducted to see if boundary layer thickness could be modulated by altering channel surface properties. The irregular projections in both channels were 200 µm in height and exposed to a volumetric flow rate of 1 mL/s. In both figures A and B, thinner color bands at the roughened surface (relative to the smooth) suggest boundary layer compression may occur. No-slip boundary conditions were set for the walls of the channel, while the inlet (black) was assigned a volumetric flow rate of 1 mL/s and the outlet (red) was assigned a gauge pressure of 0 mmHg. The material properties of the fluid were defined by density (1060 kg/m^3) and viscosity (3 cP). The fluid was assumed to be Newtonian and incompressible while the flow was unsteady. Blood is a non-Newtonian fluid, but may behave similar to Newtonian fluids under the appropriate flow conditions. Since the blood would be diluted for testing, the Newtonian assumption was reasonable. Material properties for the blood were not altered to account for dilution in order to provide a worst-case scenario. The simulations implemented quadrilateral meshes with 15000 (A) and 14500 (B) nodes that were refined via a mesh study until results varied less than 1%.

Turbulence

Bubble entrapment behind the flow obstacles was a significant issue during testing (Figure 2.9) and had to be addressed. The bubbles formed as fluid flowed into an initially empty channel. The fluid was first bifurcated on the proximal side of the flow obstacle (relative to the inlets) and then coalesced on the distal side – forming an air pocket where the two streams converged. Three options were considered for eliminating the issue. The first option was to eliminate the stream-bifurcating obstacle and replace it with a narrow flow restriction that transitions to a wide channel to destabilize flow (similar premise to the orifice plate but less extreme). This design would have eliminated bubble entrapment with the removal of the flow obstacle but may not have demonstrated effective mixing across the entire width of the miniature channel. This could be compensated for by increasing the length of the channel, but design criteria seek to limit the overall dimensions of the device. The second option was to reduce the height of the flow obstacle so fluid could pass over the top and sides of the obstacle – preventing converging streams from trapping air. The concern with this concept was that flow destabilization may become more difficult with the elimination of stagnant pockets of fluid (or 'dead zones'). The third option was to prefill the microchannel with liquid so that coalescing fluid streams could not form a bubble. Limitations of this design consideration included diminished diagnostic shelf life due to hydrolytic degradation of the ligand-coated surfaces and the dead zone behind the obstacle may entrap bubbles generated through cavitation or air pockets trapped within the reagent storage network.

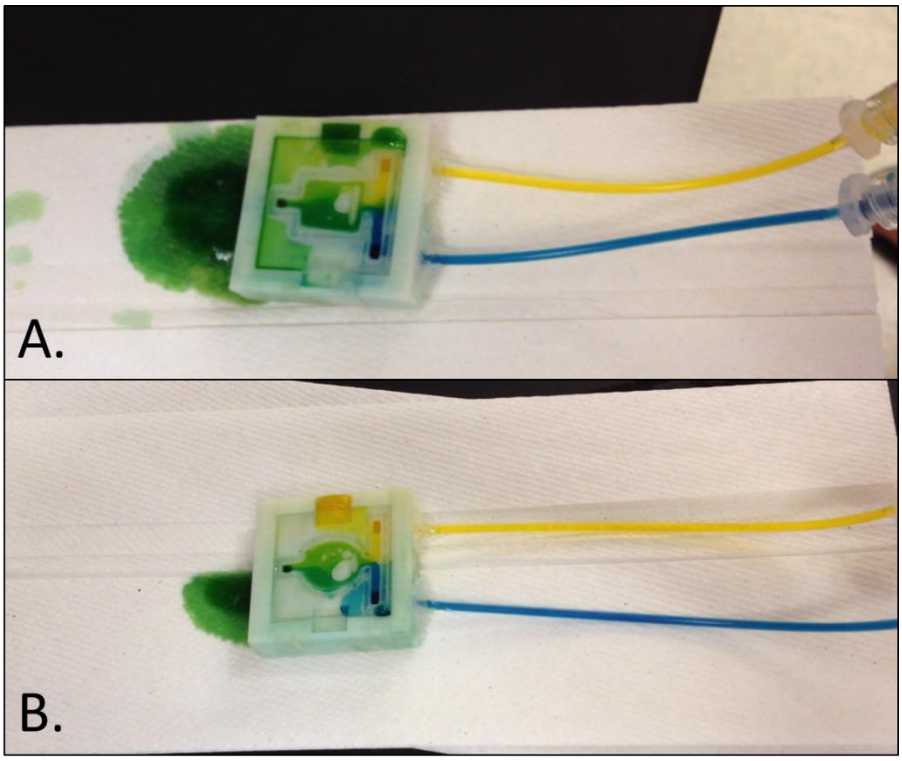

Figure 2.9. Prototype flow channels with obstructions evaluated for mixing efficiency. The rectangular flow channel (A) and elliptical flow channel (B) both demonstrated inconsistent mixing due to bubble entrapment behind the flow obstacles within the channels.

Optimal Infectious Agent Capture

Based on the counts obtained for each of the four miniature channel configurations, the elliptical channel with the flow obstruction performed the best (Figure 2.10). Interestingly, the other three channel configurations did not demonstrate any statistical differences. Even so, the elliptical channels did exhibit lower standard deviations than the rectangular channels – suggesting the elliptical configuration may promote more stable/consistent flow near the center of the channel. The rectangular channel with the flow obstruction did not perform statistically different from the rectangular channel without the obstruction, but it did demonstrate a diminished standard deviation.

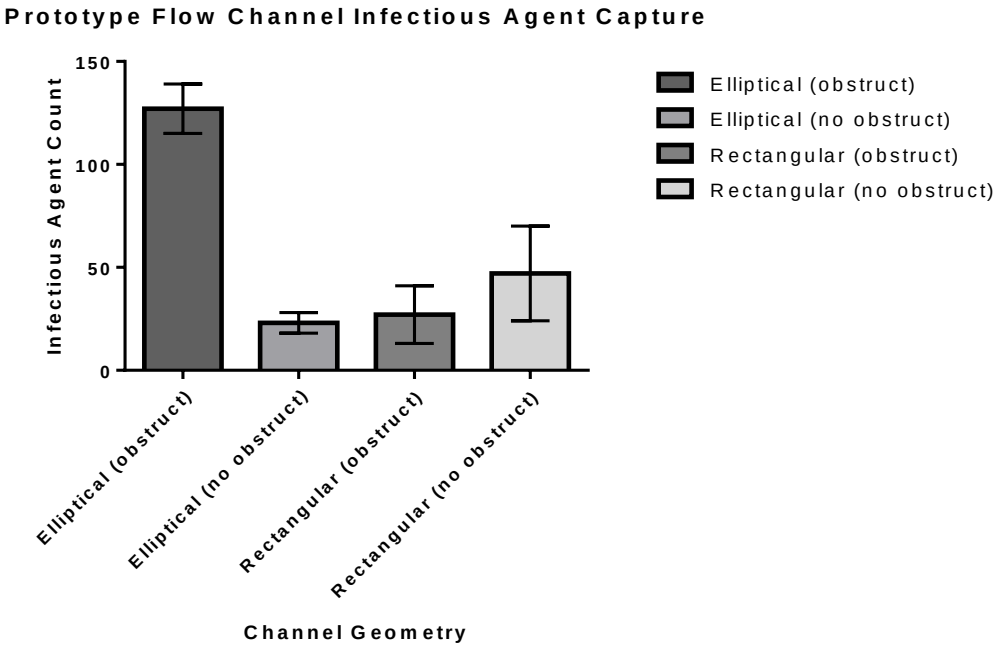

Figure 2.10. Prototype flow channel infectious agent capture. Of the four geometries tested, the elliptical sample processing channel with flow obstruction captured the most infectious agents and demonstrated improved consistency over the rectangular channel geometries. Approximate concentration of *S. aureus* was 8.52×10^9 cells/mL.

Summary of the Pilot Study

The pilot study was intended to assess the contribution of the miniature channel flow obstacles and configurations for improving infectious agent capture. One design demonstrated a statistically significant improvement in infectious agent capture relative to the other configurations. Differences in standard deviations between miniature channel configurations also may suggest particular design elements were better suited for the application than others. Based on the cursory findings from this study, the elliptical channel appeared to be the optimal miniature channel configuration and was chosen for further development and integration with the first generation diagnostic device.

The enhanced infectious agent capture and reduced standard deviation suggests that more uniform mixing may be occurring in the elliptical miniature channels. Another

possibility is that there may be a region of low flow that collects infectious agents (due to turbophoresis). Based on the simulations for the rectangular channels, there does appear to be a region of high flow in the center of the channel – which may have negatively impacted target capture for the rectangular configurations. Simulations of the elliptical channel suggest that the regions of high and low flow are more random and less stable – possibly providing enough mixing to aid in capture but not so much as to create excessively high wall shear stresses. Furthermore, the rectangular channels potentially have 2-3 regions of stagnant flow (corners of the channel and behind the flow obstruction) that possibly contribute to higher shear stresses. At the very least, the stagnant flow regions would make removal of unbound sample/reagent more difficult from the channel. The size of the flow obstacle between the two channels is also significantly different which may have played a role in disperse mixing through the channel.

In conclusion, the more narrow flow obstructions in the elliptical channels appeared to be the most suitable design elements for enhancing infectious agent capture within the first generation diagnostic device. The design must be adapted accordingly to fit within the diagnostic but, by adhering to these fundamental design specifications, enhanced mixing and infectious agent capture should be reliable and reproducible.

Reagent Storage Network

The self-containment of all reagents within a hermetically sealed reagent storage network was imperative for simplifying operational complexity, reducing variability in diagnostic performance characteristics, ensuring operator safety, and translating the diagnostic device from the laboratory to point-of-care applications. Accordingly, a novel reagent storage and circulation network was designed for the first generation handheld

diagnostic platform. Requirements governing the design of the network included: ensuring compatibility with miniature sample processing channels, use of materials compatible with reagent and sample components, simple operation, and a minimal dimensional footprint that would support a handheld diagnostic platform.

The main challenge behind designing the reagent storage network was formatting a circulatory system connecting all reagents and waste reservoirs to a bi-directional sample processing channel. The system required reagent storage reservoirs connected to the inlet of the sample processing channel, the outlet of the sample processing channel connected to waste reservoirs, and a means to drive fluid flow within the device and circulate reagents. The system that was formulated (Figure 2.11) used multipurpose reservoirs, check valves, a three-way stopcock, a hypodermic syringe septum, and pump buttons to drive fluid flow. The first prototype system was produced using a variety of components readily available for purchase but rated to maintain seals under harsh conditions. The reagent storage network was composed of PTFE tubing, nylon tube fittings and adaptors, sleeve septa, a hypodermic needle septum, and modified BD syringes with plunger caps. The hydrophobic PTFE tubing was used to lessen the risk of target analytes adsorbing to conduit surfaces before reaching the sample processing channel of the device. BD syringes were selected for two major reasons: 1) the syringe materials are specifically chosen to demonstrate compatibility with a wide range of reagent solutions for research-based applications, and 2) the form of the syringe device could be easily modified to meet the reservoir functional requirements of the device. The first prototype system was used to validate the design. After confirmation that the system worked appropriately, it was adapted to fit within the handheld device of the first generation diagnostic.

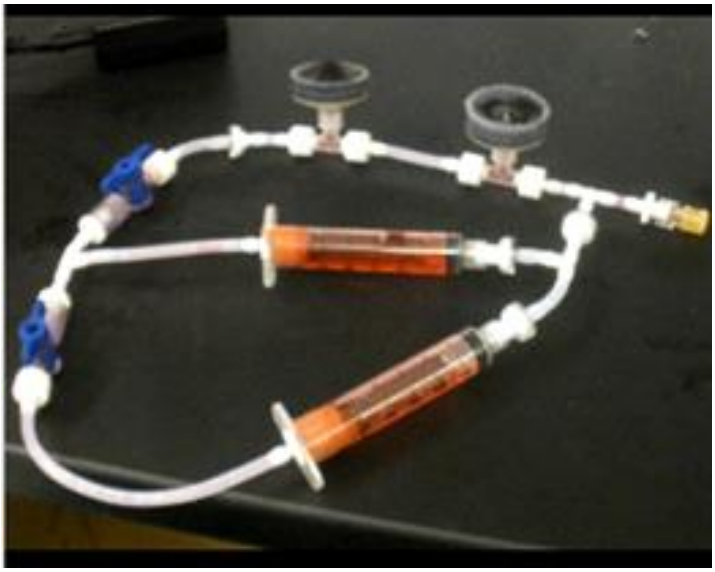

Figure 2.11. First prototype reagent storage network. The system was used to validate the design configuration and evaluate practical reagent volumes.

The multipurpose reservoirs played a significant role in minimizing the handheld diagnostic footprint. There were three reservoirs in total: the blood sample collection/hemolysis reservoir, the dye-label reagent/lysed sample waste reservoir, and the wash reagent/dye-label reagent waste reservoir. The blood sample collection/hemolysis reservoir was advantageous because it was integrated into the pump button at the inlet of the sample processing channel – saving space and reducing operational complexity for the user. The reagent and wash solution reservoirs exchanged reagent volumes with waste – eliminating the need for extra reservoirs and cutting dimensional requirements in half. Using the pump buttons to circulate fluid within the device, the selected reagent would be extracted from its reservoir and the waste from the sample processing channel would recirculate into the selected reservoir cavity. Cross contamination between the reagent and waste was prevented with a mobile plug present within the reservoir. The plug also functionally converted the reservoir into a dynamic switch. The reagent storage network was configured with check valves placed at the outlets of the reagent/waste reservoirs that

would inactivate the specific branch of the network when the plug reached the end of the reservoir tube. This would provide operator feedback to proceed to the following stage of sample processing. Initially the system was built with two one-way stopcocks separating the two reservoirs and the dynamic switch feature was critical for switching between branches of the network. The dynamic switch feature became redundant when the two valves were replaced with a single three-way stopcock to minimize design complexity and save space.

In a future generation, however, the stopcock valves were intended to be removed altogether. The process of cycling between sample processing reservoirs could have been fully automated with an improved reservoir design (Figure 2.12). These design implementations were postponed on the first generation device due to time constraints. It was also logical to wait for user feedback on the first generation platform before investing resources into the revised design. With the enhanced system design, the same protocol would be required for sample processing except the user would not have to manually select each loop via stopcock.

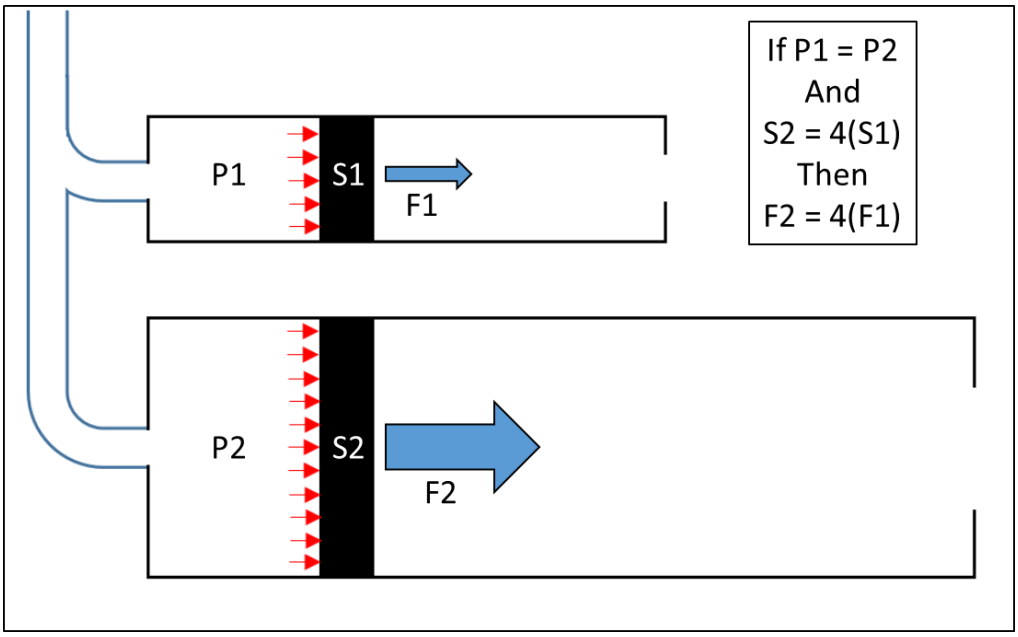

Figure 2.12. Pascal's law as a selector valve. In the diagram, there are two reservoirs connected to a strip of bifurcated tubing. Each reservoir contains a plug that creates a hermetic, semi-static seal within with the reservoir boundaries. If the internal volume of the reservoirs and tubing to the left of the plugs are treated as a closed system and pressurized, the pressure at P1 and P2 can be assumed to be equal. According to Pascal's law, the pressure acts uniformly across all internal surfaces. The force acting on the larger plug is greater than the smaller plug because the difference in surface area (stress = force/area). As a result, the plug in the larger reservoir may be triggered to actuate/move first if the frictional forces acting on the large plug are tailored to be less than the forces acting on the smaller plug. The red arrows (only depicted at the plug interface) may be assumed to be acting upon all surfaces exposed to the constant pressure.

The pump buttons were used for sample processing and reagent circulation within the reagent storage network. The buttons were placed at the inlet and outlet of the sample processing channel so that fluid may be transported bi-directionally across the ligand-coated quartz windows – achieving multipass sample processing. Two buttons were necessary because they were used to fulfill two roles. During sample processing (target capture, target labeling, and washing), the buttons would be compressed alternately by the operator. As one button was compressed, fluid would be driven through the miniature channel while and into the cavity of the second button (which would expand with increased pressure). The second button would then be compressed to drive fluid back across the ligand-coated quartz windows (Figure 2.13A) – the process would be repeated a specified

number of times to optimally extract, label, and wash sample components bound to the functionalized surfaces. During fluid circulation, reagents would be exchanged in the sample processing channel. As one button would be compressed, the other button was pumped to cyclically circulate the fluid (Figure 2.13B). The stopcock(s) would be used to select which branch (and associated sample processing stage) of the reagent storage network was active.

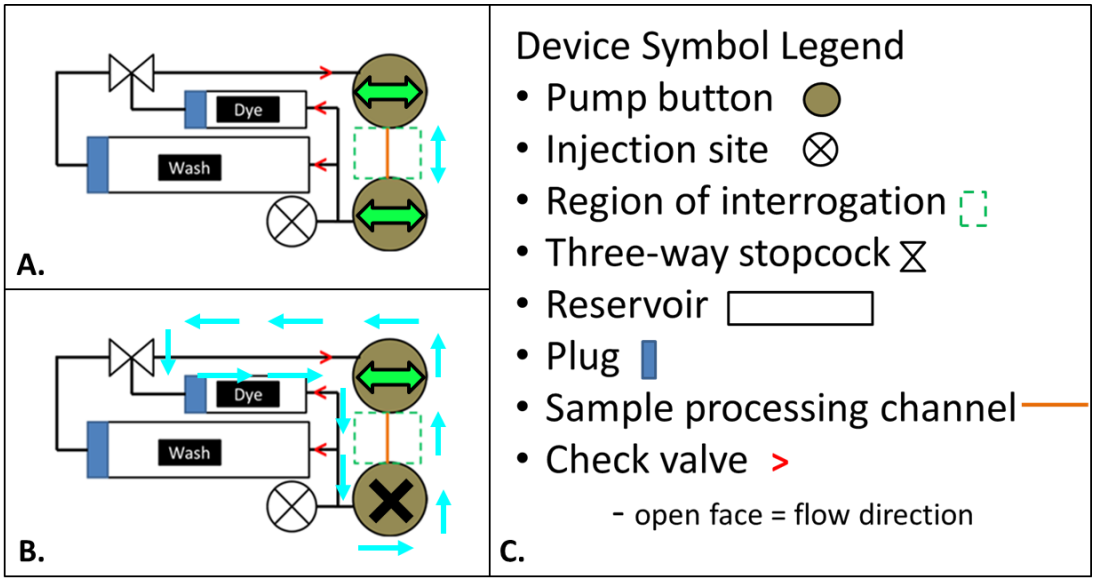

Figure 2.13. Sample processing and reagent circulation within device. (A) When the pump buttons are cyclically compressed (green double arrow) in an alternating fashion, fluid travels back and forth through the sample processing channel (blue double arrow). (B) When one pump button is continuously compressed (black X) while the remaining pump button is cycled (green double arrow), fluid circulates through the reagent storage network of the device.

Device Housing

The handheld device platform was designed alongside the fluid network so the two systems could be integrated together. One of the major design considerations for the handheld device platform was the organization of the reagent storage network components. The components had to be organized such that the body of the diagnostic device was

portable and easily fit within the operator's hands while providing sufficient room for ergonomic, operational components. The sample processing and reagent circulation system also had to function appropriately within the device – regardless of orientation. The end result was the first generation diagnostic device.

Design requirements for safety and durability were intertwined in many aspects of the diagnostic device platform. A catastrophic failure of almost any device component guaranteed compromised operator safety. The only safety concern independent of the device components was the hypodermic syringe used to collect and transfer whole blood samples. To address the operator safety concerns, the housing of the diagnostic device was designed to protect the reagent storage network and permanently retain the sample transfer vessel with a captive syringe port (Figure 2.14).

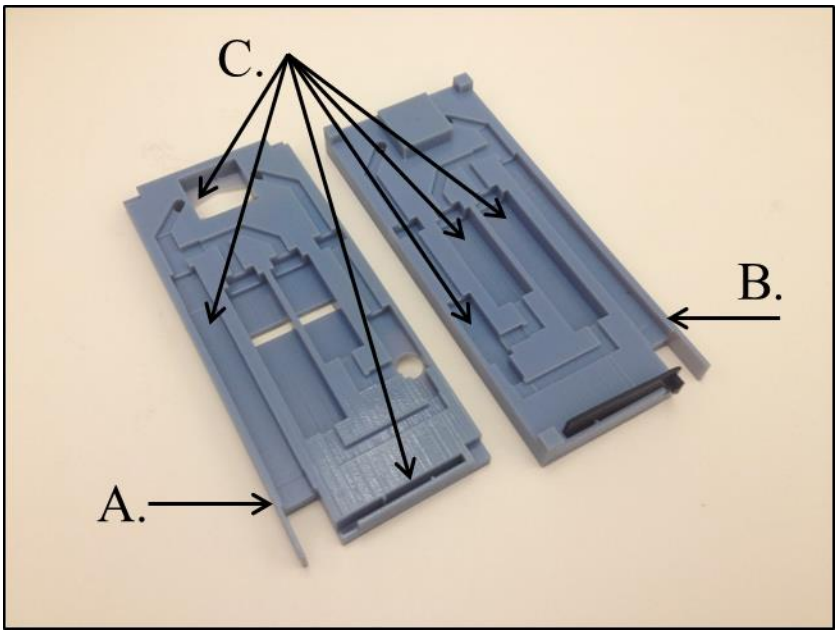

Figure 2.14. Device housing and captive syringe port designs. (A) Top housing component. (B) Bottom housing component. (C) Internal compartments for reagent storage/circulation.

The reagent storage network of the device was already composed of parts rated to maintain seals under harsh environmental conditions. Accordingly, the housing of the

device was designed to maintain the alignment of the storage reagent network components – preventing connections from being compromised and tubing from being occluded (i.e. pinched or kinked). The housing also mitigated the risk of impact and/or puncture damage. The fused deposition modeling construction of the components produced a three-dimensional woven mesh that is especially resistant to impact fracture (similar to cortical bone) because energy is significantly dissipated through the fracture of the fibers – impeding crack propagation. Delamination was a much more probable mode of failure, but easily addressed by ensuring large contact surface area between layers.

The other major risk associated with operator safety included inadvertent needle sticks by the hypodermic syringe during the collection and transfer of samples. This safety concern was addressed with the device layout and captive syringe port. The diagnostic device platform was designed to keep the operator's free hand far away from the needle during insertion into the syringe port – mitigating the risk of inadvertent sticks. Once the syringe is fully inserted into the syringe port, the locking tab is closed permanently behind the syringe – preventing withdrawal from the diagnostic. The locking mechanism design prevents the tab from being slid backwards and is insensitive to stress relaxation. In the storage position, the tab is bent in one direction. Stress relaxation will occur over time, but the locked configuration bends the tab in the opposite direction – ensuring a tight fit against the syringe plunger.

Another major concern was developing a method for safely handling the sample-transfer vessel (a 3 mL hypodermic syringe in this case) following sample acquisition and processing to mitigate the risk of operator exposure to biohazardous materials. Conceptual designs included a sheathing process (Figure 2.15) where the syringe was capped following

sample transfer, a twist-lock that captured the syringe flange in slots flanking the injection port (Figure 2.16), and a locking tab mechanism that snapped into place behind the syringe (Figure 2.17) – permanently retaining the vessel within the diagnostic device. The first two designs were dismissed based on complexity alone while the third concept was chosen for continued development.

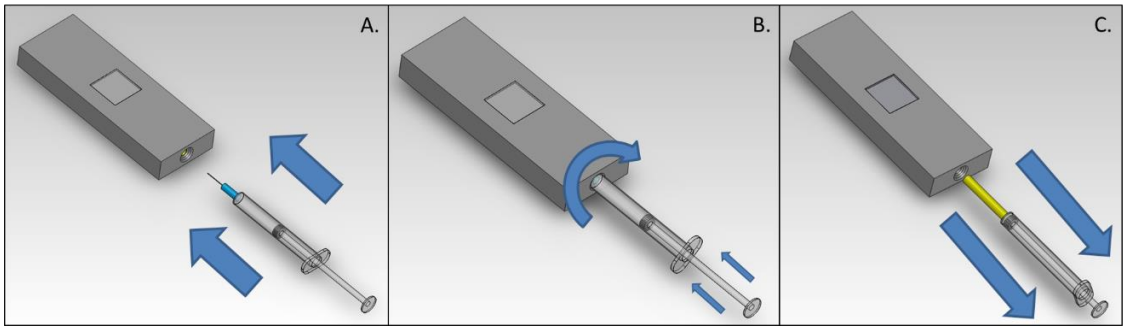

Figure 2.15. Sheath design for hypodermic syringe. (A) The sample filled syringe is inserted into the syringe port of the device containing a removable sheath that snaps on to the tip of the syringe. (B) The plunger of the syringe is depressed to inject the sample into the device. After the sample is ejected from the syringe, the syringe is twisted to disengage the sheath from the device. (C) The syringe is removed from the injection port – capped by the sheath to protect the operator from inadvertent needle pricks. The design was modeled to accept a 3 mL BD syringe and 25 gauge 5/8 inch hypodermic needle.

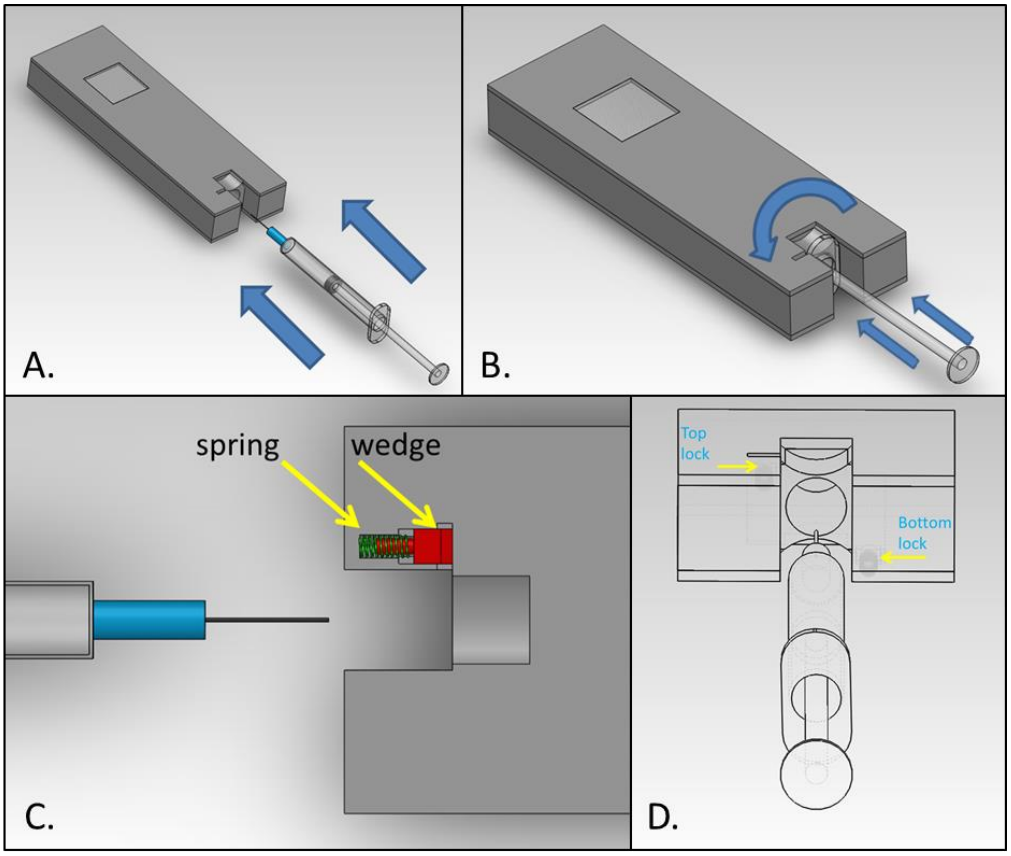

Figure 2.16. Twist-lock design for hypodermic syringe. (A) The sample filled syringe is fully inserted into the syringe port of the device. (B) After being fully seated, the body of the syringe is rotated 90° to lock the flange of the syringe into slots located at sides of the syringe port. (C) Overhead view of syringe port with shallow cross-section to expose locking mechanism. The slots contain spring-loaded wedges that allow the flange to pass but lock behind it. (D) There are two spring-loaded locks located at the top left and bottom right edges of the syringe port to securely retain the syringe after sample transfer. The design was modeled to accept a 3 mL BD syringe and 25 gauge 5/8 inch hypodermic needle.

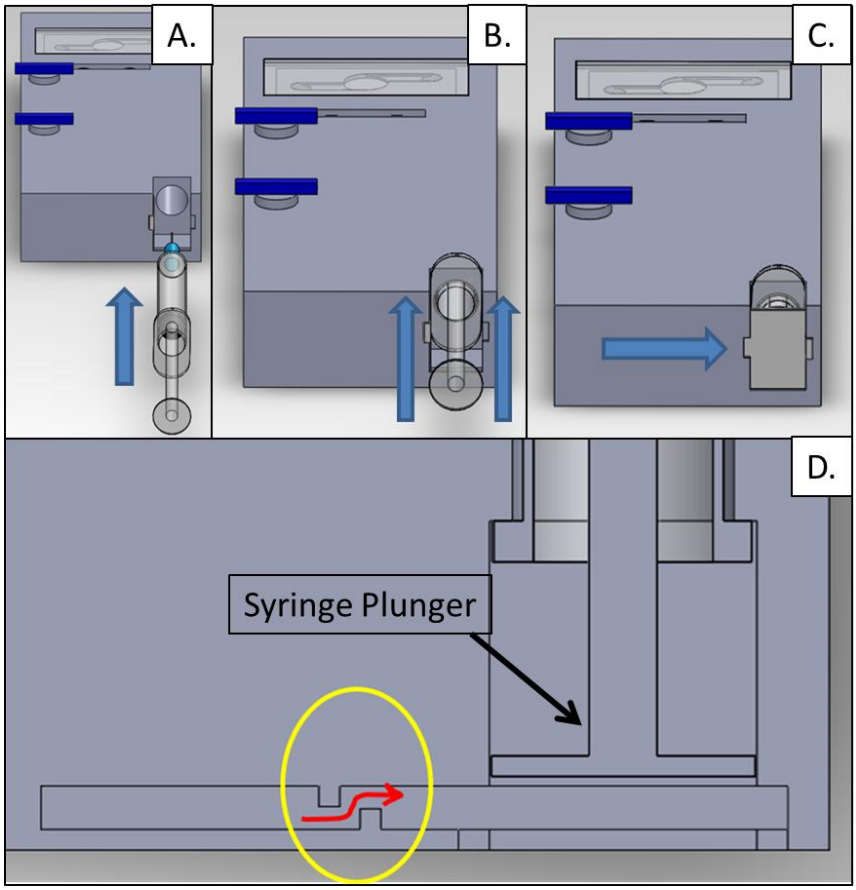

Figure 2.17. Locking tab design for hypodermic syringe. (A) The hypodermic syringe is fully inserted into the diagnostic device. (B) Once seated, the syringe plunger is depressed to transfer the sample to the device. (C) After sample transfer has been completed, the locking tab is snapped into place behind the plunger of the syringe – permanently retaining the syringe within the device. (D) The locking tab slot was designed with a tortuous slot so that the tab cannot travel backwards after being locked into place. The design was modeled to accept a 3 mL BD syringe and 25 gauge 5/8 inch hypodermic needle.

First Generation Rapid Diagnostic Device

At the end of the diagnostic platform development process, the elliptical sample processing channel, reagent storage network, and device housing components were integrated together to create the first generation diagnostic device. The first assembly was tested for appropriate functionality to make sure it operated as intended. The evaluation involved filling the device with water and checking for leaks, using a hypodermic syringe

to transfer a hypothetical sample to the reagent storage network for processing, and cycling the pump buttons to validate circulation capabilities. The device performed without any glitches and appeared ready for small batch production. Figure 2.18A and 2.18B (completed assembly), and Figure 2.19A-C (vortex shedding occurring while processing whole blood) show the completed functional prototype design of the first generation diagnostic device. This design was used to perform the limited user evaluation (LUE) described in the following section.

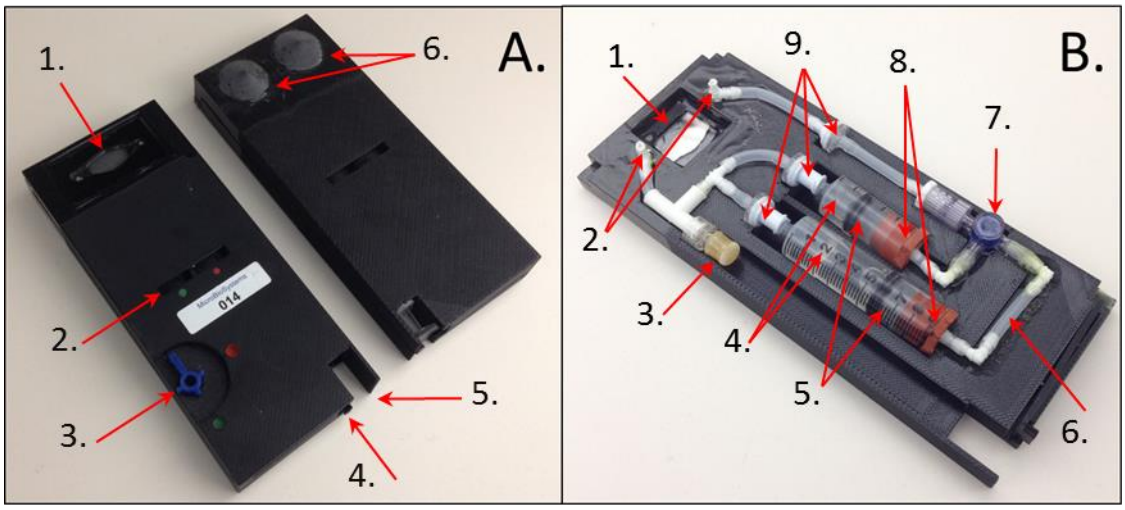

Figure 2.18. Functional prototype of first generation diagnostic. (A) Two prototype assemblies depicting the front (left assembly) and back (right assembly) of the diagnostic device. The components noted in Image A include: The sample processing channel/optical region of interrogation (1), plug visualization windows to indicate reagent exchange (2), the stopcock for selecting stages (3), the locking tab for retaining the hypodermic syringe (4), the syringe port (5), and the sample processing pump buttons (6). (B) Reagent storage network within the diagnostic device – back housing component removed to show internal components. The components noted in Image B include: the back of the sample processing channel (1), the reagent storage network tubing connections for the sample processing channel (2), the hypodermic needle septum (3), the multipurpose reservoirs (4), the plugs that maintain separation between reagents and waste during sample processing (5), the separate stage connections tubing connections to the stopcock (6), the back/bottom of the stopcock (7), the septa sleeves completing the seals of the multipurpose reservoirs (8), and the check valves (9) that directed fluid circulation within the system.

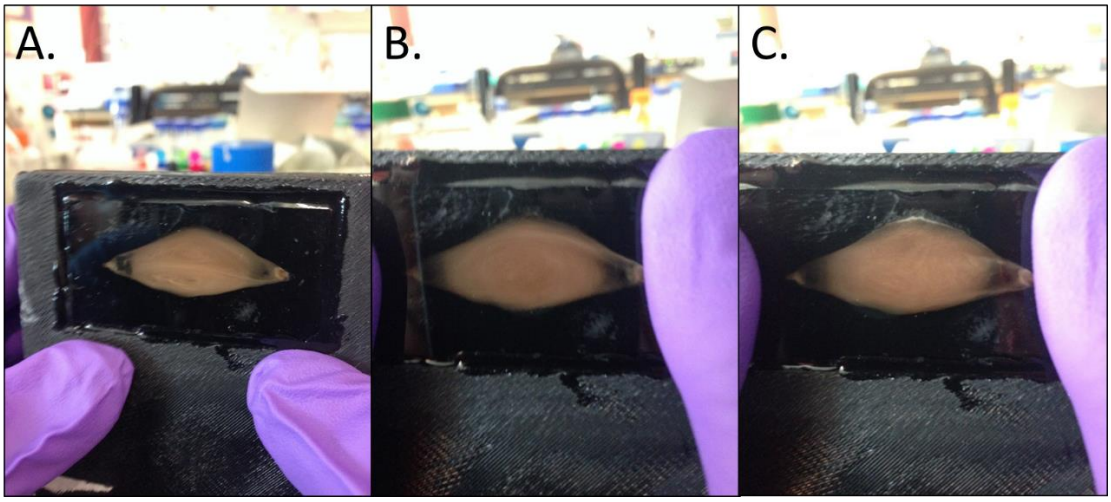

Figure 2.19. Boundary layer separation and vortex formation within the first generation rapid diagnostic device. (A) Symmetrical vortices form within the center of the sample processing channel. Irregular flow patterns occur during the mixing process. (B) A single, large vortex forms within the center of the channel. (C) Turbulent flow without clear vortex formation. The flow patterns were visible because the channel configuration induced cavitation and microbubble formation. Sample that was processed was whole bovine blood supplemented with EDTA.

Limited User Evaluation

A limited user evaluation (LUE) was conducted to assess the ease-of-use and ergonomics of the first generation diagnostic device. Overall, the LUE entailed three phases: 1) preparation, 2) first generation diagnostic device testing, and 3) acquisition of user feedback. Based on observations made during testing and the feedback provided by the evaluation participants, the device was reevaluated for fitness-of-use.

Materials and Methods

In order to prepare for the limited user evaluation, instruction materials were produced alongside a small batch of first generation diagnostic devices. The orientation materials included a user manual and an oral presentation providing guidance on the operation of the diagnostic device. These materials were administered to the evaluation participants one day prior to conducting the actual testing so the participants could ask

questions and become familiar with the operation protocol. The LUE was performed by 5 participants – each provided with 3 first generation diagnostic devices to test. To provide enough diagnostics for testing, a total of 25 diagnostic devices were assembled[2] – the best of which were used in evaluation (Figure 2.20). Participants were provided with full personal protective equipment, bovine whole blood samples to process, 3 mL hypodermic syringes (3x) for collecting and transferring the samples, and a biosafety cabinet in which to perform the device evaluation before testing commenced.

Figure 2.20. Assembly of first generation diagnostic devices for LUE. The 25 diagnostics were assessed for quality by evaluating seal integrity, component alignment, and locking mechanism function prior to final assembly steps.

During testing, participants were provided limited guidance (if unable to recollect protocol steps) and observations were recorded. The evaluation participants were specifically observed to determine if: A) the device functioned as designed; B) actuating

[2] The small batch of first generation diagnostic devices were assembled with the aid of Jonathan Wan, Hannah Curtis, Nico Contreras, and Dr. Walther Ellis.

elements of the device were easily manipulated; and C) if operators knew how to operate the device.

Results

For one of the participants, 3/3 of the diagnostic devices functioned as intended. The other evaluators experienced mixed functional performance among their devices with the primary issue of leak formation during sample transfer. When devices were investigated after testing, it was found that large syringe port tolerances resulted in an opportunity for misalignment of the syringe within the injection port – resulting in compromised seals.

Summary of Limited User Evaluation

Overall, by the end of the LUE, the first generation diagnostic device design was validated for feasibility but required significant modifications to improve ease-of-use. User feedback emphasized four main points: 1) root causes of leak formation needed to be addressed, 2) overall dimensions of the device needed to be reduced, 3) operational complexity required significant simplification, and 4) the design was too complex for production given the number of parts required to produce the prototype. Based on this feedback, the first generation diagnostic design was reevaluated to assess the feasibility for modifying the design to meet the user feedback requirements while conforming to the project design requirements. A simple solution was not readily apparent and, therefore, a design reformulation was determined to be the appropriate following step.

Conclusion

The goal of the first phase of diagnostic development was to produce a first generation diagnostic device that integrated desirable sample processing elements into a handheld platform that satisfied requirements for portability and ease-of-use. The limited user evaluation exposed significant design limitations that would hinder use in resource-limited environments. The form and function of various design components were integrated in such a fashion that the resultant platform demonstrated limited plasticity to accommodate major design modifications. As a result, a new diagnostic platform was required to meet new design specifications obtained after the limited user evaluation. This second generation diagnostic would have to be designed to be modular for sample processing applications and potential future modifications to maintain versatility and mitigate the risk of another complete design reformulation. Table 2.7, below, summarizes the major highlights of the first phase of diagnostic development along with the proficiencies and constraints of the first generation diagnostic device. The second generation diagnostic device design, testing, and evaluation is discussed in Chapter 3.

Table 2.7: First generation diagnostic device development summary	
Overall goal	To develop and produce a rapid diagnostic device to function as a starting point for the diagnostic development project
Device aims	Create easy-to-use diagnostic platform
	Produce a portable, handheld device
	Formulate and confirm design for infectious agent capture
Proficiencies	Microfluidic channels effectively destabilize flow for enhanced mixing
	Successful demonstration of infectious agent capture using *S. aureus* as a model pathogen
	Successfully designed, assembled, and tested diagnostic devices during the limited user evaluation
	Multipurpose reservoirs limited space and part requirements
	Locking mechanism successfully retained hypodermic syringes
Limitations	Diagnostic devices demonstrated variable functional capabilities due to design sensitivities, production variability, and loose tolerances
	Devices were excessively complex for operation and production
	Syringe plunger must be held down (under pressure) to operate the locking mechanism

CHAPTER 3: SECOND GENERATION DIAGNOSTIC

This chapter describes the design of the second generation diagnostic device platform (Figure 3.1). The following sections discuss the design modifications that were made to the sample processing channel, reagent storage network, and device housing with captive syringe port to improve ease-of-use and environmental resilience without compromising screening efficacy. The revised diagnostic platform was evaluated for compliance with the design criteria during military-specification (mil-spec) testing. The chapter concludes with a summary describing the results of the offsite testing and the resulting advantages and limitations of the second generation device.

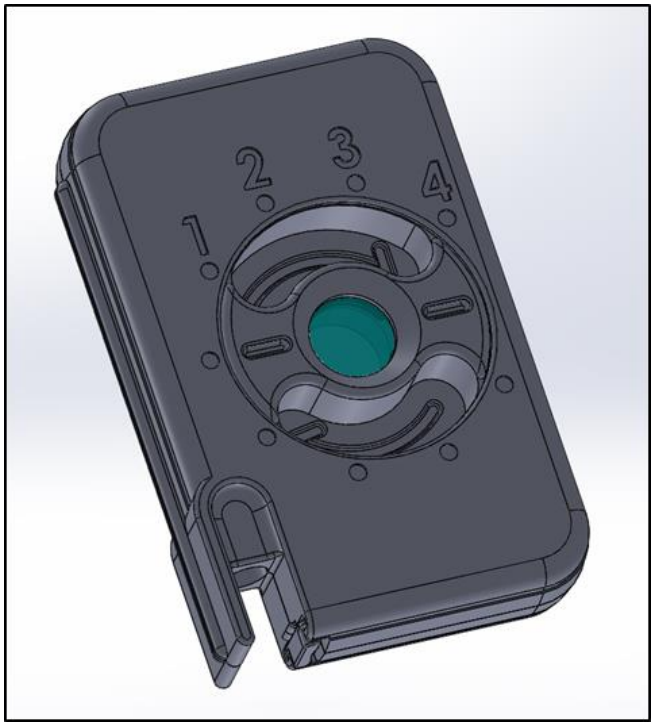

Figure 3.1. Second generation diagnostic device. Computer aided design (CAD) rendering of the second generation device. The design retained the captive syringe port component from the first generation. Remaining platform components were modified to improve ease-of-use and facilitate the simulation of slug flow for sample screening. The dimensions of the device are 138 mm X 85 mm X 26 mm (length X width X height).

Phase II Objectives

The primary objectives for the second phase of diagnostic development were to reformulate the first generation design to accommodate the limited user evaluation design criteria and produce a device capable of withstanding harsh environmental conditions. Based on user evaluation of the first generation device, the revised design criteria (Table 3.1) entailed: 1) making the platform more compact, 2) improving operational simplicity, and 3) limiting design complexity for improved manufacturability. The first generation diagnostic was not easily modified to meet the new design requirements and was therefore abandoned almost entirely. The captive syringe port was the only concept that was preserved from the original configuration. New concepts for sample processing and reagent storage were investigated to develop the second generation diagnostic platform. Designs progressed through stages of conceptual modeling, prototype testing, revision, and small batch production for evaluation. By the end of the second phase of the project, the second generation diagnostic device was substantially different from its predecessor and demonstrated a unique set of strengths and sensitivities.

Table 3.1: Phase II objectives	
1	Make platform more compact
2	Improve ease-of-use
3	Minimize design complexity

Diagnostic Device Design

Based on the feedback from the limited user evaluation, the diagnostic device required substantial simplification to be suitable for use in resource-limited settings

(RLSs). The sample processing channel and reagent storage network designs of the first generation diagnostic dictated operational complexity and limited ease-of-use. As a result, these components needed to be replaced with designs capable of automating a greater portion of the assay. After redesigning the sample processing channel and reagent storage network for the second generation diagnostic, the housing and captive syringe port were adapted to accommodate the new designs and protect the device under adverse conditions. Table 3.2 outlines the platform requirements for the second generation design.

Table 3.2: Platform operational requirements	
Configuration	
1	Accommodate 3 mL hypodermic syringe
2	Store all reagents within hermetically sealed device
3	Facilitate multiple passage sample processing for pathogen capture, labeling, and preparation for optical interrogation
4	Store processed sample, dye-conjugate, and wash solutions within waste reservoirs
Screening	
1	Lyse blood sample to release intracellular pathogens
2	Separate pathogens from sample matrix via capture substrates
3	Label bound pathogens with fluorescent marker
4	Rinse unbound sample and reagent residues from optical region of interrogation

Prototype Sample Processing Channel Configurations

A literature review was conducted to evaluate potential fluid transport schemes that would facilitate sample processing while remaining compliant with the project requirements for optimized infectious agent capture. An attractive alternative to boundary layer separation and vortex formation was to design the diagnostic platform around a sample processing channel that simulated slug flow. Slug flow is a passive form of

multiphase fluid transport driven by differential fluid densities that result in slugs of liquid separated by gas bubbles. The flow regime is characterized by enhanced mixing within the liquid slugs and optimized mass transport through the thin fluid film formed between the gas pockets and channel walls [80-87]. This method for enhanced sample processing was not subject to the limitations of the previous design and could process large sample volumes under variable conditions with reproducible results. Two prototype sample processing channel configurations were developed to simulate slug flow and assessed for compatibility with the project design criteria.

Pump-Driven Slug Flow

The first concept design for the sample processing channel employed a pump to circulate air through a fluid-filled vessel to simulate slug flow and produce a bubble train (Figure 3.2). The circulatory network of the design included a fluid reservoir (modeling the sample processing channel) connected to a check valve, pump button, another check valve, and small diameter tubing connected back to the inlet of fluid reservoir to create a closed-loop system. When held upright, pressing the pump button would circulate gas through the system – creating a bubble train within the fluid reservoir. When held upside down, pressing the pump button would circulate fluid – emptying the reservoir.

Figure 3.2. Image of early slug flow system in operation. This closed system design reliably generates bubble trains by circulating air through liquid trapped within a reservoir. The reservoir may be replaced with any sample processing channel configuration desired. Scaling the design to accommodate the various sample processing steps required for the device overcomplicated the system.

The system was advantageous because it could be easily adapted to produce a slug flow bubble train within the sample processing channel and a single pump button performed both sample processing and reagent circulation. The pump-driven flow would also allow the gap distance between quartz windows to be minimized since forced convection (rather than passive flow) would not be at risk of plug formation. While the design demonstrated proof of concept, it had limitations that negatively impacted production feasibility and fitness-for-use. The main limitation was extrapolating the prototype design concept to the full diagnostic device system – requiring the exchange of multiple reagents throughout the stages of sample processing. The design would likely exhibit the same drawbacks as the first generation platform associated with complex

production and operation. Accordingly, the pump-driven slug flow design was eliminated from consideration for the second generation diagnostic device.

Gravity-Driven Slug Flow

The second concept design for simulating slug flow utilized gravity and channel inversion to drive flow and yield the desired flow regime (Figure 3.3). The prototype was composed of two quartz slides separated by a rubber gasket with interior channel dimensions of approximately 70 x 15 x 2.5 mm (length x width x height). The rubber gasket was permanently mounted to the base quartz slide with cyanoacrylate adhesive while a capture ligand-coated top slide completed the channel seal through a combination of surface tension and compressive forces. This prototype made it possible to evaluate the ability of heparan sulfate and lignosulfonic acid surface coatings to capture a broad spectrum of infectious agents (and virus surrogates) under slug flow conditions.

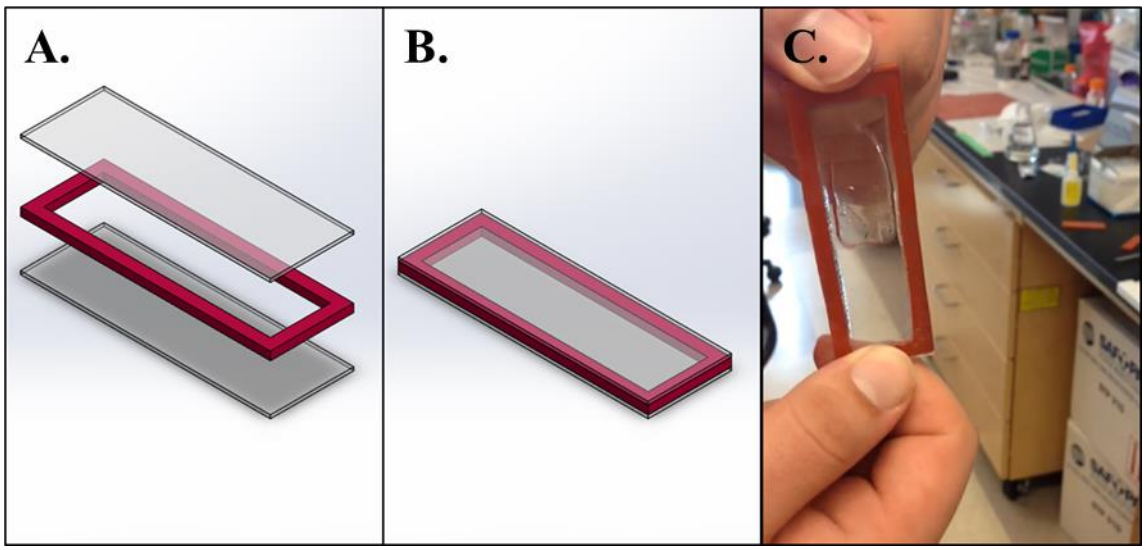

Figure 3.3. Second generation sample processing channel prototype. The prototype simulated slug flow in order to enhance sample exposure to functionalized surfaces within the channel. This was achieved through the formation of thin liquid films between the rising bubble and boundaries of the channel. The rising bubble also generated trailing vortices for increased mixing. (A) Exploded view of sample processing channel prototype (B) illustrating the two quartz slides and gasket. (C) Demonstration of simulated slug flow.

The advantage of the gravity-driven slug flow design was low complexity and an improved scalability for processing multiple reagents. The use of passive convection also presented a few design challenges for the system. Without forced convection, the hydraulic cross-sections of channels within the device would have limitations for minimization. This resulted in an increased gap distance between the quartz windows to prevent fluid viscosity and surface tension from plugging the channel. The passive induction of simulated slug flow would also require a more complicated reagent storage network design that would store sample screening reagents, facilitate reagent exchange, and store waste products without the use of a pump mechanism. Before proceeding with the development of the second generation diagnostic platform, the sample processing channel required validation.

Staphylococcus aureus was the first infectious agent used to evaluate capture efficiency of the prototype sample processing channel. Under simulated slug flow, the infectious agents clumped together and bound to the surface of the ligand-coated quartz slides (Figure 3.4A). Clumping of the *S. aureus* indicated that the simulated slug flow did not develop excessive wall shear stresses that could impair capture. The test was repeated a second time with aggressive shaking (Figure 3.4B) to determine if shaking had any negative impacts upon infectious agent capture. Shaking disaggregated the *S. aureus* clumps and generated a large volume of bubbles within the channel. While shaking produced a more uniform coating than the simulated slug flow, high shear stresses stripped otherwise captured infectious agents from the quartz surface. When processing samples with lower microbial loads, the high shear stresses could impair infectious agent contact with the ligand-coated surface. The bubbles also posed an issue if they became trapped within the optical region of interrogation (ROI) where they would negatively impact

fluorescence-based measurements. Based on these preliminary observations, simulated slug flow appeared to be suitable for enhancing infectious agent capture as long as shaking could be minimized. While brainstorming concepts for developing a diagnostic platform around the new sample processing channel prototype, the prototype was tested for broad spectrum infectious agent capture capabilities.

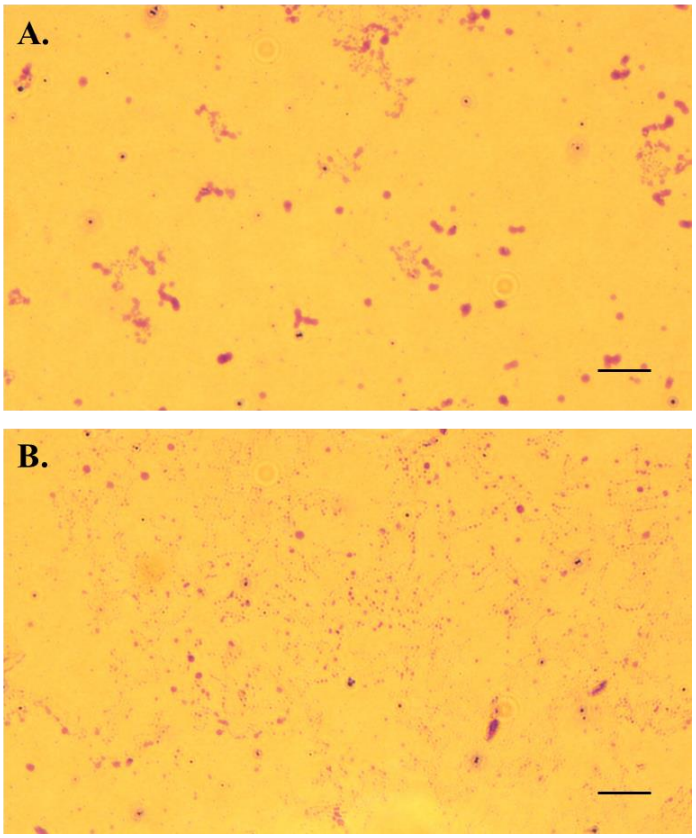

Figure 3.4. Validation of infectious agent capture using new channel geometry. (A) Simulated slug flow. (B) Sample shaking. Scale bars are 10 µm long.

Following the preliminary *S. aureus* capture tests, the second generation sample processing channel was used to confirm the versatility of the ligand-coated quartz surfaces for capturing more diverse infectious agents including viruses, bacteria, and parasites

(Table 3.2)[3]. Confirmation of diverse infectious agent capture suggested that a diagnostic device with flow conditions similar to the prototype channel should also be effective. Accordingly, the next step in the diagnostic development process was to design a device platform compatible with the new flow regime.

Table 3.3. Infectious agents and surrogates captured with slug flow prototype channel	
1	HIV - I (VLPs*)
2	HTLV - I (VLPs*)
3	Hepatitis B virus (VLPs*)
4	Hepatitis C virus (VLPs*)
5	HPrPsc (recombinant human scrapie-like prions)
6	MRSA (clinical strain)
7	VRE (clinical strain)
8	*Enterobacter aerogenes*
9	*Streptococcus pneumoniae*
10	*Neisseria gonorrhoeae* (clinical strain)
11	*Neisseria meningitidis* (clinical strain)
12	*Cryptococcus neoformans*
13	*Chlamydia trachomatis*
14	*Babesia microti*
15	*Leishmania donovani* and *braziliensis*
16	*Treponema phagedenis*
17	*Plasmodium falciparum*
18	*Plasmodium vivax*

*VLP: virus-like-particle

Prototype Device Platforms

Two conceptual designs were formulated for the new diagnostic platform based on different operational methodologies compatible with the new sample processing flow

[3] The experiments investigating infectious agent/surrogate capture using the prototype sample processing channel (listed in Table 3.2) were performed by Nico Contreras, Hannah Curtis, Niki Lajevardi-Kosh, and Jonathan Wan.

regime. These concepts were assessed for production feasibility and fitness-for-use to determine which design was ideal for the final device. One of the main goals of the diagnostic redesign was to simplify device complexity. After a simplified platform was designed, other design goals could then be pursued without risk of having to make substantial revisions to the device structure or layout. A major obstacle that impaired design adaptability for the first generation diagnostic was the use of off-the-shelf parts. As a result, the new platform designs were entirely custom with the exception of the quartz windows.

Thumbwheel-Based Platform

The first concept design sought to develop slug flow through the use of paired reservoir sets positioned radially around and connected to a central sample processing channel via an elastomeric reagent storage network. The main design challenges for this configuration was developing a method for selecting between the paired reservoir sets while progressing through the multiple stages of sample processing, maintaining a hermetically sealed system, and producing prototype platforms with this configuration. For this configuration, a thumbwheel would be used to independently open selected reservoir sets while isolating the other compartments of the system through compression.

The design assembly for the thumbwheel-based device platform was composed of a total of seven parts – only two of which moved (Figure 3.5). The self-contained reagents were stored in reservoirs located radially around a central, miniature channel used to capture, label, and wash infectious agents. The reagent storage network and sample processing channel were designed as a single, continuous part where reservoirs were connected to the miniature sample processing channel with collapsible lumen. Reservoirs

would be sequentially selected for sample processing using a thumbwheel that functioned similarly to a pinch valve. The thumbwheel was designed to selectively allow the lumen of paired reservoir sets to open while compressing and occluding the lumen of the remaining reservoirs based on the alignment of two notches cut into the underside of the component. A ratchet arm and complimentary saw-tooth ratchet groove were radially incorporated into the thumbwheel to aid operators using the device to select progressive stages for screening samples. The ratchet design provided tactile feedback to the device operator as they progressed through the various stages of sample processing and prevented unintentional regression to a previous stage.

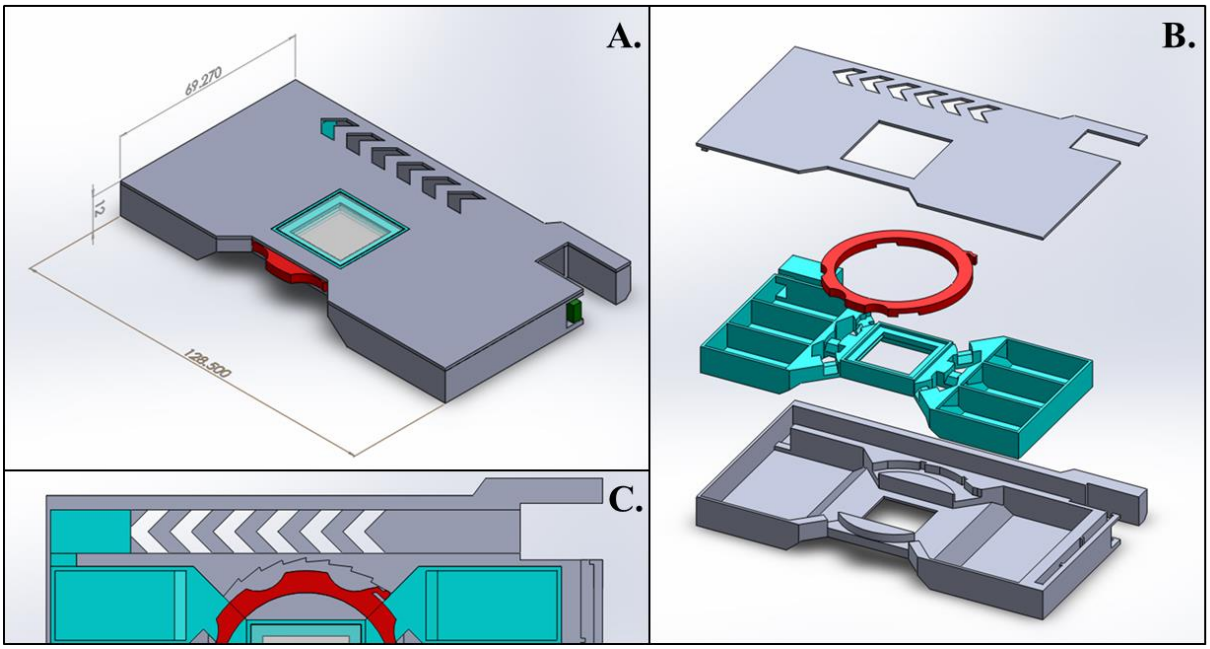

Figure 3.5. Thumbwheel platform prototype CAD. (A) The platform was significantly smaller in size than the first generation diagnostic with dimensions 128.5 mm X 69.27 mm X 12 mm (length X width X height). (B) An exploded view of the assembly illustrates the top and bottom device housing components, elastomeric reagent storage system, and thumbwheel for selecting the stages of sample processing. (C) A ratchet was built into the thumbwheel so that operators could not regress to previous stages.

The thumbwheel-based design demonstrated advantages and potentially significant limitations/obstacles. The advantages included only two moving parts in the device

assembly, which led to a significantly easier device to operate compared to the first generation. Limitations and design obstacles included dimensional constraints, risks of impaired function due to stress relaxation after prolonged channel compression during storage, multiple inlets and outlets surrounding the miniature channel may impair the removal of unbound sample and reagent residues from the optical ROI, and molding of the reagent storage network. A significant amount of design effort would have to be invested to successfully interface the compression fit and function of the thumbwheel. Preliminary design prototypes were produced and assessed for feasibility (Figure 3.6) which confirmed these concerns regarding thumbwheel ergonomics and compression capabilities. Additionally, only 3 paired reservoir sets could fit within the compact handheld device due to the spacing requirements for selectively opening and closing the reservoirs – four sets were necessary for efficient sample processing.

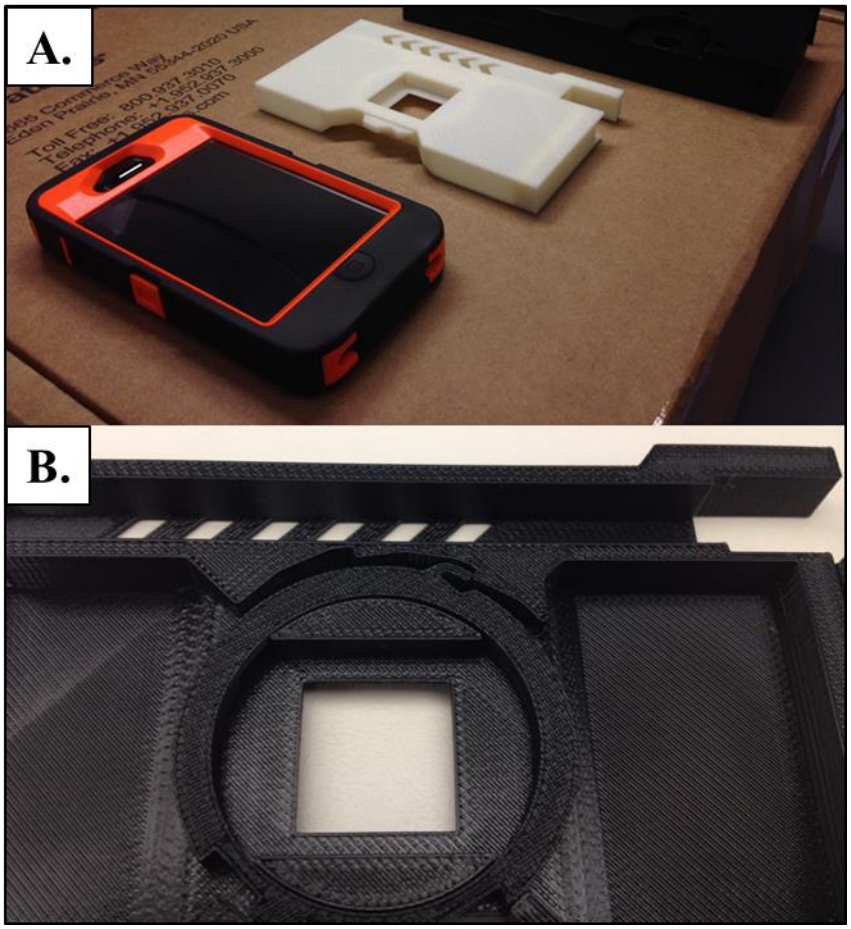

Figure 3.6. Preliminary thumbwheel-based platform prototype. (A) Dimensional comparison relative to smartphone. (B) Radial ratchet mechanism for stepwise sample screening stage selection.

The first reagent storage network produced was cast in urethane (Figure 3.7). The lumen connecting the paired reservoir sets to the sample processing channel were difficult to compress due to the material stiffness, narrow lumen, and thick lumen walls (2 mm). Based on these issues the overall dimensions of the prototype were increased, a softer silicone elastomer was selected for the reagent storage network, and the thumbwheel was modified into a compression ring that the operator could actuate using an axial interface rather than radial thumb grooves (Figure 3.8).

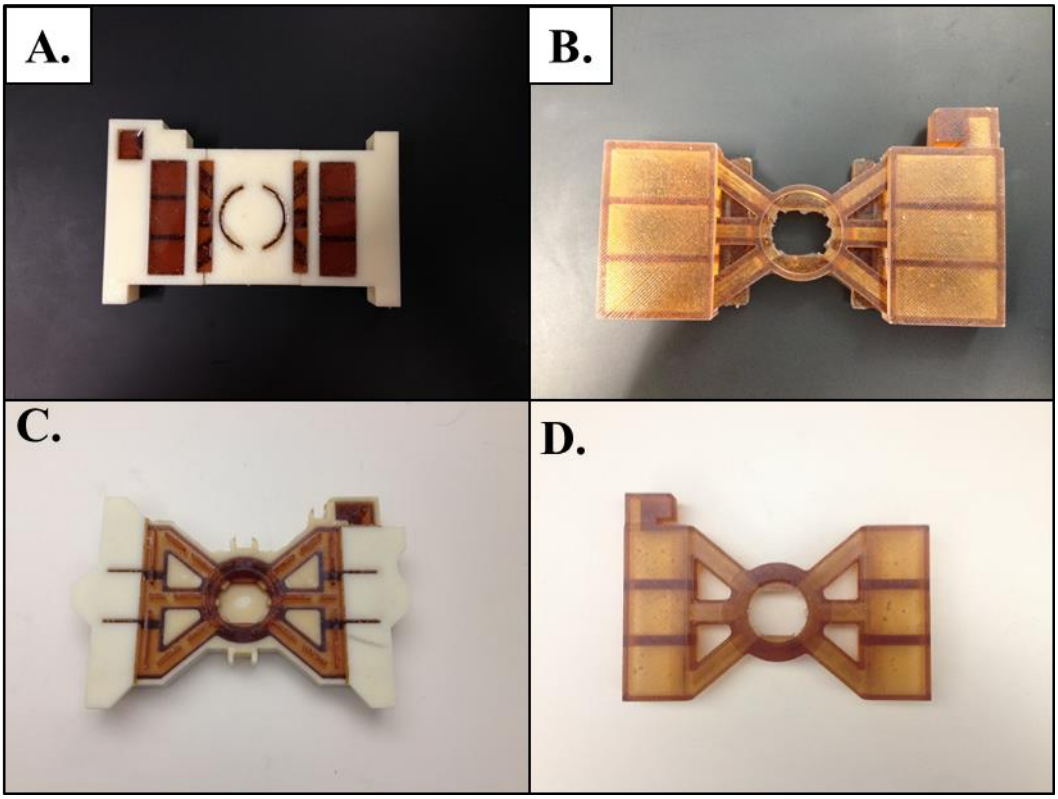

Figure 3.7. First and second generation reagent storage network components for thumbwheel-based platform. (A) Full mold assembly used to cast reagent storage network in urethane elastomer (60 Shore A). (B) Demolding reagent storage network component. (C and D) Second generation design and molding components improved part quality for more reliable evaluations.

The modified design continued to pose compression-based design obstacles after the walls of the lumen were made thinner (1.5 mm), separated further apart with wider lumen dimensions, and produced in a less stiff silicone (40 Shore A). After inspecting the prototype and assessing options for modification, it was determined that the reagent storage network lumen would have to be produced as flat tubing to make the design work. The flat channels would be easy to compress, facilitate thumbwheel rotation, and passively open when appropriately aligned with the thumbwheel by the weight of the reagent solution stored in the reservoir. Although the concept had potential, production would be exceedingly difficult. The technical and design obstacles for creating such a reagent storage network deterred continued development and led to the next logical platform design.

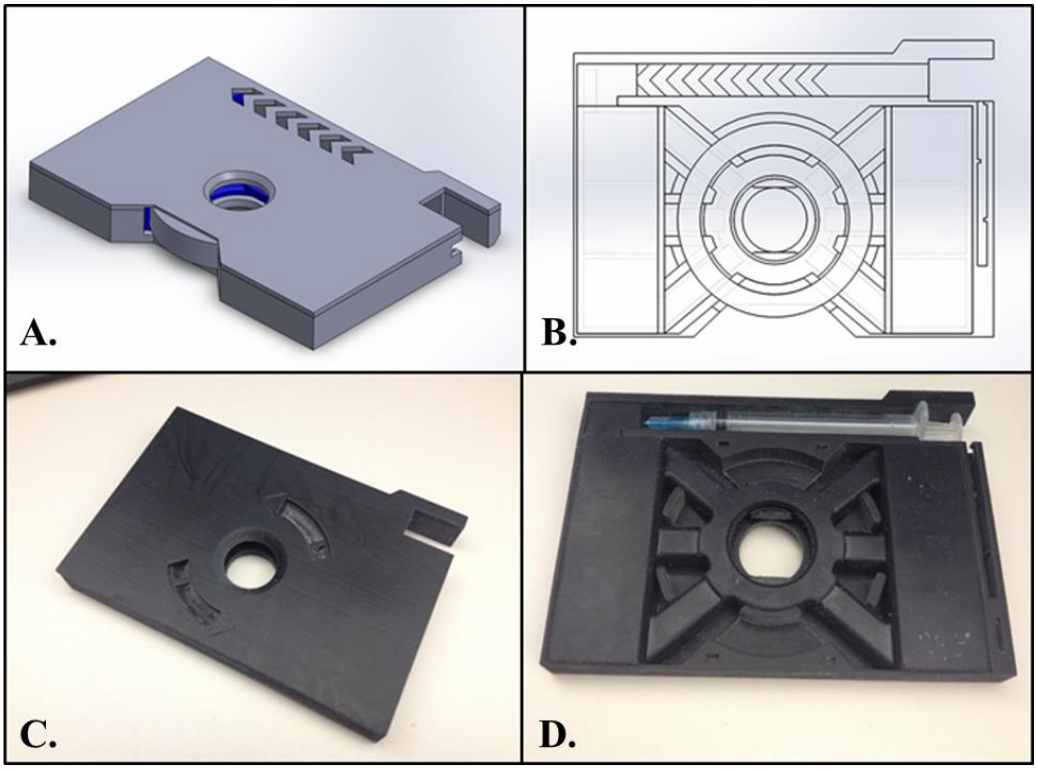

Figure 3.8. Second thumbwheel-based diagnostic prototype iteration. (A and B) The thumbwheel-based platform was modified to account for compression limitations noted in the first prototype. Concern over achieving adequate compression without compromising ease-of-use associated with frictional resistance led to the development of an intermediate prototype (C and D) that transitioned from the thumbwheel-based platform to the dial-based platform.

Dial-Based Platform

The dial-based design concept was very similar to the thumbwheel design according to the platform layout of the reagent storage network. The main difference, however, was that the sample processing channel was made as an independent component. The dial-based design concept (Figure 3.9) consisted of nine parts in total that composed the main assembly (the diagnostic device) and a subassembly (the dial of the device). The dial was intended to be used similarly to the thumbwheel of the alternative design except the compression channels linking the reservoirs to the central, miniature channel were eliminated and replaced with radial seals at the dial-reagent storage network interface. The

ratchet component of the design was also significantly different from the alternative platform as it was relocated to the base of the device but ultimately served the same purpose.

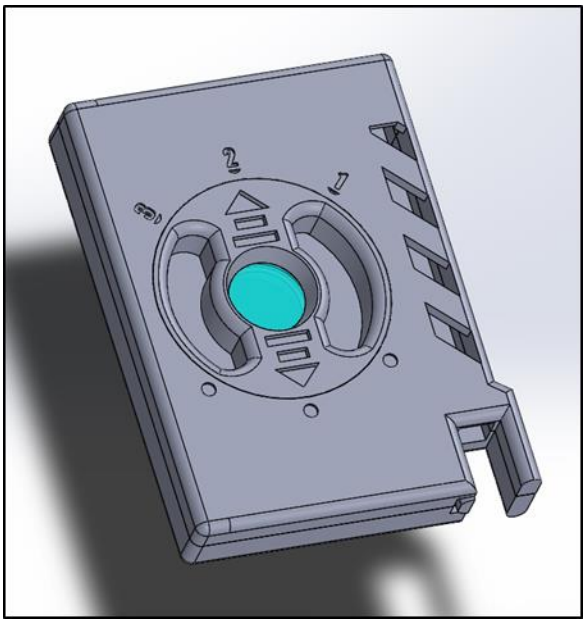

Figure 3.9. CAD rendering of preliminary dial-based platform prototype.

The dial-based design demonstrated advantages and potential limitations for production and efficacy. The advantages of the design included greater dimensional freedom, a more modular design, and reduced functional complexity. The greatest potential limitation of the design was the design of the dial-reagent storage network sealing interface. Preliminary design prototypes confirmed design feasibility and fitness-for-use (Figure 3.10). The semi-static dial seal was a complex component of the design that would require incremental iterations of development to achieve functional requirements, but offered greater simplicity and ergonomics than the thumbwheel-based design. Thus, the dial-based design was selected for the second generation diagnostic platform and continued development.

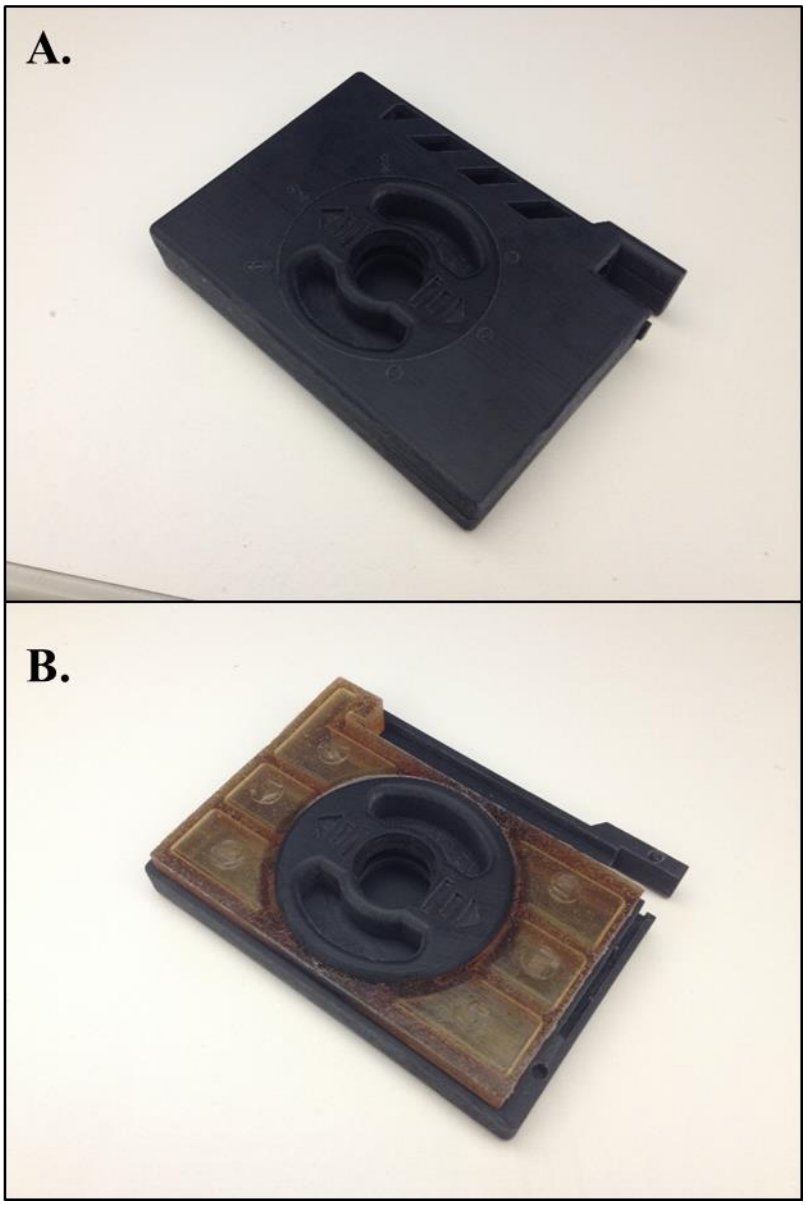

Figure 3.10. First physical prototype of dial-based diagnostic platform. (A) Full assembly minus the quartz windows. (B) Assembly without top housing component – depicting dial interface with reagent storage network. The first prototype was used to evaluate form, fit, and ergonomic operation.

Second Generation Diagnostic Device

The second generation diagnostic device (Figure 3.11) utilized the dial-based platform configuration. This configuration was divided into three fundamental elements

including the dial subassembly, reagent storage network, and device housing to aid in the development process.

Figure 3.11. Second generation diagnostic device platform. (From left to right) CNC machined ABS, CNC machined aluminum, and SLS glass-filled nylon second generation diagnostic device prototypes.

Dial Subassembly

The dial subassembly of the second generation diagnostic device was composed of three main design elements including the sample processing channel, ratchet, and the dial itself (Figure 3.12). The sample processing channel was designed to reliably generate bubble formation within the ROI to improve sample screening efficiency. The dial was designed to form stable, semi-static radial and axial seals with the reagent storage network and prevent leak formation under harsh operational conditions. The ratchet provided audible and tactile feedback during sample processing stage selection, prevented inadvertent regression to previous stages, and locked the dial into a final position after sample processing was completed.

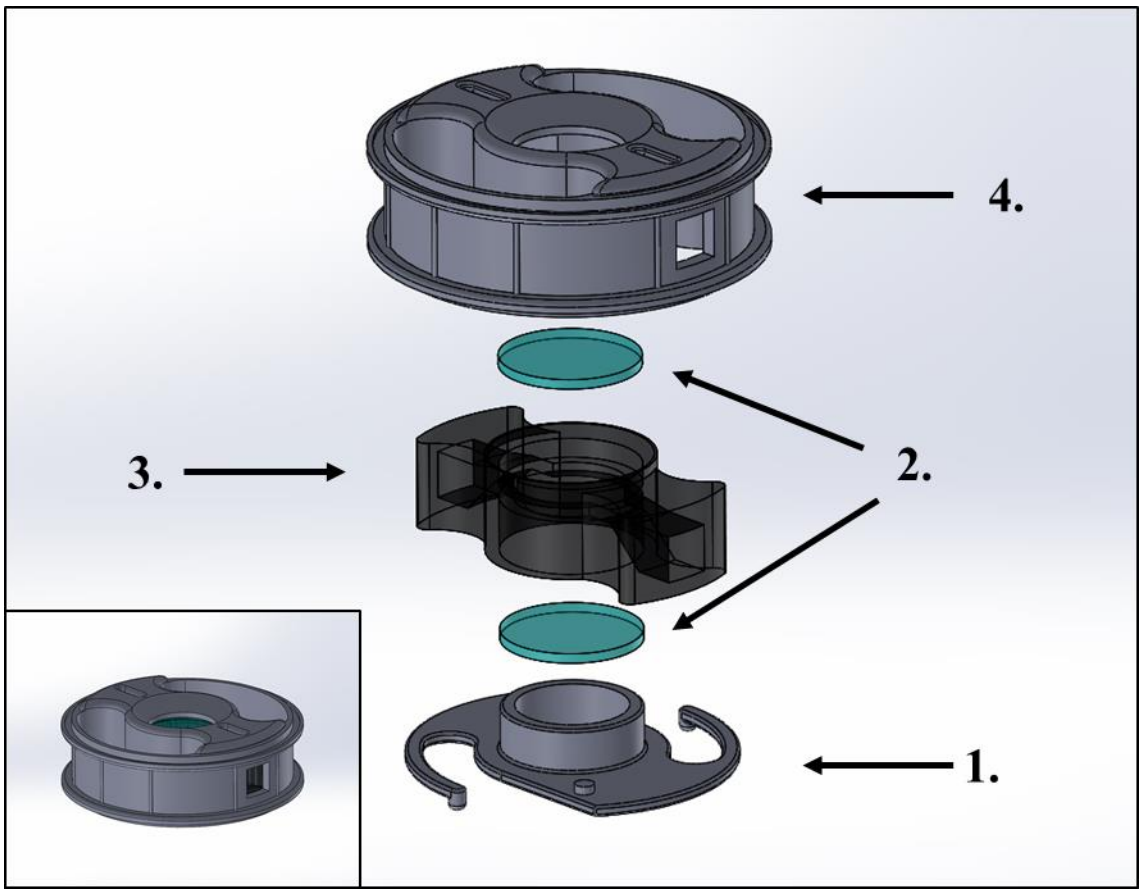

Figure 3.12. Dial subassembly. The dial subassembly was composed of a ratchet (1), two quartz windows (2), an elastomer channel (3), and the dial (4).

The major design obstacle for the second generation sample processing channels was determining the appropriate dimensions of the channel restriction to induce bubble formation. After several design iterations, an appropriate hydraulic cross-section was determined along with a channel geometry to facilitate flow. The flow restrictions immediate before and after the optical region of interrogation were designed with hydraulic cross-sections of 16 mm^2. The channel leading toward the flow restriction began with 64 mm^2 hydraulic cross-section that tapered down to the flow restriction. The taper served to accelerate rising gas and destabilize the liquid/gas interface. The channel rapidly expanded within the ROI and served to decelerate and spread the rising gas – allowing fluid within

the region to converge and collect back at the flow restriction before the next bolus of gas passed through. This oscillating process is repeated until the exchange process completed.

The second generation channels were produced independently of the dial using elastomer resins for modularity and ease of modification. Completely integrating the channel into the dial would have simplified design complexity from a production standpoint, but would also make revisions more costly and time consuming. Urethane was selected mainly for thermal stability and compatibility with a wide range of chemicals and aqueous solutions. The medium durometer urethane casting resins also have low viscosities that help with the molding process – leading to production of higher quality parts without casting under vacuum.

A mold assembly was designed in SolidWorks to cast the second generation sample processing channels (Figure 3.13). The mold components were produced using a stereolithography (SLA) additive manufacturing process with VeroBlackPlus model resin. After production, the mold components were cleaned and coated with a urethane demolding reagent to facilitate casting the sample processing channels. A two-part casting urethane was used in the process and dyed black to limit light scattering during optical interrogation.

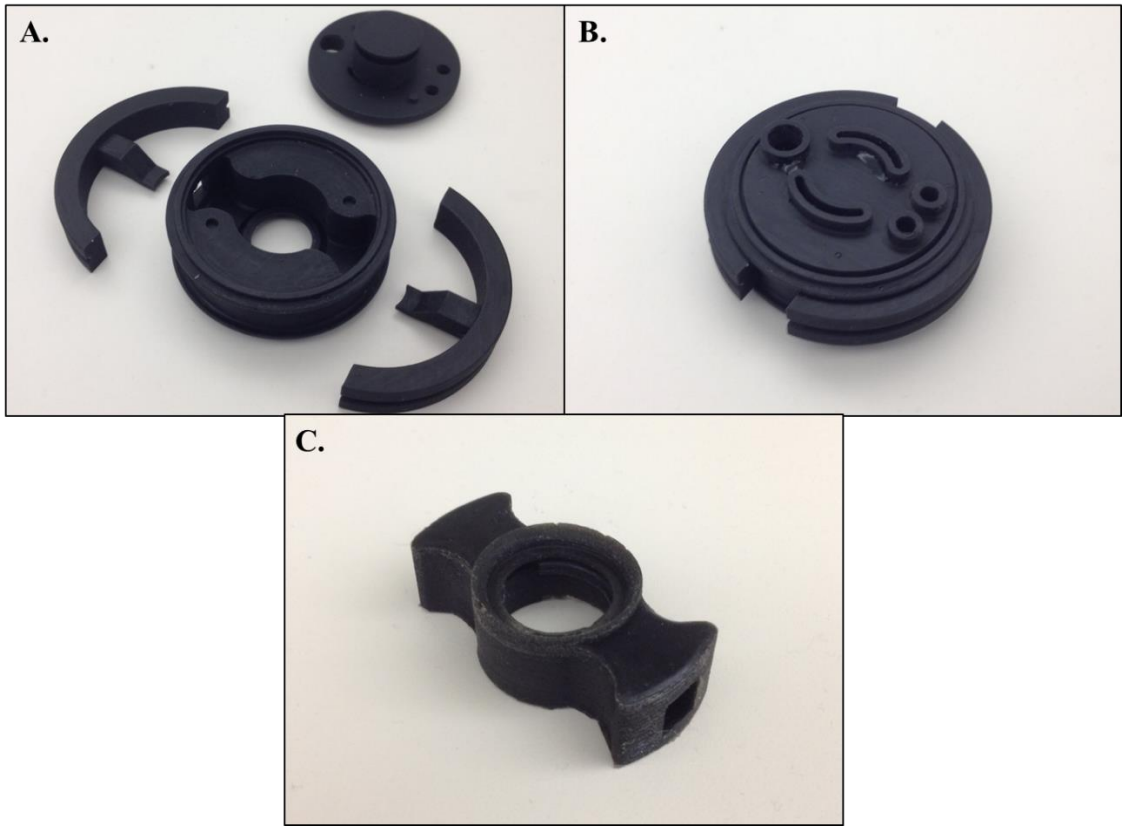

Figure 3.13. Mold assembly for casting sample processing channel. (A) Mold assembly components. (B) Complete mold assembly ready for casting elastomer channel. (C) Elastomer sample processing channel produced from mold.

The major design obstacle for the dial component was developing reliable, semi-static seals at an interface with a large surface area. The seals had to withstand harsh environmental and handling conditions, but could not impede diagnostic operation (i.e. rotating the dial). Two categories of seals were used – radial and axial. Radial seals prevented cross-contamination and fluid migration within the device while axial seals prevent fluid migration from the interior to exterior of the device. Radial seals were achieved by oversizing the diameter of dial relative to the internal cavity of the reagent storage network to induce radial compression generated from 5% stretch of the elastomeric storage network. Pillars were also integrated into the radial face of the dial to reinforce radial seals. Axial seals were achieved with compression rings designed to crimp reagent

storage network gaskets (20% strain) between the top and bottom of the dial and the top and bottom device housing components.

The main design obstacle for the ratchet component of the dial subassembly was developing the ratchet arms to be stiff enough to provide audible and tactile feedback without damaging the ratchet. The stiffness of the ratchet arms could be tailored by modifying the length of the arms and their cross-sectional dimensions. Damage was addressed by modifying the degree of strain the arms were exposed to while traversing the ratchet groove integrated into the base of the device housing. After several iterations of prototypes, an optimal configuration was determined.

The dial and the ratchet were also designed using SolidWorks. The parts were produced out of glass-filled nylon through an additive manufacturing process of selective laser sintering (SLS). The nylon parts were dyed black (DuraForm Ex Black) and sealed (Imprex) with post-processing treatments. The sealant was necessary to make the components watertight and improve their resilience to adverse environmental conditions.

Reagent Storage Network

The reagent storage network of the second generation diagnostic device was designed as a single, elastomeric component that performed a variety of functions within the device (Figure 3.14). These functions included storing the reagents necessary for sample processing and ensuring safe sample transfer. There were multiple benefits to creating the reagent storage network as a single part. Production and operational complexities were substantially reduced, the design became more compact, and the design was much more durable with fewer components that could malfunction.

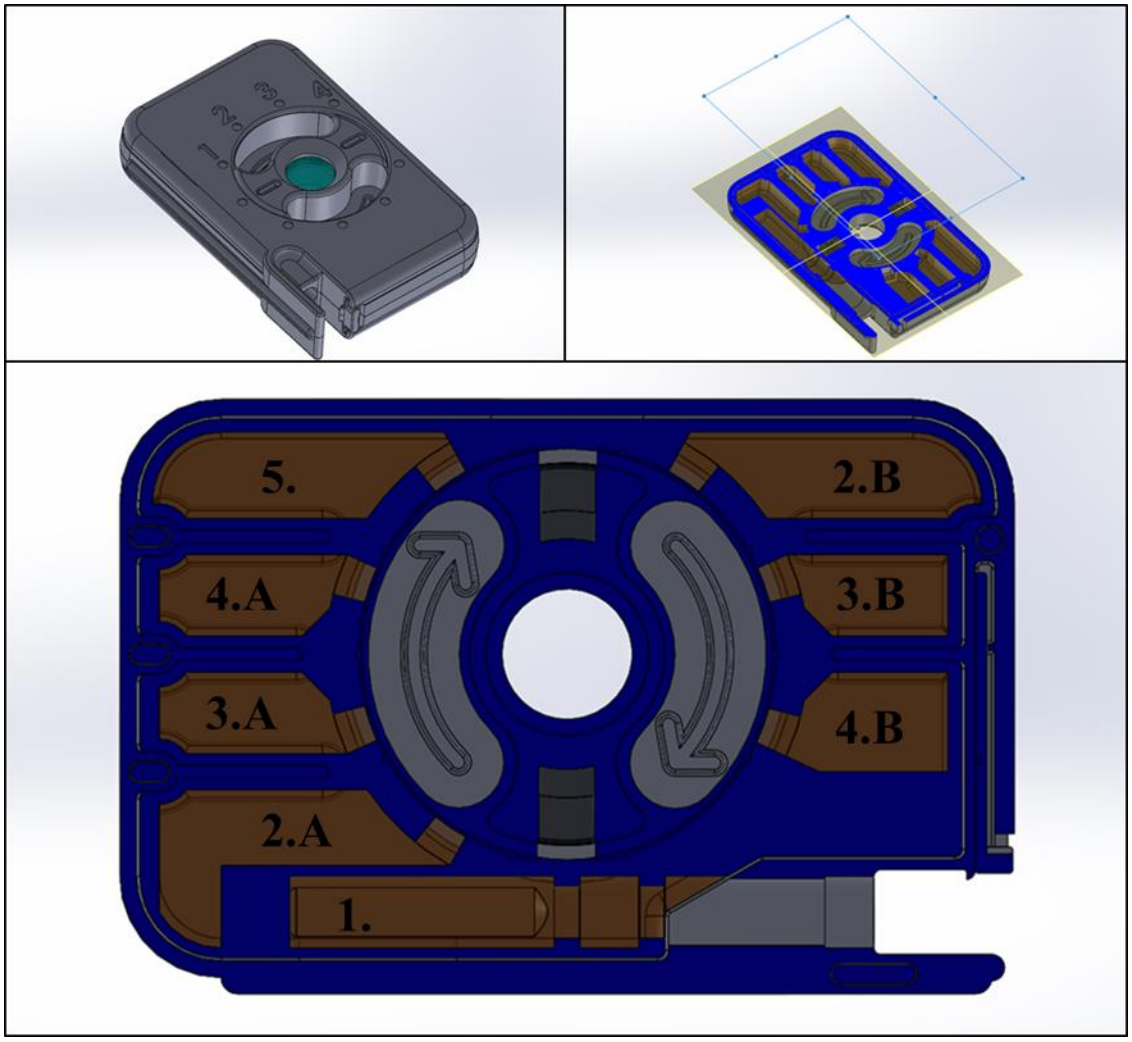

Figure 3.14. Urethane reagent storage network. (1) Syringe port. (2.A) Distilled water reservoir. (2.B) Distilled water/blood waste reservoir. (3.A) Dye-conjugated reagent solution reservoir. (3.B) Dye-conjugated reagent waste reservoir. (4.A) Phosphate buffered saline (PBS) rinse reservoir. (4.b) PBS rinse waste reservoir. (5) PBS solution to flood the optical region of interrogation prior to analysis.

The reagent storage network was composed of seven reservoirs positioned radially around a central cavity designed to interface with the dial assembly. Six of the reservoirs were designed as paired sets – each for a specific stage (1-3) of sample processing. The seventh reservoir (stage 4) did not require a waste reservoir because the solution stored in the reservoir was intended to be transferred to the sample processing channel for optical interrogation. The first and fourth stage reservoirs were designed to hold 5 mL of liquid while the second and third stages held only 3 mL. The larger volumes of reagents were

required to dilute and lyse blood samples (stage 1) and fill the sample processing channel (stage 4) leaving no gas pockets that could interfere with optical measurements. Overall, the reservoir volumetric capacities were made larger than necessary to provide versatility for future generation design optimization.

Features to facilitate radial and axial seals with the dial were designed into the central cavity of the reagent storage network. Radial seals were achieved by under sizing the inner diameter of the cavity relative to the outer diameter of the dial to produce 5% stretch. Axial seals were achieved with gasket ledges integrated to top and bottom of the central cavity – positioned above and below the dial shelves. Offset compression rings located on the dial and device housing were designed to crimp the elastomer with 20% compression.

Based on the septa issues experienced during the limited user evaluation, the septum of the reagent storage network was made thick and with a large surface area to provide a strong seal and mitigate alignment sensitivities. A segment of the syringe port was also integrated into the design with compression collars to seal against the body of the syringe (Figure 3.15). This design provided a redundant safety feature to prevent leak formation should the syringe fail to successfully transfer the sample to the interior of the diagnostic device. The strength of the compression collar seals were tested by inserting a 3 mL syringe (without the hypodermic needle) into the syringe port and ejecting 3 mL of distilled water into the cavity. The design was validated with no visible leak formation.

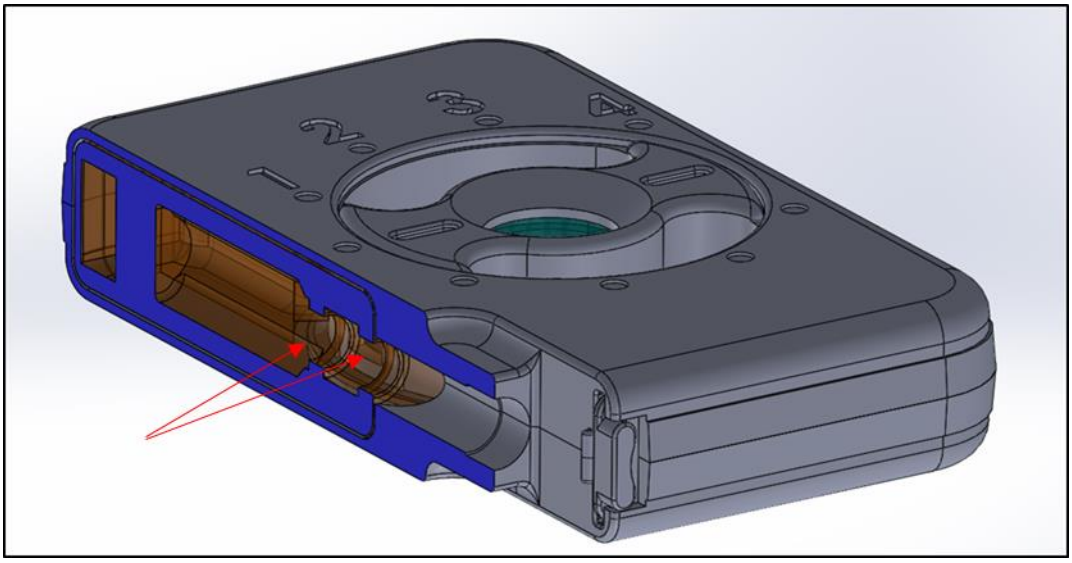

Figure 3.15. Cross-sectional illustration of the syringe port with compression collars. Arrows indicate locations of compression collars.

A complex mold was designed in SolidWorks to cast the reagent storage network components in a medium durometer urethane elastomer (Figure 3.16). The mold components were produced similarly to the sample processing channel molds. The main difference, from a production standpoint, was that elastomer components were not dyed black since they did not reside within the optical ROI of the device.

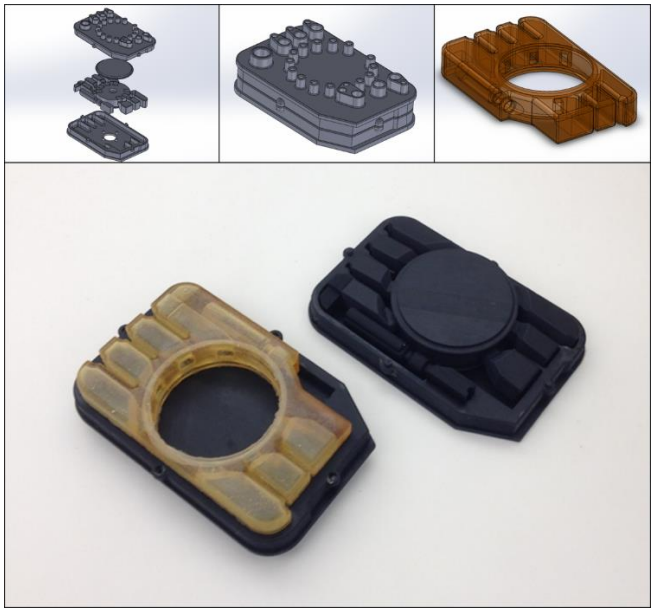

Figure 3.16. Mold assembly for reagent storage network.

Device Housing

The housing was designed to protect the device from harsh conditions in an ergonomic, handheld platform. The housing included a variety of design elements (Figure 3.17) integral to device operation, as well. These elements included a ratchet groove system for stage selection during sample processing, the captive syringe port and locking tab, and compression rings to complete the axial seals between the reagent storage network and dial subassembly. The housing of the device was symmetrically divided into top and bottom components that fit together with alignment pins. This particular structural format was selected so that uniform compression could be generated for axial seals during device assembly. If the housing components were divided into a lid and enclosure, the lid would not be stiff enough. The housing components and locking tab were designed in SolidWorks and produced in glass-filled nylon through the SLS process similarly to the dial and ratchet.

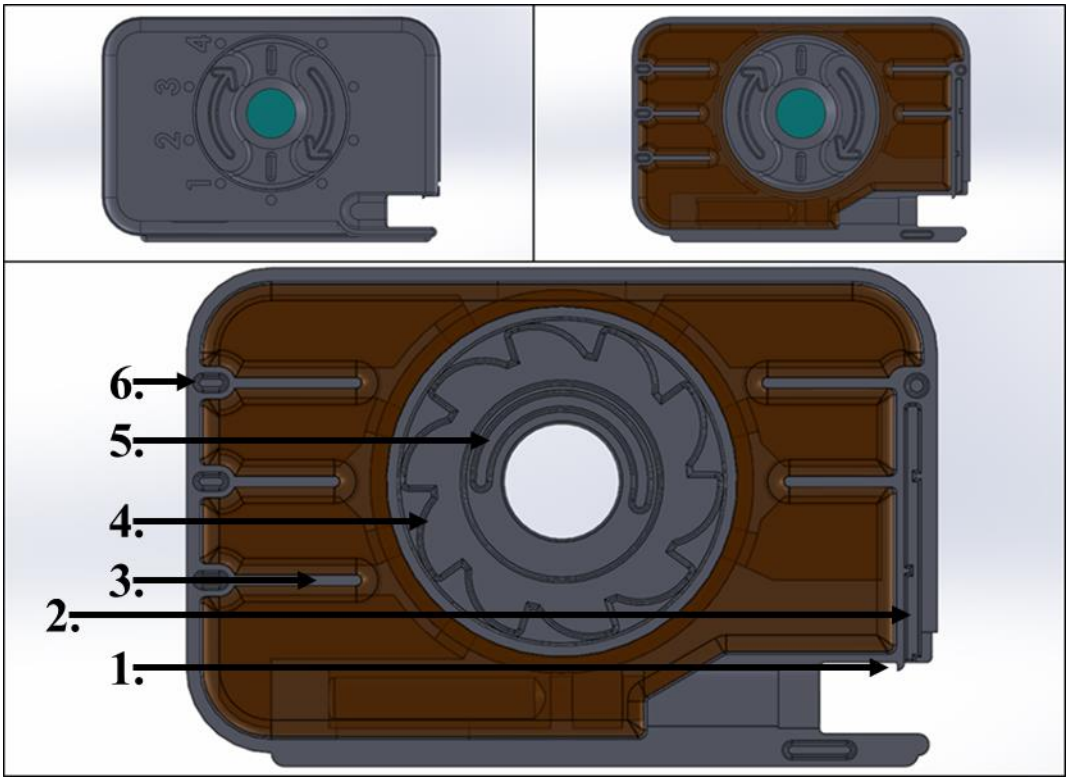

Figure 3.17. CAD rendering of diagnostic device illustrating device housing features. (1) Syringe plunger retaining shelf. (2) Locking tab slot. (3) One of the five reagent storage network dividers. (4) Ratchet arm groove. (5) Semi-circular slot to lock dial into final position after sample processing. (6) One of four alignment pins to help mate top and bottom housing components together.

Diagnostic Device Operation

The blood screening protocol for the second generation diagnostic device (Table 3.4) was substantially different from the first generation due to the reconfigured platform design. The protocol for processing a whole blood sample included a total of 10 steps divided among four stages. The role of the first stage was to lyse and dilute the whole blood sample before concentrating infectious agents upon the functionalized surfaces of the sample processing channel. The second stage labeled any bound infectious agents with dye-conjugated ligands while the third stage washed away unbound sample and reagent residues. The fourth stage of the sample processing procedure filled the sample processing

channel with phosphate buffered saline to improve optical interrogation efficiency. The protocol required less than ten minutes to complete.

Table 3.4: Second generation diagnostic operation		
Stage	Step	Process
1	1	The dial is rotated to the first stage position
	2	Holding the device upside down, the sample is transferred to the device.
	3	Locking tab is closed behind hypodermic syringe.
	4	The lysed/diluted sample is reciprocally washed across the sample processing channel (25x) by inverting the device followed with a gentle shake to induce bubbling.
2	5	Holding the device upright, fluids drain into a waste reservoir and the dial is rotated to the second stage position.
	6	The dye-conjugate solution is reciprocally washed across the sample processing channel (25x) following the same inversion and shake procedure performed for the first stage of processing.
3	7	Holding the device upright, fluids drain into a waste reservoir and the dial is rotated to the third stage position.
	8	The wash solution is reciprocally washed across the sample processing channel (25x) following the same inversion and shake procedure performed for the first two stages of processing.
4	9	Holding the device upright, fluids drain into a waste reservoir and the dial is rotated to the fourth stage position.
	10	After the fluid from the fourth stage reservoir fills the sample processing channel, the dial is turned to its final (horizontal) position and automatically locked in place. The device may now be interfaced with the fluorescence-based reader.

The operational protocol was validated for infectious agent capture using a complete second generation diagnostic device to screen a whole blood sample spiked to yield a clinically relevant concentration of *S. aureus* ($ID_{50} = 10^5$ cells/mL [88] where ID_{50}

represents the infectious dose required to infect 50% of experimental subjects). After the first stage of sample processing, the quartz windows from the optical ROI were extracted from the device, stained with crystal violet, and inspected using brightfield microscopy (Figure 3.18).

Figure 3.18. *S. aureus* capture with second generation diagnostic. Scale bar is 10μm long

Evaluation

Enhanced Limit of Detection: Pilot Particle Study

The pilot particle study was performed to determine if device detection limits could be improved for samples containing low concentrations of infectious agents by supplementing the samples with inert silica microspheres[4]. In theory, the particles should aid in the capture of infectious agents by increasing the effective concentration of the

[4] The pilot particle study was performed with the aid of Hannah Curtis. Hannah cultured the *S. aureus* for testing and assisted with experimental protocol execution.

pathogens within the fluid film formed by the slug flow by displacing fluid within the film. The increased number of particles within the film should also increase energy within the system resulting in more collisions between particles, infectious agents, and functionalized surfaces coated with capture ligands.

Materials and Methods

To evaluate the impact of the silica microspheres on infectious agent capture, serial dilutions of a stock *S. aureus* solution were screened until capture could not be confirmed using brightfield microscopy – establishing a crude limit of detection. At this point, a new sample of the low concentration solution of *S. aureus* was supplemented with silica microspheres and processed to determine if visual confirmation of capture could be regained.

S. aureus was cultured overnight in Luria-Bertani (LB) medium to provide a stock solution of infectious agents for experiments. A Petroff-Hausser counting chamber was used to determine the beginning concentration of *S. aureus* used in the experimental procedure (10^{10} cells/mL) and provide an estimate for the limit of detection using brightfield microscopy. The experiment was conducted by screening a series of samples with lower and lower infectious agent concentrations (10^{-1} dilution/test) until an approximate sample concentration of 10^4 cells/mL (10^{-6} final dilution) was evaluated and could not be visualized under the microscope. At this dilution, 50 µL of glass particles suspended in solution (1.6^{12} particles/mL) with a mean diameter of 1 µm were added to the diluted *S. aureus* sample and the screening process was repeated. Samples were stained for microscopic evaluation using the previously described method. The prepared slides

were then inspected using the oil immersion objective of the brightfield microscope (1,000x).

Results

The addition of silica microspheres to the low concentration *S. aureus* sample restored visual detection of infectious agent capture under the brightfield microscope (Figure 3.19). The result from this study suggests that the limits of detection of the device could potentially be augmented by adding inert particles to the reservoirs of first stage of the sample processing protocol within the diagnostic device.

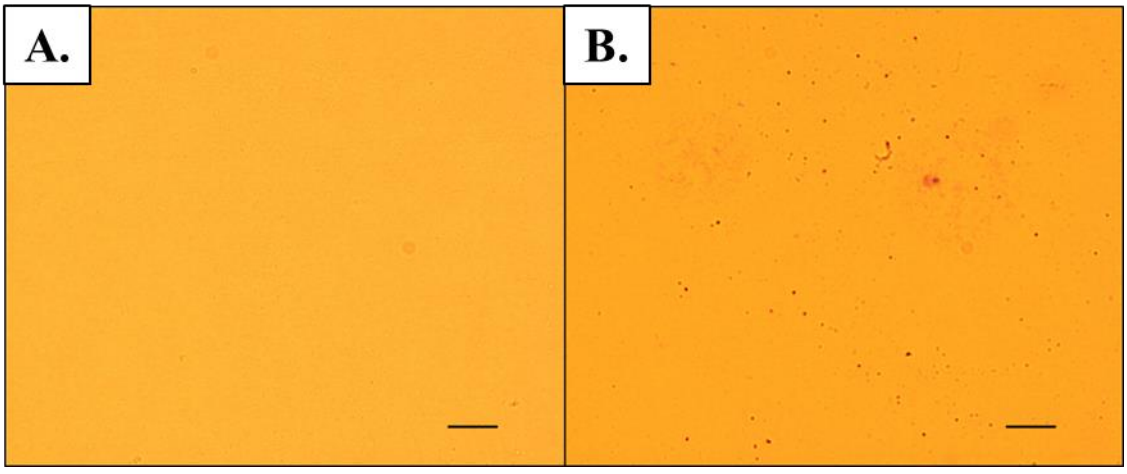

Figure 3.19. Visual confirmation of enhanced limit of detection. (A) Ability to visually confirm capture of *S. aureus* lost after serial dilution of test sample. (B) Restored ability to visually detect capture of *S. aureus* after diluted test sample was supplemented with silica microspheres. Scale bars are 10μm long.

Discussion and Conclusion

More work is required to fully elucidate the advantages and limitations of this possible modification, but the pilot study results were promising. A potential implication beyond enhanced infectious agent capture could be improved residue removal from the optical ROI but would require further testing to evaluate. Potential limitations associated

with the process may result from impurities in the silica microspheres and entrapment within the ROI – potentially increasing noise and impairing the instrument-based limits of detection.

Environmental Resilience Evaluation

A small batch of second generation diagnostic devices were produced for military specification (mil-spec) testing at the United States Army Aeromedical Research Laboratory (USAARL). These tests were conducted to assess the suitability of the diagnostic for use in resource-limited settings through exposure to harsh environmental and handing conditions. Feedback gained from the evaluation would expose design weaknessesand guide future design modifications.

Offsite Testing

For offsite testing, 50 second generation diagnostic device assemblies were produced (Figure 3.20) and shipped to USAARL[5]. To conduct the evaluation, diagnostic devices were exposed to a specific test condition, cycled through the sample screening protocol, and interfaced with their corresponding fluorescence-based reader to simulate field operation. The fourth-stage reservoirs of the reagent storage network were filled with a rhodamine dye solution so that the instrumentation would take an actual reading and confirm successful device function.

[5] Assembly of the 50 diagnostic devices was performed with assistance from Hannah Curtis, Niki Lajevardi-Kosh, Jerrie Fairbanks, Dr. Walther Ellis, and Dr. Linda Powers.

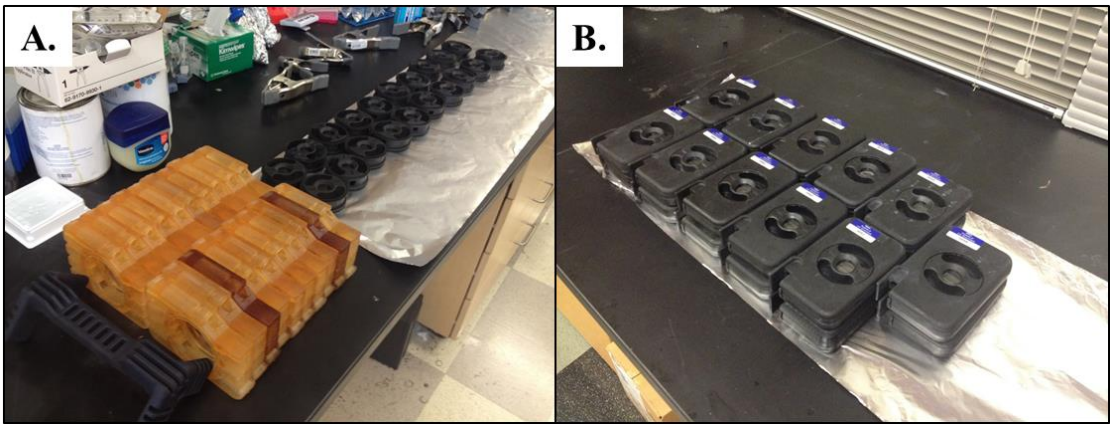

Figure 3.20. Small batch production of second generation diagnostic device. (A) An assembly line process was used to build 50 diagnostic devices for testing where dial sub-assembly were produced first, inserted into the pre-filled reagent storage networks, and sealed with the device housing components. (B) Completed assemblies were inspected for integrity and labeled with part numbers for tracking purposes during testing.

For altitude testing, the diagnostic device must survive pressure fluctuations associated with ascending from 0 to 18,000 ft. (MIL-STD 810G 500.5, Procedure II – Operational) [89]. For temperature testing the diagnostic device must be operational at temperatures ranging from 10 - 40°C, withstand storage at temperatures ranging from -26 – 60°C, and remain functional when exposed to high temperature and humidity at 41°C and 88% RH. For vibration testing (MIL-STD 810G 501.5, 507.5, 502.5) [89]. For vibration testing, the diagnostic device must survive vibrational frequencies and magnitudes associated with rotary-wing/fixed-wing/jet composite lifetime curves and ground composite lifetime curve to simulate convoy transport (MIL-STD 810G 514.6, Procedure I) [89]. For environmental elements, the diagnostic device must survive blowing sand, dust, and rain (MIL-STD 810G 510.5 Procedures 1, II; 506.5 Procedure I) [89]. Lastly, for environmental testing, the device must survive repeated drops from 4ft. within transport case and 3ft. drops without (MIL-STD 810G 516.6 Procedure IV) [89].

Results

The second generation diagnostic device passed the evaluation process with only two significant issues – one of which was unrelated to the testing that was performed. The functional issue that was reported during testing was associated with compromised seal integrity during testing at 18,000 feet above sea level with no pressurization. Second issue pertained to a material compatibility problem between the dye reagent and the urethane of the reagent storage network that was discovered prior to the evaluation process. The dye apparently adsorbed to the urethane surface – preventing the fluorescence-based reader detection. To overcome the issue, the small batch of second generation diagnostics were loaded with an excess amount of dye to saturate the urethane and maintain a detectable concentration of dye in solution.

Discussion and Conclusion

Based on the results of the military specification testing, the second generation diagnostic device would be suitable for use in resource-limited settings with only a couple minor revisions. The first revision that was required was replacement of the urethane reagent storage network with another material compatible with the dye. The second revision that was necessary for the design was an improved axial and radial seal design between the reagent storage network and dial subassembly. This was likely due to gas expanding within the reagent storage network – forcing separation between the network and the dial and thus compromising the radial and axial seals. The issue could have been exacerbated by part variations associated with production, but the design itself could be improved to eliminate sensitivity to elevated internal pressures.

Summary

The goal of the second phase of diagnostic development was to produce a second generation diagnostic platform that remedied the deficiencies of the first generation design and could withstand exposure to harsh operational conditions. To achieve this goal, a completely customized platform was designed. By eliminating the use and modification of off-the-shelf parts, it was possible to tailor the design to meet performance requirements and design specifications. The primary source of design complexity in the first generation diagnostic device was the sample processing channel. The second generation diagnostic simplified sample processing by implementing a passive technique for enhanced infectious agent capture. The design simplification propagated throughout the remaining components of the design to yield a platform with desirable attributes. Even though the second generation diagnostic was a substantial improvement over the previous platform, military specification testing highlighted design features that required further development and modification. Table 3.5, below, summarizes the major highlights of the second phase of diagnostic development along with the proficiencies and constraints of the second generation diagnostic device.

Table 3.5: Second generation diagnostic device development summary	
Overall goal	To produce a rapid diagnostic device with acceptable operational simplicity and enhanced durability to survive harsh conditions
Device aims	Simplify operational complexity and improve ergonomics
	Implement simulated slug flow for sample processing
	Enhance safety features
	Reduce device size
Proficiencies	Significantly reduced operational complexity (only two moving parts)
	Intuitive and ergonomic configuration
	Robust seals at dial interface and injection port
	Ruggedized design passed offsite testing for environmental resilience
	Plunger retaining shelf secures pressurized syringe body prior to lock
	Syringe port arm enlarged for improved strength
	Prototype channels confirm infectious agent capture for virus-like-particles, bacteria, and parasites
	Second generation diagnostic assembly confirmed target capture capabilities
	Generous joint and edge fillets enhance durability
	Paired reservoir sets enhance modularity and conserve space
	Design may be multiplexed for greater diagnostic specificity
	Diagnostic design may be used to screen a variety of different samples for alternative applications
Limitations	Design weaknesses to variability associated with part production and assembly process
	Selected inlay material incompatible with dye reagents
	Syringe port arm still sensitive to direct impacts, but at significantly elevated force

CHAPTER 4: THIRD GENERATION DIAGNOSTIC

The purpose of this chapter was to describe how the results of military specification testing helped shape the design of the third generation diagnostic device as it was prepared for manufacture and assembly. The following sections specifically address how the dial subassembly and device housing were modified to enhance performance and safety, what revisions were necessary to prepare the device for manufacture and assembly, and the implications the design features had on production costs. The finalized designs were reviewed by companies specializing in injection molding and ultrasonic welding services to determine production feasibility and obtain quotes. While the designs were production-ready, manufacture and assembly of the custom device were outside of the budget for this phase of development. The chapter concludes with a summary describing the advantages and limitations of the third generation diagnostic device and what was learned from the evaluation process.

Phase III Objectives

The primary objectives for the third generation diagnostic device (Figure 4.1) were to mitigate second generation design weaknesses discovered during military specification testing at USAARL and format the revised designs for injection molding production and ultrasonic welding assembly. The design weaknesses of the second generation device, reported in the previous chapter, included: 1) leak formation under elevated device internal pressure, and 2) material incompatibility between the urethane reagent storage network and

dye reagent used to label captured pathogens. These issues were resolved by improving device seals and eliminating urethane components from the platform. After modifications to the diagnostic device were completed, designs were formatted for injection molding and assembly using readily available design guides [90-96]. Finalized engineering designs were sent out for third-party review by companies specializing in the respective manufacturing and assembly processes.

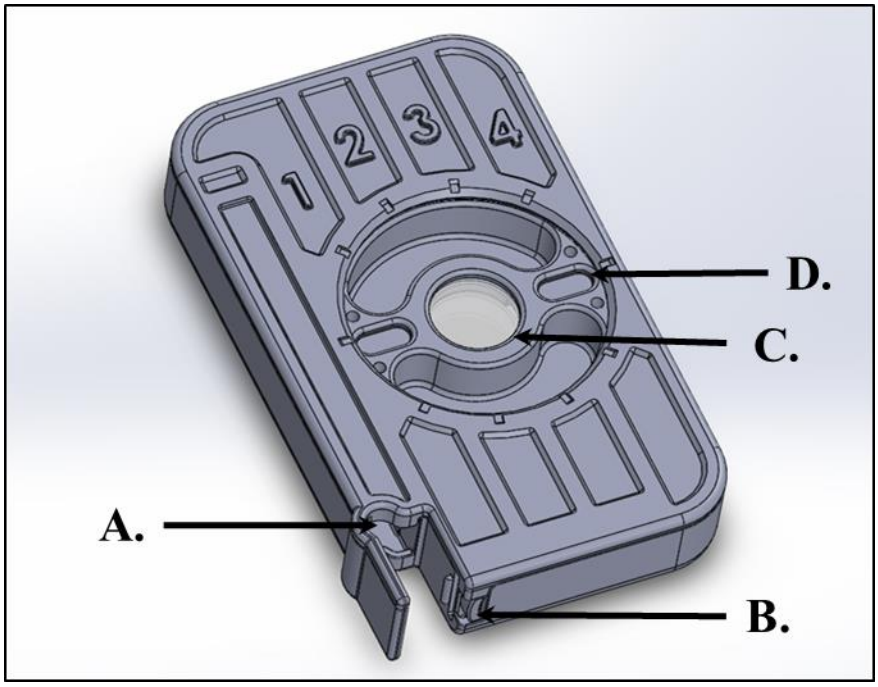

Figure 4.1. Third generation diagnostic device. The computer aided design (CAD) rendering of the third generation diagnostic illustrates the captive syringe port (A) with locking tab (B) used to safely transfer blood samples to the device. The optical region of interrogation (C) and dial (D) are also indicated. The overall device dimensions were 138mm length X 83mm width X 23 mm height.

Diagnostic Device Design

The development process for the third generation diagnostic device had two priorities. The first priority was to resolve platform design weaknesses. The design modifications are described as they pertained to the dial subassembly and device housing.

While major design weaknesses were discovered during military specification testing, other less significant weaknesses were identified after thoroughly reviewing the design. It was important to make all necessary design revisions before performance testing of the final diagnostic design.

The second priority of the development process was to prepare the third generation diagnostic for injection molding production and ultrasonic welding assembly. The design elements and criteria for designing production-ready components for these processes are largely universal but method specific.

Resolution of Design Weaknesses

Two major design weaknesses identified during the evaluation of the second generation diagnostic platform included leak formation under elevated internal pressures and a material incompatibility. These issues were resolved by simplifying the dial subassembly sealing system and integrating the reagent storage network into the housing of the device. Once the two most significant issues were addressed, the platform was reviewed for other design flaws that may adversely affect the safety or efficacy of the device. Final modifications were made to the device components to complete the platform design before reformatting for production.

Dial Subassembly

During the altitude phase of military specification testing, the radial and axial seals of the diagnostic device were compromised. This was problematic because it posed a safety risk for operators and limited the versatility of the diagnostic for field use. It was hypothesized that elevated internal pressures generated leaks by separating the reagent

storage network from the dial subassembly – compromising the integrity of the interface-based seals. To prevent this from reoccurring, the dial-based seals needed to be simplified and reinforced. Design simplification was achieved by consolidating axial and radial seal elements on to the radial surface of the dial (Figure 4.2). This design configuration made seal integrity completely reliant upon radial compression rather than both radial and axial. The seals were reinforced, in part, by increasing the thickness of the gaskets generating the seal so that they would be less sensitive to part variability. The final design modification made to complete the enhanced dial-based seal, described in the following section, was integrated into the housing of the device in the form of a stiff-walled cavity.

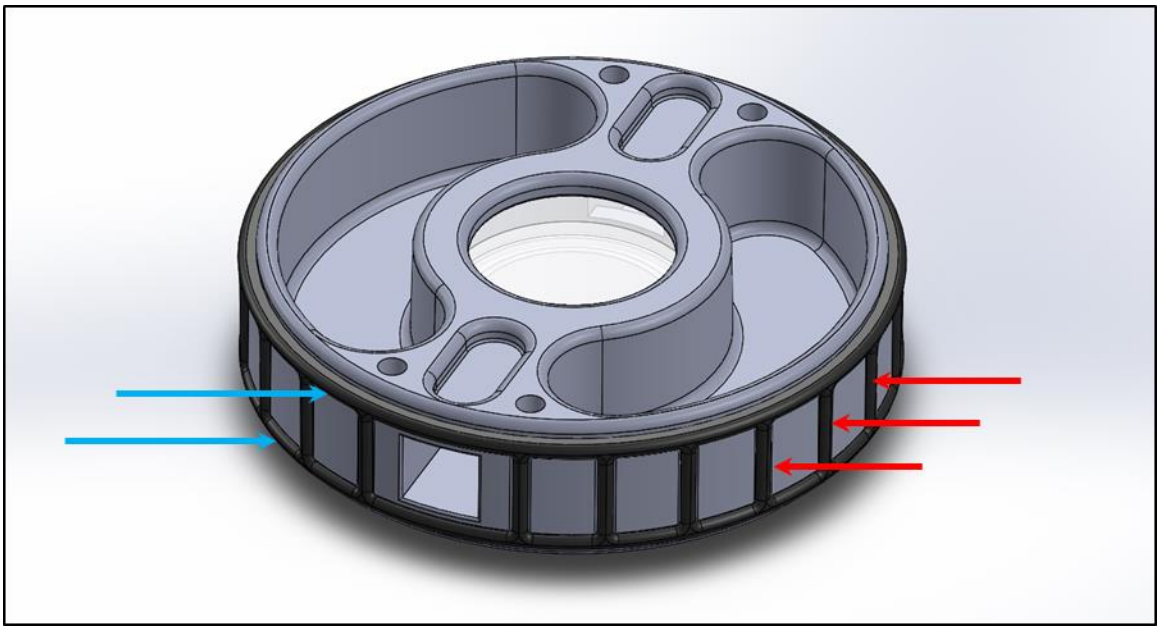

Figure 4.2. Third generation platform semi-static gasket seal design. (Blue arrows) Axial seals intended to prevent fluid migration from the interior to the exterior of the device were relocated onto radial dial face. (Red Arrows) Radial seals evenly spaced along the circumference of the dial prevent contamination between reagent reservoirs of the reagent storage network.

The revised designs established a new set of potential advantages and limitations for the diagnostic device. In addition to reinforcing the integrity of the seals, consolidating the seal elements to the radial face of the dial also reduced the overall surface area of the

semi-static seals. This should help improve the ergonomics of device operation by reducing frictional resistance to dial rotation. The design also reduces the number of critical design dimensions influencing seal integrity and subsequently simplifies device manufacture. The main limitation, however, was that the simplified design was potentially more complex to produce and assemble. The radial seals could be formed through an expensive over-mold process directly on the dial or as a separate gasket component that would increase assembly complexity.

After the seals of the dial subassembly were revised, the designs were reviewed for any additional opportunities to make modifications that would further decrease the complexity of the system, improve seal integrity, or augment functional reliability. As noted in the previous chapter, the sample processing channel was not required to be an independent component within the subassembly. Accordingly, the channel was integrated into the dial. This effectively reduced platform design complexity and increased reliability by eliminating a component from the assembly and minimizing the total surface area requiring permanent seals during assembly (Figure 4.3). Once dial subassembly modifications were finalized, the next step in the development process was to address the design weaknesses inherent in the reagent storage network and device housing for the diagnostic platform.

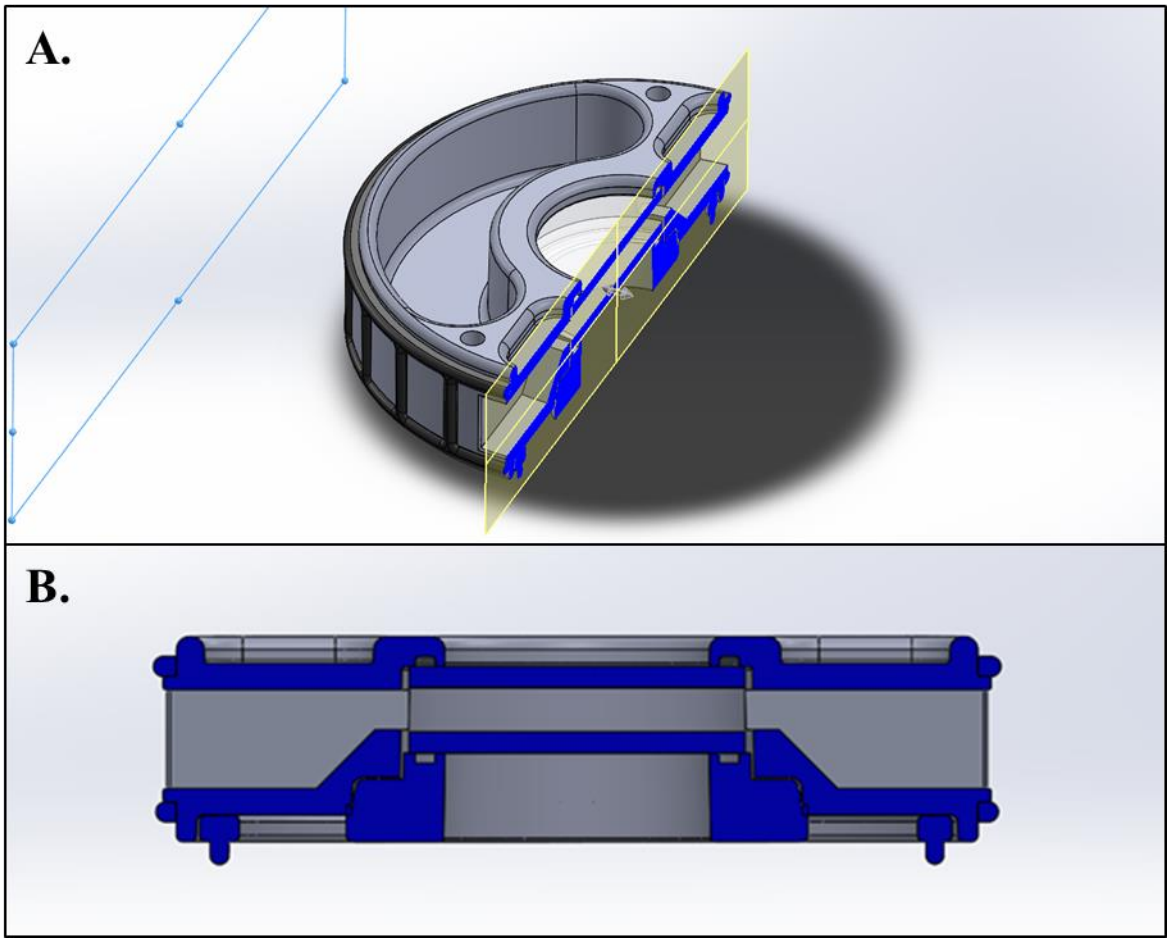

Figure 4.3. Cross section of dial subassembly illustrating sample processing channel integration. (A) The CAD rendering of the dial subassembly was cross-sectioned along the longitudinal axis of the sample processing channel. (B) The sample processing channel was fully integrated into the dial component of the dial subassembly.

Device Housing and Captive Syringe Port

Material incompatibility posed a significant problem for the diagnostic device. When dye solutions were loaded into the urethane reagent storage network, a rapid drop in fluorescence emission intensity was observable within minutes. The short term solution for this problem was to store highly concentrated dye solutions in the reagent storage network with the expectation that, once an equilibrium was reached, a fraction of the dye molecules would remain in suspension. This was adequate for military specification testing but too expensive to qualify as a long term solution. Possible long term solutions included

modifying the urethane elastomer casting resins to alter material properties, storing the reagent in a dried form (such as lyophilized powder), or producing the reagent storage network out of an entirely different material. The most expedient solution was to reconfigure the device housing to replace the elastomer reagent storage network – eliminating the need for the urethane elastomer. This modification also made it possible to form the stiff-walled dial cavity necessary to complete the dial-based seals designed to mitigate the risk of leak formation under elevated internal pressures (Figure 4.4).

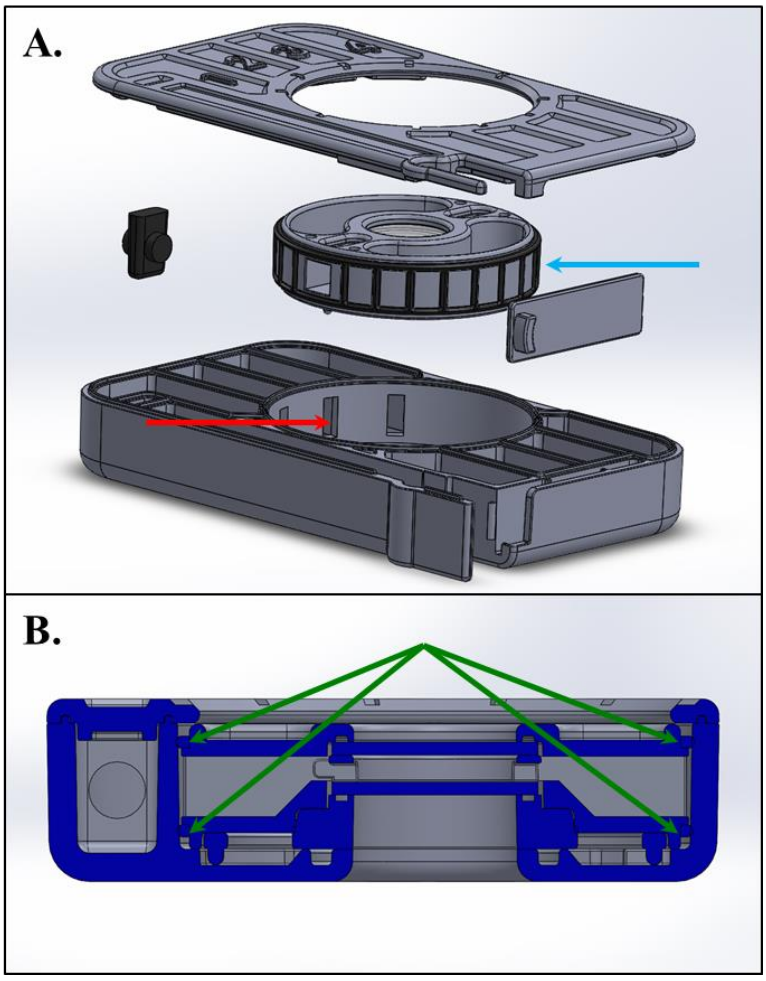

Figure 4.4. Exploded view and cross-sectional view of third generation diagnostic platform. (A) A dial cavity (red arrow) was designed into the base of the device housing to provide a stable seal with the dial subassembly (blue arrow). (B) The axial and radial seals were formed with an interference fit (green arrows) where the dial gasket was compressed 20%.

Integrating the reagent storage network into the device housing resulted in a unique set of advantages and limitations for the diagnostic platform. The design was advantageous because it eliminated a complex design component and interfaced well with the dial subassembly. This solution was also compatible with dry reagent storage which could augment the device shelf life. The limitation, however, was that the requirements for the material properties of the device housing became significantly more complicated. The housing had to demonstrate thermal stability, resist impacts and adverse environmental conditions, and exhibit suitable compatibility with the device sample processing reagents. As a result, a series of materials were evaluated for compatibility that could be used as the substrate material for the housing, as a housing over-mold, and/or used to produce custom gasket components.

Additional modifications made to improve design function and durability were implemented through adjustments to the diagnostic device housing components. The second generation diagnostic device used a clamshell-style of housing that primarily served structural and protective roles. The clamshell-style of housing formed a seam with limited protection from penetration along the perimeter of the device. Even though the seam was sealed with epoxy, the seam provided a direct path from the exterior of the device to the internal reagent storage network if the seal was compromised. Also, the syringe port arm was noted for being sensitive to fracture after severe, localized impacts associated with drops or rough handling. Both design weaknesses were addressed by modifying the housing components of the device. The clamshell-style housing components were replaced with a more conventional body and lid design configuration. The lid of the design simply served to seal the device hermetically. Step joints were incorporated into the lid in such a

fashion that they inserted into the cavities of the housing base – reinforcing the walls and forming a tortuous path leading from the exterior to interior of the housing components (Figure 4.5A). To improve the durability of the syringe port arm, the interior joint of the arm was restructured with a larger radius to effectively distribute stresses during sudden loading and prevent excessive stress concentrations from forming (Figure 4.5B).

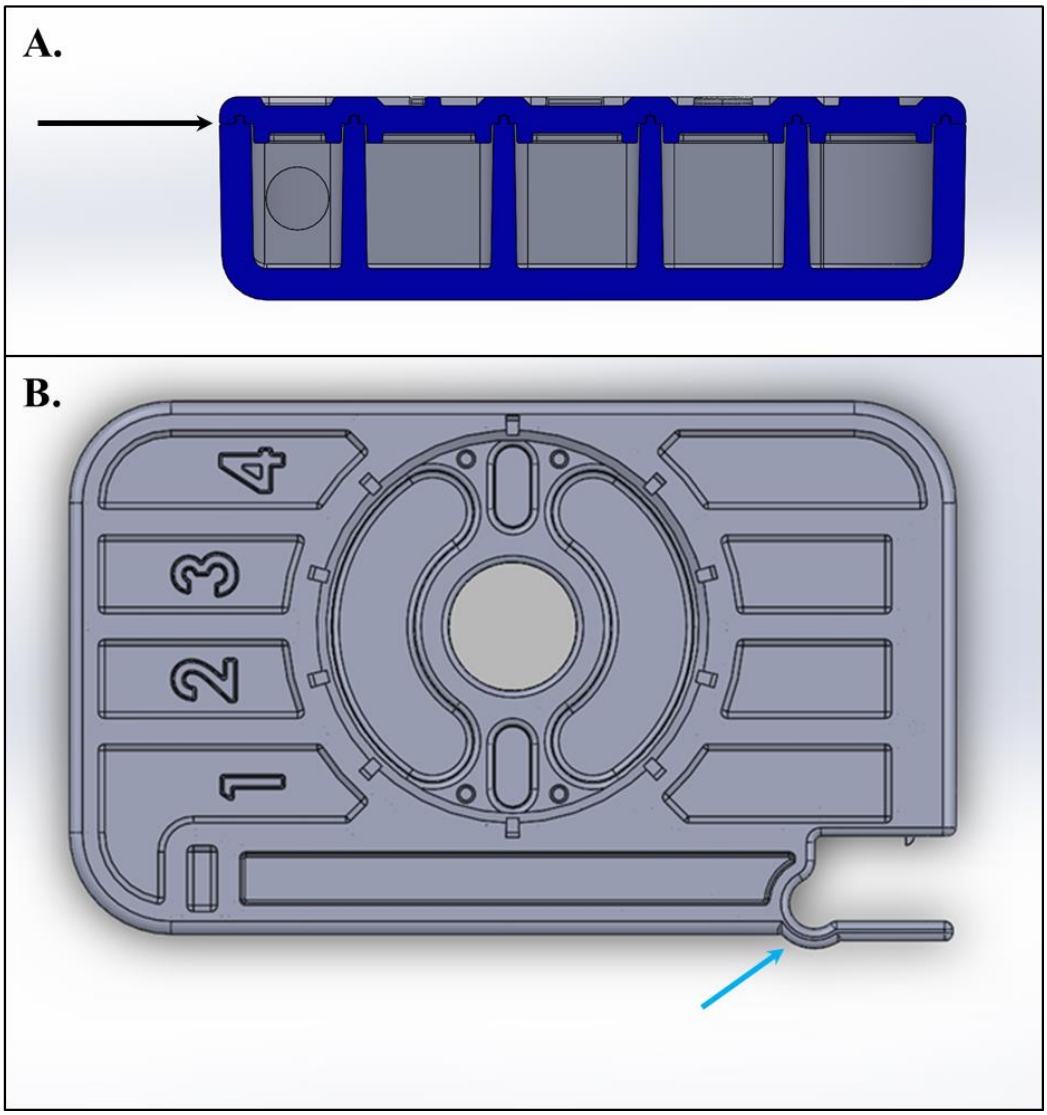

Figure 4.5. Device housing enhancements. (A) The base and lid components of the housing were designed to fit together with a step joint configuration to eliminate a direct path from the exterior to the interior of the device (black arrow). (B) The joint connecting the syringe port arm to the body of the device was modified with a large, semi-circular loop to decrease the magnitude of hoop stress concentrations that may result from impacts.

After completing the desired diagnostic device modifications, the components were ready to be configured for injection molding and ultrasonic welding. These methods of production and assembly were well suited for manufacturing the disposable diagnostics and mitigating product variability associated with alternative methods of prototyping. Even though the diagnostic device would undoubtedly require future adjustments, it was critical to begin design configuration for manufacturing early in the development process in order to prevent minor changes/adjustments from becoming exceedingly expensive.

Design for Manufacture and Assembly

In order to successfully translate this diagnostic technology from the laboratory to resource-limited settings (RLSs), the platform design was required to be inexpensive to manufacture and assemble. Injection molding was an obvious choice for production because the process is commonly used to rapidly manufacture inexpensive, disposable products with consistent quality. Less obvious, however, was the means by which the diagnostic devices should be assembled. There are a variety of plastic joining techniques available for use (i.e. adhesive bonding, solvent welding, mechanical fastening, etc.). The seals of the diagnostic platform were required to withstand harsh operational environment conditions and rough handling while processing potentially biohazardous materials. As a result, the joining (assembly) strategy for the diagnostic devices was required to produce durable, hermetic seals using a methodology that could be scaled to high throughput manufacturing. The third generation diagnostic device was first configured to comply with injection molding requirements and then modified for ultrasonic welding since a variety of different ultrasonic weld joints may be used depending on the circumstance. After designs

were completed, they were submitted to third-party companies specializing in these processes for review.

Designs intended for injection mold production must be structured to resist deformation/warping and sink mark or knit line formation. Part warping/deformation and sink mark formation occur when parts have inconsistent wall thickness or rapid transitions in wall thickness. The most simple way to avoid cooling defects was to maintain consistent nominal wall thicknesses throughout each part (if all parts features are consistent, they may be produced in 'family molds'). More complex parts with external walls and internal features must be configured with thicker features on the exterior of the part with thinner features toward the interior. Formatting parts in this fashion aids filling the injection mold tooling with molten resin and reduces the risk of channels 'freezing off' before reaching the mold core. Thinner interior features also help prevent sink mark formation as they must be drafted (demolding) and include joint fillets (durability) – reducing base thickness. Features must also be appropriately spaced apart to aid in uniform cooling. Knit lines are potentially problematic because they result in anisotropic material properties and that may generate stress concentrations leading to fracture inception and propagation. Knit lines form when resin flows bifurcate/separate passing around a flow obstruction and coalesce again at the distal side of the feature. Knit lines are more problematic when these features/obstacles are located in thin parts near the center of the part. If the features cannot be implemented near the edge of the part they should generally be removed from the design entirely or added via a secondary process (i.e. milling). The third generation diagnostic components were reconfigured accordingly.

Obviously, designs intended for injection molding must be capable of being demolded. For this project, the majority of parts were simple and qualified for 'short-pull' injection molding requirements. Accordingly, draft angles of 1.0° were added to all vertical surfaces and all joint seams and edges were filleted. The two complex parts of the design included the base shell component and the dial. The base shell component must be produced using complex tooling to create the ports that connect each reservoir to the core cavity (where the dial resides) and over-molding for the syringe port septum. These undercuts must be made with collapsible tooling. The dial was complex because it required two sliding elements within the tooling to produce the inlet and outlet of the dial. Furthermore, the dial was designed for two-shot molding so an elastomer gasket could be over-molded upon the radial surface.

After configuring the third generation diagnostic device for injection molding, ultrasonic weld joints were added to the design components requiring hermetic seals. A variety of conventional joint designs (i.e. step joints, tongue-in-groove joints, etc.) were available to join parts using the ultrasonic welding technique. These joints were unique because they incorporated energy directors or interference fits between parts (i.e. shear joint) to concentrate vibrational energy at focused contact surfaces to generate selective heating and bonding. The process is capable of producing welds with mechanical properties greater than or equal to the parent material [97-99]. For the housing of the diagnostic device, energy director tongue-in-groove joints were added to all mating surfaces requiring hermetic seals (Figure 4.6A). To seal the dial subassembly, an ultrasonic shear joint was added to the ratchet component of the design (Figure 4.6B).

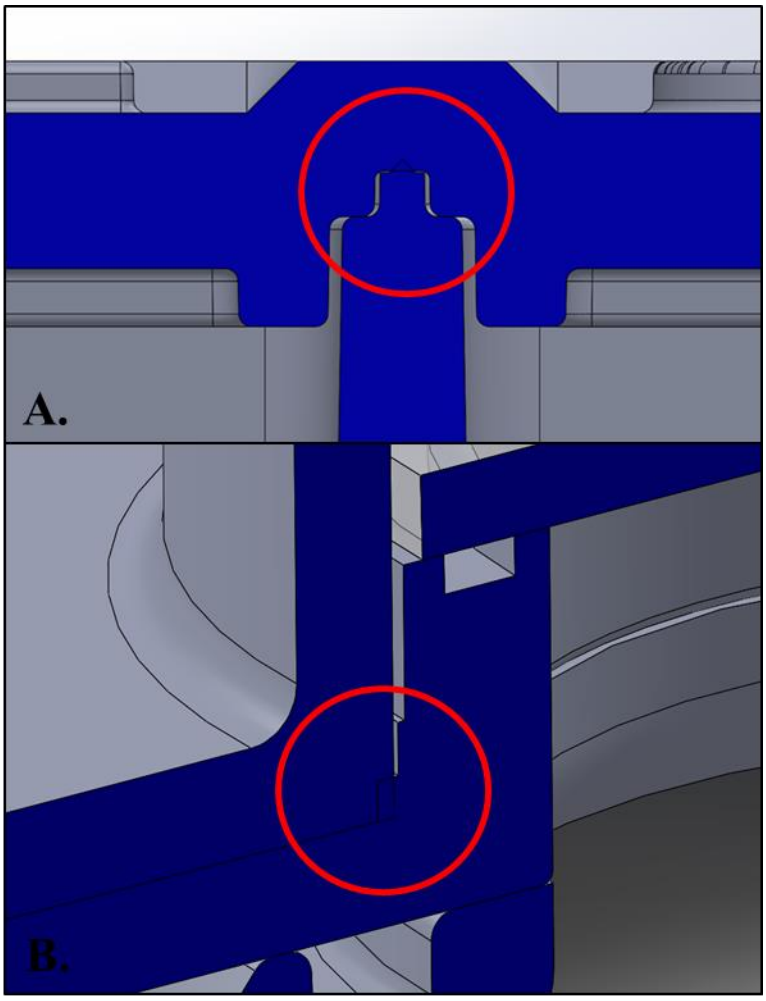

Figure 4.6. Images of platform ultrasonic weld joints. (A) Tongue-in-groove joints were designed into the base and lid components of the device housing to provide hermetic seals for all the compartments of the reagent storage network. (B) A shear joint was used to create the hermetic seal for the dial subassembly between the dial and the ratchet components.

The assembly process was designed to be conducted by producing the dial subassemblies first and the housing second after loading the dial subassembly, reagents, and locking tab. The risk of mobile parts tacking to other parts during assembly was addressed through material selection (for the locking tab) and configuration (for the dial subassembly). A crystalline polymer was selected for the locking tab which would not bond to the surrounding amorphous polymer structures it contacted. The dial was more

complex to protect because the amorphous polymer forms a molecular bond with the elastomer selected for over-molding and gasket seal formation. The gasket prevents the radial surface of the dial from tacking to the walls of the core cavity and the bottom of the dial was located far enough away from the ultrasonic welding surface that it would not bond to the base shell component (Figure 4.7).

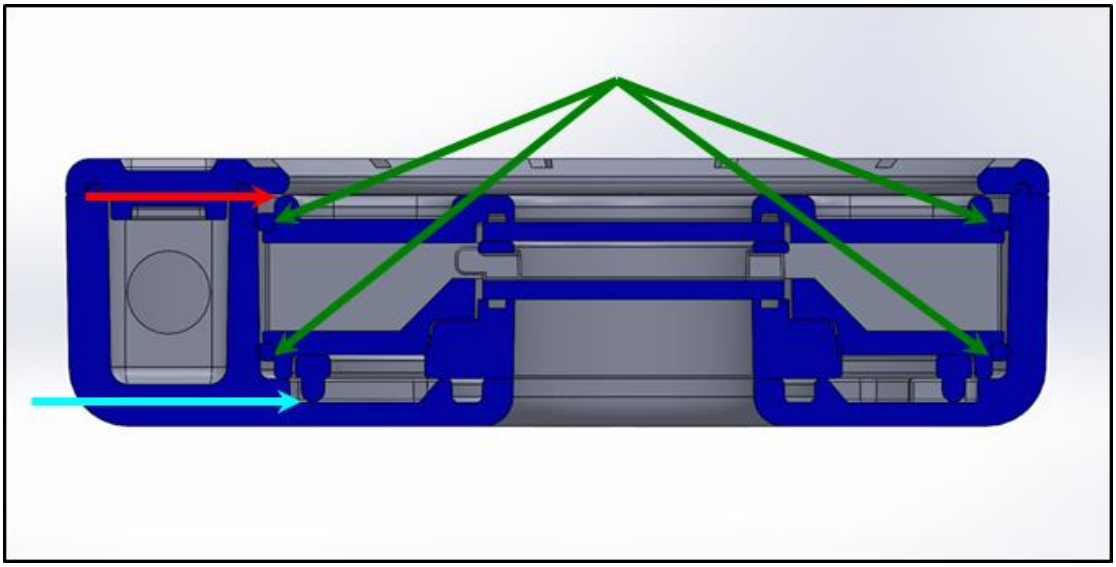

Figure 4.7. Platform design to prevent tacking (transverse cross-section). The lid of the housing was offset from the dial subassembly to prevent direct contact and tacking (red arrow). The base of the dial was distanced sufficiently far enough away from the device lid (where the ultrasonic vibrations would be focused) to prevent secondary tacking (blue arrow). The gasket material making contact with the walls of the dial cavity was designed as an elastomer (green arrows) that would dampen ultrasonic vibrations and prevent taking due to dissimilar material properties.

Evaluation

There were two significant evaluations performed during the third phase of the diagnostic development project. The first evaluation entailed screening a variety of polymers for compatibility with the rhodamine dye reagent that was the fluorescent tag used in the diagnostic to help label and detect infectious agents stripped from screened samples. It was imperative for device function that compatible materials were identified –

at least one plastic and one elastomer. After materials had been specified for production, designs for manufacture and assembly could be completed. The first section describes the process used to screen materials for compatibility and what conclusions were made.

The second evaluation involved sending computer aided design (CAD) files to companies specializing in injection molding and ultrasonic welding for review. The review process would determine whether the designs were production-ready and inexpensive. The affordability of the diagnostic had multi-faceted implications. For example, the device had to be inexpensive to manufacture because it was a disposable intended to extend blood transfusion safety to resource-limited settings. The device was also required to progress through a diagnostic evaluation and optimization phase of development before device finalization. If the design was too expensive to produce, the platform could be modified to reduce costs but still yield data from production-grade prototypes. The second section describes the feedback received from the review processes for injection molding and ultrasonic welding and the implications for the third generation diagnostic device.

Material Compatibility

The protocol for conducting the material compatibility experiment involved immersing material samples in rhodamine solution for 20 hours at room temperature and measuring changes in fluorescence emission of the rhodamine solution after prolonged exposure[6] (Figure 4.8). The measurements were then compared to a control sample that was not exposed to any sample materials. A total of 19 materials were selected for evaluation – 12 plastics and 7 elastomers.

[6] Experimental preparation and data acquisition for material testing was conducted with the help Hannah Curtis.

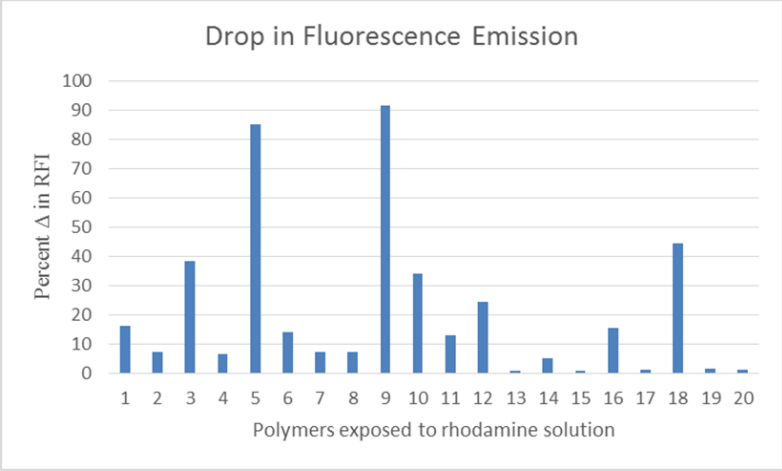

ID	Material
1	Styrene-butadiene rubber (1)
2	High density polyethylene
3	Natural Rubber
4	Polytetrafluoroethylene
5	Styrene-butadiene rubber (2)
6	Butyl Rubber
7	Polyethylene
8	Polycarbonate (1)
9	Nitrile
10	Latex Rubber
11	ABS/PC copolymer
12	Polypropylene
13	Acrylonitrile butadiene styrene (1)
14	Polycarbonate (2)
15	Acrylonitrile butadiene styrene (2)
16	Polycarbonate (3)
17	Delrin
18	Nylon
19	Santoprene
20	Control

Figure 4.8. Material compatibility testing. Based on the drop in relative fluorescence intensities (RFIs), a select few materials appeared to demonstrate acceptable dye compatibility. These materials included Santoprene, Delrin (POM), and ABS.

Based on the results of the 20 hour compatibility testing, two plastics and one elastomer appeared to exhibit acceptable properties suitable for use in the diagnostic device. The two plastics were acrylonitrile butadiene styrene (ABS) and polyoxymethylene (POM) and the elastomer was Santoprene. Since Santoprene was the only elastomer to demonstrate acceptable reagent compatibility, it was the obvious material of choice for the elastomeric components of the platform. With more than one option for compatible plastics, the choice material was based on moldability and cost. ABS plastic was selected for diagnostic device production because it demonstrated relatively consistent performance and could be used to form the thick-walled components of the third generation device. While POM also demonstrated reagent compatibility, the polymer undergoes anisotropic shrinkage following injection molding. Anisotropic shrinkage would make it difficult to achieve uniform, low-tolerance dimensions for the dial cavity of the device housing – potentially compromising seal integrity. POM is also a considerably more expensive polymer than ABS – further reinforcing the decision to use ABS for production.

Injection Molding and Ultrasonic Welding Design

Before sending the finalized design to a third party company for review, the assembly components were rapid prototyped via fused deposition modeling (FDM) with black ABSplus. The diagnostic device prototype was produced to confirm form, fit, and function (ratchet mechanism and locking tab). This was necessary because the review process independently evaluated platform components and features for moldability – not fit or function. Based on the prototype, the components fit together appropriately and functioned as intended (Figure 4.9). Form was assessed from an ergonomic perspective – the finger grooves of the dial were sufficiently large and deep for operator use, the locking tab was easily operated, and the overall device fit well within the hand. According to the evaluation, the design was ready to be reviewed for production.

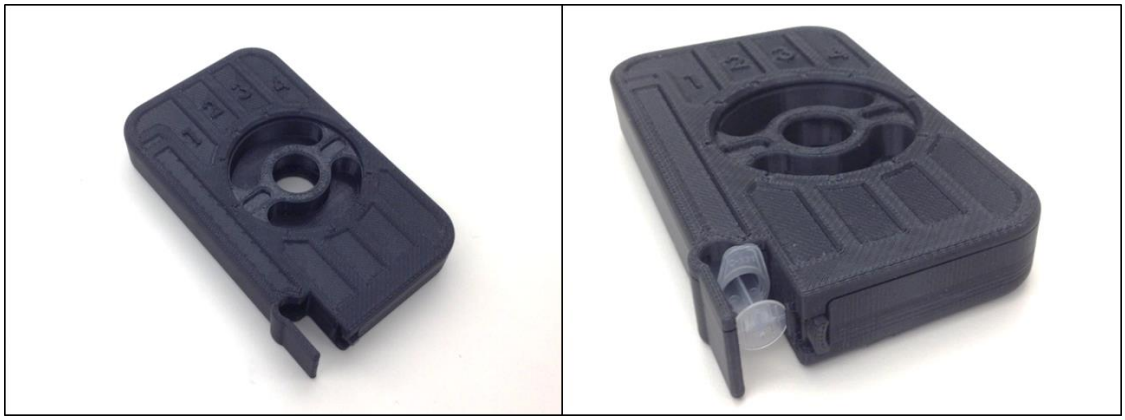

Figure 4.9. Image of FDM prototype used to confirm design accuracy.

This device design was sent to separate companies specializing in injection molding and ultrasonic welding for review. The injection molding review process assessed production feasibility and provided a quote for production of 500 assemblies. The ultrasonic welding review process entailed reviewing the designs for structural integrity (withstanding the assembly process), ultrasonic weld joint design, material compatibility

with the welding process, and providing a quote for purchasing/renting equipment to assemble the devices. The designs were approved by both review processes.

Unfortunately, the cost for injection molding was greater than anticipated due to the complex tooling requirements for the device housing base. Each port positioned within the central cavity formed an undercut that required a custom lifter (collapsible tooling element) for production. This complex tooling significantly added to the cost of production. A variety of design alterations were investigated for eliminating the undercuts without significantly modifying the third generation diagnostic platform configuration. A reasonable solution that dropped production costs without compromising function was not readily apparent and even after investing a significant amount of time in developing alternative solutions, the most cost-effective and functionally reliable designs resulted in the formation of seams on critical surfaces for seals. The seams may be mitigated with post-processing steps but not necessarily resolved. Also, alignment between mating parts may compromise the seals independent of seam-based surface irregularities.

Summary

The goal of the third phase of diagnostic development was to produce a third generation diagnostic platform that mitigated design weaknesses discovered during military specification testing and was ready for injection molding production and ultrasonic welding assembly. To resolve the design sensitivities, the reagent storage network was integrated into the device housing and dial-based seals were simplified and reinforced. These modifications would considerably enhance device performance under adverse conditions in resource-limited settings. Designs were reformatted to comply with design requirements for injection molding and ultrasonic welding after platform modifications

were completed. Production-grade diagnostics were desirable to minimize cost and improve consistency while evaluating and optimizing diagnostic performance characteristics. Even though the designs were approved for production for both processes, the design required complex tooling for production that was outside the allotted budget for this phase of diagnostic development. Table 4.1, below, summarizes the major highlights of the third phase of diagnostic development along with the proficiencies and constraints of the third generation diagnostic device.

Table 4.1: Third generation diagnostic device development summary	
Overall goal	To enhance the second generation design and produce a rapid diagnostic device ready for manufacture and assembly
Device aims	Improve dial seals
	Select alternative material for inlay or eliminate inlay altogether to meet dye compatibility requirements
	Configure design for injection molding
	Configure design for ultrasonic welding
Proficiencies	Enhanced rapid diagnostic design simplicity, durability, and efficacy
	Approved design for injection molding
	Approved design for ultrasonic weld assembly
Limitations	Outside of budget for production and assembly
	Dial sealing surface still represents a design sensitivity given the large surface area that must be sealed

CHAPTER 5: CONCLUSION

Project Summary

Over the course of three years, the rapid diagnostic device designed for this project continually evolved to enhance performance and reduce production costs. The experience was instructional and the process yielded a promising product that may benefit society in the near future. This was made possible by clearly defining a medical need, establishing specific aims for the project, and implementing a product development strategy to achieve the aims. By the end of the project, the third generation diagnostic device:

1) Ensured operational safety and simplicity through ergonomic design and the use of a hermetically sealed device with completely self-contained reagents.

2) Provided a robust and reliable platform resilient to adverse environmental conditions.

3) Optimized for infectious agent capture by implementing design features that maximize screening efficacy (i.e. multipass sample processing, simulated slug flow, etc.) and improve reagent-material compatibility.

Product development strategy was a key factor in terms of establishing probability of success and must anticipate the unforeseen obstacles that inevitably present themselves despite tedious planning. However, even a well-planned strategy supported by contingencies cannot substitute for a thorough understanding of translational research requirements and the challenges they present beyond simple safety and efficacy considerations.

The product development strategy used for this project involved explicitly defining the problem the diagnostic device was intended to solve, establishing boundary conditions and design specifications to govern product evolution, generating numerous concept models to provide best-fit alternative options, and designing modular platforms that may be readily modified as the proficiencies and constraints of specific designs were determined. The advantages associated with this approach encompassed: reduced time and resource expenditure, enhanced product adaptability and quality, simplified root cause diagnosis during troubleshooting, and streamlined problem resolution. Difficulties experienced while applying this design strategy were primarily associated with the parallel path design process and a narrow perspective that focused on diagnostic design elements within modular platforms – addressing manufacture and assembly concerns later than ideal. Regardless of the strength and weaknesses of the design strategy, the end product was a notably improved and inexpensive rapid diagnostic design compared to the first generation prototype that is readily deployable in the near future – detecting infectious agents in resource-limited settings (RLSs).

Without question, the design strategy helped the rapid diagnostic development process navigate obstacles that were presented over the course of the project. While the benefits were evident throughout the development process, the advantages were most notable during phases of diagnostic device platform design generation and reformulation. At the beginning of the project, computational modeling, evaluation of multiple prototype designs, and experimental observations made it possible to achieve enhanced fluid mixing within the miniature channel of the first generation diagnostic device. This was produced in parallel with the reagent circulation and storage network of the diagnostic – saving time,

expense, and minimizing troubleshooting complexity while resolving preliminary design limitations for each system. Addressing these design elements improved the probability of successful diagnostic assembly production and operation for the limited user evaluation. Based on the observed design sensitivities, inadequate design features were readily diagnosed and addressed with the development of the second generation diagnostic device. Producing multiple design concepts for the second generation device made it possible to quickly eliminate designs with unacceptable limitations, simplify operational complexity, and produce a device capable of passing third-party military specification testing. Furthermore, the design was readily adapted for injection molding and ultrasonic welding without compromising the platform.

As mentioned previously – this project required a thorough understanding of translational research requirements beyond safety and efficacy for success. These requirements emphasize ergonomics, operational simplicity, and inexpensive product manufacturing and assembly. Design requirements pertaining to these categories were a primary cause of design reformulation. During the development of the first generation diagnostic device, it was not recognized how simple the device must be in order to qualify as 'easy-to-use.' As a result, feedback from the limited user evaluation requesting simplified diagnostic operation resulted in a complete redesign of the diagnostic device because the manual methods of sample processing and reagent circulation were inextricably designed into the platform. Given the design of the first generation diagnostic device, automation (reduced operational complexity) would only be achieved through more sophisticated and expensive means. Similarly, the third generation diagnostic device required a platform change because requirements for inexpensive prototype manufacture

and assembly were not well defined in terms of third party prototype constraints. The third generation diagnostic device was capable of being injection molded and assembled through ultrasonic welding, but too expensive for dynamic prototyping. Ultimately, these major design reformulations were necessitated by the dynamic process of design development.

Based on these observations, future product development projects will benefit from involving manufacturing engineers early in the design process during prototype development and obtaining explicit definitions for ambiguous design criteria governing design goals. While these design strategy improvements may seem obvious, they are not trivial. Had they been implemented, considerable time and effort would have been saved that could have been applied to design optimization. However, some elements are not or cannot be defined explicitly during the preliminary stages of product development if the customer does not want to overly constrain the development process or if the customer does not know what they are willing (or not willing) to accept. Additionally, it may be difficult to secure manufacturing engineer consultation early in the product development process as designs may be subject to significant alteration during preliminary feasibility assessments.

The design elements that performed the best in each diagnostic platform shared one common trait – simplicity. These elements included the captive syringe port locking mechanism designed for the first generation diagnostic and the slug/modified-slug flow regime implemented in the second generation diagnostic. It was essential to keep design elements as simple as possible in order to reduce production costs, increase device reliability, ensure operational reproducibility, and improve device versatility – properties essential for a diagnostic device intended for use in resource-limited settings (RLSs).

Complex design features breed increasing complexity in the product development process. Elements that did not perform well in the diagnostic device designs tended to be complex. These elements included the vortex forming miniature channel of the first generation design, the external inlay of the second generation device, and the port-forming undercuts of the third generation diagnostic.

Future Work

A significant amount of work remains to translate the diagnostic device produced over the course of this project from the laboratory to point-of-care use in resource-limited settings. Future work may be divided among three categories including design optimization, testing for FDA approval, and exploration of alternative applications. These categories may be pursued in series or parallel. Given the potential for the diagnostic to benefit society with the early detection and diagnosis of infectious disease, a parallel path design strategy would be desirable for bringing the device to market as soon as possible.

The final prototype produced through this project requires design optimization in order to achieve the greatest diagnostic performance characteristics possible at the lowest disposable, diagnostic device unit cost. Elements for optimization include sample volume, reagent concentration, and the total number of inversions for sample processing; platform dimensions; manufacture and assembly formatting; and a multiplexed diagnostic design configuration. The sample processing related variables for design optimization require a series of pilot studies to investigate the impact variable alterations have on the limits of detection for various different infectious agents. After optimization of the sample processing variables, device structural considerations may be addressed. The end products

would be two diagnostic devices primed for FDA approval and validation of alternative applications.

In order for the rapid diagnostic device to be commercialized, the FDA must approve the device. Before receiving approval, clinical data must be collected with an investigational device exemption (IDE) that may supplement a premarket approval (PMA) application or 510(k) premarket notification. For the best chance of approval, the design optimization prior to conducting clinical studies is essential. However, experiments challenging safety and efficacy may be conducted prior to design finalization to demonstrate thorough and exhaustive evaluation of the device. With the emphasis on safety and efficacy, high quality diagnostic devices must be produced for data acquisition. Rapid prototypes are sufficient for proof of concept, but still lack the properties of production grade assemblies. For efficient evaluation of the device, device class and approval process must be determined before data collection for FDA approval.

Alternative applications for the diagnostic device involve screening a wide variety of different sample types for various target analytes. These applications include urinalysis, quality control for food processing/packaging services, and even cell culture screening – just to name a few. The modular nature of the design makes exploration of alternative applications straightforward and simple. The ligand coatings within the target capture region of the diagnostic device may readily adjusted to bind target analytes specific to the desired application. Furthermore, for less demanding applications, different methods of detection may be employed. For example, the fluorescence-based detection system (which provides the highest sensitivity) may be substituted with other detection systems compatible with the sandwich-style assay format.

Exploration of alternative applications should begin as soon as possible so they may be listed in the FDA approval application and modular adaptations may be included in the finalized diagnostic designs. Investigation of alternative applications prior to design finalization is also important because inexpensive modifications/fittings/adaptors/or ports may be developed to achieve suitable device versatility.

SECTION II

DEVELOPMENT OF A NOVEL BIOPROCESSING TECHNIQUE FOR ENRICHING ADIPOSE-DERIVED STEM CELLS WITH ENHANCED FUNCTIONAL CAPACITY

CHAPTER 6: INTRODUCTION

Overview

Cell-based regenerative medicine has significant therapeutic potential for treating a broad variety of tissue disorders ranging from myocardial infarction to articular cartilage defects [100, 101]. Cell-based regenerative therapy may be used to improve wound healing in conjunction with cosmetic surgery or impede tissue necrosis associated with myocardial infarction [102]. The fundamental premise behind regenerative treatment is that damaged or dysfunctional tissue can be repaired by transplanting viable cells to the affected site where they will be engrafted, they will proliferate, and they will synthesize components of the extracellular matrix necessary to regenerate healthy tissue. Successful cell transplant and engraftment would restore tissue function, reduce pain, and/or impede further tissue degeneration [103]. While this treatment strategy is conceptually simple, effective application has proven difficult and has demonstrated variable results in laboratory and clinical settings [104, 105]. In this research, cell therapy procedures will be evaluated and modified with the goal of developing focal articular cartilage repair with the long term goal of impeding joint degeneration and the progression of osteoarthritis.

One of the primary factors limiting the efficacy of current cell-based regenerative therapy is acute-phase cell death following cell transplant [106-111]. This phenomenon is commonly described as “massive cell death” and studies report high percentages of cell loss ranging from 30 – 90% with a tendency toward higher percentages [109]. This cell loss occurs within the first few days post transplantation. Acute-phase cell death is clearly detrimental to treatment efficacy as viable cells are eliminated and subsequently unable to

proliferate or contribute to tissue repair. The cell death is also counterproductive because not all cells are cleanly eliminated through apoptosis and a portion of the cells undergo necrosis [111, 112]. Cell necrosis causes cell lysis and resultant cytotoxic intracellular components are released into the surrounding microenvironment where they may adversely affect viable cells in the native tissue [112].

Several elements contribute to the accelerated and widespread death of transplanted cells. These elements include host inflammatory response, mechanical injury, maladaptation, hypoxia, and the quality of the transplanted cell sample [108, 113, 114]. A simple strategy for improving transplanted cell engraftment and treatment efficacy is enhancement of desirable cell attributes. The quality of a cell sample may be evaluated by three parameters: cell viability, regenerative capacity, and resilience. A deficiency in any of these three attributes could limit process efficiency and efficacy [100, 115, 116]. Cell sample quality may be enhanced through selective enrichment, preconditioning, improved extraction and handling techniques, and by obtaining cells from younger donors [115-120]. Selective enrichment techniques include fluorescence-activated cell sorting (FACS), magnetic-activated cell sorting (MACS), dielectrophoretic cell sorting (DEP), filtration, centrifugation, and a slew of variations capable of targeting cells based on selective physiochemical properties [121]. Many of the more selective approaches require a high degree of sample processing (more than cell culture expansion and differentiation) and have limited clinical applicability [121]. Methods for preconditioning cell samples before transplant include exposure to stressors, culture expansion with growth factors, and genetic modification of cells [108]. Based on experimental evidence amassed through several studies, one highly effective method for improving transplanted cell survival has been

exposure of cells to stressful stimuli. Stressors used to precondition cells include hypoxia and hyperthermia [122]. Cells exposed to these harsh conditions are stimulated to express pro-survival genes, develop tolerance, and ultimately exhibit improved resilience to the adverse conditions of the transplant microenvironment [122]. Current methods of cellular preconditioning are limited by the amount of time required to condition cells to tolerate adverse environmental conditions and safety concerns associated with gene manipulation [122]. Improving extraction and handling techniques to minimize cell injury and enhance cell sample viability pose the least risk of compromised treatment safety but have generally been restricted to minor protocol adjustments producing relatively small benefits.

The goal of this research was to develop a novel process for enhancing extracted cell sample quality to improve the efficacy of cell-based regenerative therapies. By combining advantageous characteristics of cellular preconditioning and cell separation techniques, we have created a selective process for enriching metabolically active cells within extracted cell samples. The rationale for targeting metabolic activity as the basis for separating cells is multifaceted. Metabolic activity is an intrinsic cellular property directly associated with cell survival and therefore a consistent, robust mechanism for selective enrichment. Furthermore, metabolic activity characteristics serve as an indication for cell viability, regenerative capacity, and resilience. Accordingly, the selective enrichment of metabolically active cells should subsequently address the three parameters that constitute cell sample quality. We hypothesize that extracted cell samples contain substantial populations of less-efficient, senescent, damaged, and dying cells that contribute to the massive cell loss during acute-phase cell death post transplantation.

Eliminating the dysfunctional cells from extracted cell samples should improve cell survival and therapeutic efficacy.

Articular Cartilage Structure and Function

Cartilage is classified into three categories: hyaline, elastic, and fibrous cartilage [123]. These classes of cartilage tissue share general characteristics but differ in biochemical composition, biomechanical properties, and ultrastructural architecture. Articular cartilage, which covers all diarthrodial joints, is a specialized form of hyaline cartilage [123]. While articular cartilage is only 2 – 4 mm thick, the tissue exhibits exceptional mechanical properties and durability [124]. The primary function of articular cartilage is to provide a low friction surface [125]. It is also capable of absorbing some shock [125]. Articular cartilage is considered a biphasic material composed of immiscible solid and fluid phases [125, 126]. The solid phase includes a network of collagen (primarily type II) fibrils, proteoglycans, chondrocytes, and non-collagenous proteins. Non-collagenous proteins include anchorin CII, cartilage oligometric protein, fibronectin, and tenascin. Water within the tissue constitutes the fluid phase and accounts for 65 – 80% of the total tissue weight [125]. The nature of the interaction between the phases is responsible for the mechanical properties of articular cartilage.

Articular cartilage is aneural, avascular, and alymphatic [127]. The absence of these networks severely limits the intrinsic regenerative capacity of the tissue. Chondrocytes within the tissue rely on diffusion for nutritional support and anaerobic metabolic activity to support cellular functions due to the low oxygen concentration within the interstitial environment [125]. The structure of the tissue is characterized by four zones and three regions. The articular cartilage layers include the superficial, transitional, deep,

and calcified zones [125]. The outermost layer is the superficial zone and constitutes the articular surface. This zone is characterized by a fibrillar collagen network oriented parallel to the surface, elongated chondrocytes, low interstitial proteoglycan content, and a high concentration of water. The transitional zone is adjacent to the superficial zone and is composed of less organized and slightly larger collagen fibrils. Chondrocytes within this zone are morphologically more spherical. Approaching the subchondral bone, the following layer is the deep zone. This zone of the articular cartilage contains the largest collagen fibrils. The collagen fibrils are oriented perpendicular to the subchondral bone and parallel to columnar stacks of spherical chondrocytes. The proteoglycan content is the highest in this zone and inversely proportional to the water content, which is at its lowest concentration. The final layer of the articular cartilage ultrastructure is the calcified zone. The calcified zone is a transitional tissue that anchors the overlying cartilage to the subchondral bone. Based on the proximity to chondrocytes interspersed throughout these zones, the extracellular matrix is divided into three regions. Relative to the chondrocytes, the pericellular matrix is the most proximal region and composed of proteoglycans and non-collagenous matrix components. The pericellular matrix is believed to aid in mechanical signal transduction from the extracellular matrix to the chondrocytes during mechanical loading. The pericellular region is surrounded by the territorial matrix, which is composed of thin collagen fibrils. The fibrillar network of the territorial matrix region provides mechanical protection for chondrocytes during joint articulation and mechanical loading. The final region is the interterritorial matrix. This region encompasses the entire matrix existing between chondrons (a chondrocyte and its surrounding territorial matrix) and changes as a function of articular cartilage zones [125].

The biomechanical properties of articular cartilage are a product of the complex interactions between the solid and fluid phases of the tissue. The three main functional characteristics of articular cartilage include shock absorption, low-friction, and high wear-resistance. Articular cartilage is a load bearing tissue and, when placed under compression, the biphasic properties become apparent. Fluid pressurization is believed to be the primary mechanism by which mechanical loading is supported by the tissue [128]. Proteoglycans within the interstitial space make a substantial contribution to fluid pressurization and the overall compressive stiffness of articular cartilage. Proteoglycans consist of a long protein core and numerous sulfated glycosaminoglycan side-chains. The sulfates on the branched side-chains are negatively charged and cause the glycosaminoglycan side-chains to spread apart and remain dispersed while attracting and retaining significant numbers of water molecules. Without the proteoglycans, cartilage would permanently deform under compression. The fluid within the tissue bears 95% of the compressive load and dampens shock – it also serves to enhance lubricity and durability of the tissue. Over the past few decades, a variety of mechanisms have been proposed to account for the low-friction and high wear-resistant properties of articular cartilage. It has been clearly demonstrated that synovial fluid contains lubricant macromolecules that aid in articular cartilage lubrication. These macromolecules adsorb to the surface of the articular cartilage and the mucinous glycoproteins (such as lubricin) generate a lubricious film and significantly reduce friction. The fluid film is also believed to help protect the joint surface from abrasion and degeneration. More importantly, however, the low hydraulic permeability of the fluid phase in conjunction with the tensile strength of the fibrillary collagen network generates substantial interstitial fluid pressurization. As a result, tissue deformation and

consequently contact area are minimized while the interstitial fluid bears the majority of the mechanical load. This interactive process protects the articular cartilage solid phase while minimizing friction [129, 130]. Damage to the complex articular cartilage architecture compromises the material properties of the tissue and results in progressive degeneration as the balance of mechanical forces shift from the fluid phase to the solid phase with increased stress concentrations, surface contact, and wear [128].

Articular Cartilage Damage and Degeneration

Articular cartilage has a limited capacity for self-healing following traumatic injury. Once damaged, the tissue undergoes progressive degeneration and the intrinsic mechanisms for mitigating abrasive wear are compromised. The avascular nature of articular cartilage plays a primary role in the limited regenerative capacity of the tissue as inflammatory mediators and cells that can repair tissue damage are unable to access the damaged cartilage. Furthermore, the dense extracellular matrix prohibits cellular migration of native chondrocytes to the wound site. They are therefore unable to repair the tissue. Direct trauma (e.g. impact), chronic degeneration (e.g. that is caused by joint malalignment), and subchondral bone abnormalities are common factors associated with articular cartilage lesion formation.

According to the International Cartilage Repair Society (ICRS), there are five grades of cartilage lesions based on defect severity. In order of increasing defect severity, grade 0 refers to intact undamaged cartilage; grade I describes articular cartilage softening, blistering, and superficial fissure formation; grade II lesions are focal defects that penetrate less than half of the full tissue thickness; grade III lesions exhibit deep ulceration greater

than half of the full tissue thickness; and grade IV lesions are characterized by full-thickness tissue defects that expose the underlying subchondral bone.

Once compromised, the fibrillar collagen network loses its ability to effectively retain proteoglycans and pressurize the interstitial fluid when the damaged articular cartilage is placed under compression. The solid phase of the articular cartilage bears a more significant proportion of the mechanical load and subsequently is subjected to increased wear. The irregular surface of the articular cartilage surrounding lesions generates stress concentrations where incongruities distribute compressive loads over small surface areas. As increased wear occurs between the joint surfaces, the reduced cartilage surface area causes increasingly higher mechanical stresses leading to additional degeneration and tissue damage, which becomes self-propagating.

Articular Cartilage Cellular Therapy

There are a variety of therapeutic strategies available for treating articular cartilage lesions. Approaches for relief from pain due to cartilage damage and/or articular cartilage repair include: palliative treatments, intrinsic repair enhancement, whole tissue transplantation, and cell-based regenerative therapy [125, 131]. Each of these strategies has specific advantages, limitations, and indications for application. While the most effective treatment remains a controversial topic, increasing clinical experience and post-operative monitoring have demonstrated cell-based regenerative therapies are effective for correcting articular cartilage lesions.

Palliative strategies include arthroscopic debridement, lavage, and chondroplasty. The purpose of these treatments are to reduce pain and improve the mechanical function of joints by removing surface irregularities. The treatment strategy does not restore tissue

and lesions persist, but degradation of the articular cartilage is temporarily mitigated. Cartilage degeneration will continue to progress with time and extended use, but the treatment is generally acceptable for older patients with low physical demand. These treatments are often used as a first step for patients of any age who have small amounts of damage [131].

Intrinsic cartilage repair strategies include subchondral bone microfracture, drilling, and abrasion arthroplasty, collectively termed marrow stimulation. These forms of treatment result in temporary vascularization of the articular cartilage lesion and cells from the bone marrow infiltrate the site where they can repair joint tissue. The cartilage formed through this process is often fibrocartilage and results in a partial filling of the lesion [125]. The fibrocartilage has dissimilar ultrastructural architecture compared to the native articular cartilage and inferior material properties [125]. The irregular collagen network and low proteoglycan content of the fibrocartilage promote tissue degeneration under repetitive dynamic loading and limit the longevity of the treatment [125].

Autologous osteochondral transplant (OATS) and allogenic osteochondral transplant are examples of cartilage repair strategies that rely on whole tissue transplantation. These treatments are fundamentally the same except the allograft is not subject to the constraints of healthy autologous tissue availability and donor site morbidity associated with autografts. Autologous osteochondral transplant is performed by harvesting one or more osteochondral cylinders from a lesser weight-bearing surface and transplanting them into a focal defect. OATS is recommended for treating focal lesions 1 – 4 mm^2. The cartilage tissue is hyaline and exceptional performance characteristics have been reported lasting 5 – 20 years. A limitation associated with this style of treatment is a

lack of surface congruity following osteochondral transplantation and an absence of circumferential cartilage tissue integration. In fact, there is substantial cell death along the margin of the implant. With the removal of subchondral bone for the transplant, reparative fibrocartilage is generated within the margin surrounding the osteochondral unit. Even though the osteochondral transplant has limited circumferential tissue integration above the subchondral bone, osteointegration securely fixes the transplant in place.

Cell-based regenerative strategies include autologous chondrocyte implantation (ACI) and matrix-associated autologous chondrocyte implantation (MACI). These approaches to repairing damaged articular cartilage appear to produce hyaline-like cartilage and may be used to treat large or diffuse defects. However, these therapies require a two-stage treatment process where tissue is extracted from the patient, cells are isolated from the tissue, and then expanded *in vitro* before implantation. After a sufficient population of cells has been cultured, the cells are harvested and injected into the articular cartilage lesion during the second stage of the treatment process. The injected cells are localized and held in place by periosteal or collagen patches sutured in place and sealed with fibrin glue. ACI has shown excellent performance characteristics for 5-11 years without any reported complications within the first 2 years following surgical intervention [125]. ACI post-operative monitoring, however, has shown evidence that implanted cells undergo acute-phase cell death (a common problem for transplanted cells) – potentially limiting treatment efficacy [132].

Of the cartilage repair strategies reviewed, ACI and OATS are generally regarded as superior treatments for larger focal defects and demonstrate improved treatment efficacy and longevity when compared to other available therapies [131, 133, 134]. Microfracture

continues to remain popular because of the low costs of this procedure, but production of fibrocartilage limits therapeutic performance and longevity [125, 134, 135]. Depending on the application and lesion characteristics, ACI or OATS may be more suitable for articular cartilage repair [133, 135]. ACI has exhibited greater therapeutic efficacy and longevity when treating large cartilage defects, but OATS has shown clinical superiority when treating patients with smaller focal defects [134]. Regardless of which strategy is used, both have proven effective for reducing pain, restoring function, and impeding joint degeneration when treating severe articular cartilage lesions. The phenomenon of massive cell death following cell transplant limits the therapeutic efficacy of cell-based regenerative therapies. The addition of scaffolding when used with cellular implants has improved engraftment and cell survival.

Therapeutic Potential of Adipose-Derived Stem Cells

Limited donor cartilage tissue availability has helped fuel the investigation and research on alternative cell sources that provide high quality samples for cell-based regenerative therapies [136]. Adipose tissue is an example of a cell source often termed a cell depot that can in some cases provide cells for therapy [137]. There are several types of adipose tissue within the human body that may be accessed with minimally invasive surgical techniques or as a secondary procedure in conjunction with highly invasive surgical interventions intended to address auxiliary pathologies. White, brown, and mechanical adipose tissue constitute three of the main types of adipose tissue found throughout the body [138]. White adipose tissue is found subcutaneously in the human body. Two main functions of white adipose tissue include insulation and energy supply. Brown adipose tissue is highly vascularized and located around the heart, aorta, and

kidneys of newborns. The supply of this type of adipose tissue decreases with age. The primary function of brown adipose tissue is thermogenic regulation. Mechanical adipose tissue provides specialized structural support for the musculoskeletal system. Infrapatellar and palmar fat pads would be examples of mechanical adipose tissues [138]. The diverse variants and widespread distribution of adipose tissues throughout the body could provide an abundant supply of cells for cell-based regenerative therapies that are easily accessed and less sensitive to supply constraints associated with underlying pathologies or traumatic damage.

During the early stages of embryo development, adipose tissue is derived from the mesoderm germ layer [137]. As a result, a subpopulation of cells obtained from adipose tissue exhibits the phenotypical and functional characteristics of adult mesenchymal stem cells capable of differentiating along adipogenic, chondrogenic, myogenic, and osteogenic lineages [137, 139]. These adipose-derived stem cells (ASCs) have also been shown to participate in the formation of endothelium, hepatocytes, and neurons. ASCs are typically extracted from adipose tissue as part of a heterogeneous cell population known as the stromal vascular fraction (SVF). The stromal vascular fraction is composed of multiple cell types in addition to adult mesenchymal stem cells. This includes: fibroblasts, endothelial cells, pericytes, hematopoietic progenitors, and blood cells [139, 140]. Adipose tissue may be collected by surgical resection or lipoaspiration. The SVF is extracted from the tissue after mechanical mincing (not necessary for lipoaspirates) and enzymatic digestion of the sample. The tissue slurry is centrifuged and density gradient separation yields a SVF cell pellet that may then be used or expanded in culture [141].

In their native environment, ASCs are responsible for the continuous replacement of damaged, dysfunctional, or senescent cells, which support subsequent tissue regeneration and maintenance [142]. Once the SVF is extracted from the adipose tissue, the ASCs within the cell population can be differentiated to cells, which generate a wide variety of tissues. As mentioned previously, the ASCs are capable of differentiating along adipogenic, chondrogenic, myogenic, and osteogenic lineages. Clinically, the SVF cell extracts may be used to aid in wound healing and subcutaneous tissue formation, bone formation and osteointegration, cardiac repair and angiogenesis, and cartilage regeneration.

Currently, clinical trials utilizing ASCs are being investigated for safety and efficacy relative to autologous chondrocyte implantation, microfracture, and osteochondral transplants [143, 144]. Mesenchymal stem cells are ideal because acute-phase cell death may be mitigated by providing a surplus number of cells during transplant. This is an option that is unavailable when using chondrocytes due to low chondrocyte concentrations in cartilage tissue collected for cell harvest. Furthermore, the use of mesenchymal stem cells may reduce the two-stage surgical process for cell-based transplantation to a single surgery. This would eliminate the need for cell culture expansion.

Bioprocessing Extracted Cell Samples

It is well established that the efficacy of cell-based regenerative therapies is limited by massive cell death following transplantation [106, 108, 109, 111-114, 122]. Host inflammatory response, mechanical forces, and hypoxic environmental conditions are believed to contribute to this phenomenon [113]. Articular cartilage is avascular and subsequently protected from the host immune response (assuming the subchondral bone remains intact) [125]. Excessive mechanical loads and hypoxic conditions, however, are

relevant environmental conditions found within damaged diarthrodial joints that contribute to maladaptation of cellular transplants and compromised transplant engraftment [145, 146]. Extracted cell samples will exhibit variable performance characteristics under such harsh environmental conditions, which will depend on extracted sample quality. The quality of a cell sample may be assessed by monitoring cell viability, regenerative capacity, and resilience [147]. Numerous bioprocessing techniques are currently available or under development for enhancing extracted cell sample quality and utility for regenerative therapy [148-150]. These sample bioprocessing strategies include cell sorting, preconditioning, and improved sample extraction and handling practices.

Cell sorting allows target cells within a sample to be selectively enriched through positive and negative selection strategies. Cell sorting strategies may be further categorized as "active" or "passive" based on the method and extent of sample processing. Examples of active cell sorting would include filtration, fluorescence-activated cell sorting (FACS), and magnetic-activated cell sorting (MACS). For these bioprocessing techniques, cell samples are manipulated by directly binding to cell surface markers using magnetic particles or fluorescent dyes conjugated to ligands with selective binding affinities (i.e. MACS, FACS), or the cell sample may be separated by passing a cell suspension through a selective filter [148, 150].

Passive cell sorting does not directly manipulate cell samples with processes that require intimate contact, but relies on indirect manipulation that targets intrinsic cellular properties for selective enrichment or depletion of select cells. Examples of passive cell sorting techniques include density gradient separation, explanted tissue cell migration, and dielectrophoretic (DEP) cell sorting. For density gradient separation, a cell suspension is

centrifuged and heavier cells travel faster and further than less dense cells within the suspension. For explanted tissue samples placed within culture flasks, viable cells will migrate from the tissue and adhere to the culture vessel surface for further expansion. DEP sorting enriches viable cells with intact membranes based on their charge. Nonviable cells with compromised membranes will lose charge.

The advantages of active cell sorting include rapid sample processing and greater selective capabilities for enriching or manipulating cell samples. Disadvantages include the use of expensive reagents, the fact that direct cell manipulation raises regulatory agency concerns regarding safety, the fact that the biocompatibility of samples may be compromised with exposure to various reagents, and the fact that a high degree of processing may cause undesirable changes within the sample cell population [150].

Passive cell sorting techniques may not be as rapid or have as much selective flexibility as active cell sorting, but indirect sample manipulation has advantages that make it suitable for translational medicine. Advantages of passive cell sorting include cost-effective sample processing, minimal sample manipulation and a lower risk of inducing undesirable changes or compromising biocompatibility. In addition, these selective enrichment or depletion processes are less variable and more consistent [151].

Cell sample preconditioning is implemented with the intention of improving or promoting cell survival by exposing extracted cell samples to stressful environmental conditions and stimuli. This style of bioprocessing differs from cell sorting or separation techniques in that it does not attempt to deplete undesirable cells from the sample through a sorting process. The cell stressors may eliminate some cells within the cell cultures, but the number of cells affected in this manner are presumed to be negligible based on

published results. Methods for preconditioning include exposing extracted cell samples to moderate hyperthermic or hypoxic environmental conditions. Cell cultures in which preconditioning treatments are applied demonstrate adjustment to the adverse environmental conditions within 2 – 5 days of culture and marked increases in cell survival [108, 122, 149].

Current tissue resection and cell extraction techniques are inherently destructive processes and adversely affect the viability of extracted cell samples. Accordingly, protocols used to isolate cells from tissue are continually evolving to process samples faster, improve cell yield, and minimize cell damage. For example, when extracting the SVF from explanted adipose tissue, the extracellular matrix may be digested for a long period of time with a low concentration of collagenase to improve cell viability and yield. A high concentration of digestive enzymes may be used to expedite the process of cell isolation but typically result in lower cell yields. Human error can represent a substantial contribution to variable sample quality and, as a result, automated systems have been developed for use in laboratory and clinical settings to improve extracted cell sample quality.

Summary and Specific Aims

The purpose of this research was to develop a process for enhancing extracted cell sample quality for cell-based regenerative therapeutic applications. Current methods for cell sample bioprocessing focus on selective enrichment of target cells, preconditioning to promote cell survival, and improved sample handling practices. Most processes focus on addressing only a single parameter such as sample viability, regenerative capacity, or cell resilience. We have developed a protocol for processing extracted cell samples and

simultaneously enhancing all three characteristics. Furthermore, the process is expedient, reproducible, scalable, and as such compatible with the requirements of translational medicine [152]. Limitations of current viable cell enrichment strategies are contingent on the method used for measuring cell viability. One of the most common methods for determining cell viability is assessing membrane integrity. Cell membrane integrity may be compromised temporarily in living cells and membrane integrity is not compromised in dying cells until the later stages of apoptosis and necrosis. Accordingly, measurements based on cell membrane integrity are susceptible to false results both positive and negative. These measurements are also limited and unable to provide any feedback concerning cellular functional capacity. Limitations with regenerative cell enrichment strategies are associated with the use of surface markers to selectively label and isolate stem cells. No singular, definitive marker exists to distinguish a stem cell from other cell types. In addition, this active cell sorting strategy may stimulate the cell in an undesirable fashion or compromise their biocompatibility after processing. Furthermore, resilient cell enrichment practices may improve cell survival under certain conditions but inefficient or damaged cells are not removed from the samples. They present a cytotoxic risk to the rest of the population. In addition, the inefficient cells occupy a portion of the space that could otherwise be populated by productive cells.

We hypothesize that extracted cell samples contain a relatively large population of inefficient, damaged, or senescent cells. More importantly, this population of cells may detract from the efficacy of cell-based regenerative therapies by exacerbating issues of cell survival post transplantation and synthesis of inferior matrix components while wasting nutrients and space. We have developed a selective process for enhancing extracted cell

sample quality based on metabolic activity. By exposing extracted cell samples to nutrient deficient conditions we aim to:

1) enhance sample quality with minimal processing in a timely manner,

2) retain the regenerative capacity of adult mesenchymal stem cells exposed to the treatment process, and

3) create a cost-effective, scalable protocol for processing cell samples that may be applied in clinical settings to enhance a wide range of cell-based regenerative therapies.

In the following two chapters, I describe a process for enhancing extracted cell sample quality through selective enrichment. I summarize the results, discuss implications of our experimental findings, and describe future work which should be conducted to further elucidate the bioprocessing impact on cell samples and the utility of the samples for use in regenerative medicine, diagnostics, and biopharmaceutical production.

CHAPTER 7: A NOVEL BIOPROCESSING TECHNIQUE FOR ENHANCING CELL SAMPLE QUALITY

Introduction

Tissue-extracted cell sample quality likely has a direct impact on the safety and efficacy of cell-based therapies for regenerative medicine. The quality of a cell sample can be predicated based on several factors, which include cell viability, regenerative capacity, and resilience. Processes used to extract cells from tissues are inherently destructive and can yield inconsistent results. Tissues must be mechanically disrupted and enzymatically digested *in vitro* in order to detach cells from the surrounding extracellular matrix. Factors such as tissue health, donor age, tissue handling, and processing time can affect the cell viability and yield. Traditionally, cell extraction procedures are performed manually exacerbating issues with extracted cell sample quality and reproducibility [100]. In order to mitigate variation and improve quality, automated cell extraction devices have been developed and are being prepared for use in the clinical setting. Even so, different automated cell extraction devices exhibit inconsistent performance characteristics – especially with respect to cellular viability. The goal of this research was to develop a means to selectively enrich stromal cell extracts with viable cells having the regenerative capacities necessary for clinical therapy in part to mitigate the damaging effects of cell extraction.

Current strategies for enhancing cell sample quality consist of automated cell isolation and cell culture preconditioning. Methods for automated cell isolation may

further be categorized as active or passive processes. Active cell isolation technologies rely on direct sample manipulation to enrich target cells within a sample using positive or negative selection strategies. Laboratory techniques, which fall under this category, include fluorescence activated cell sorting (FACS) and magnetic activated cell sorting (MACS). In both cases, cell separation is contingent on the selective binding of cell surface antigens of a target cells with either fluorescent labels (FACS) or magnetic particles (MACS) which may subsequently be used to enrich or deplete the identified cells. FACS may also be used to enrich viable cells by selectively labeling intracellular components of cells with compromised membranes. Passive cell isolation technologies rely on intrinsic cellular properties to selectively enrich cells within a sample and the separation process is primarily regulated by the cells themselves. Examples of intrinsic cellular properties for passive cell isolation include differential surface binding kinetics of adherent cells suspended in media and cellular migration from tissues to other surfaces for cell culture expansion. Active cell sorting techniques are capable of processing samples more rapidly than passive approaches, but passive cell sorting is less detrimental to the sample and mitigates the risk of compromising biocompatibility and clinical utility. Cell sample preconditioning treatments have been developed in the interest of improving transplant cell survival and preventing the phenomenon of massive cell death. For this strategy, cells are exposed to stressors under controlled conditions to induce expression of cell survival mechanisms by elevating heat or oxidative stress. The conditioned cells are then better suited to survive the inhospitable, wound environment where they are placed. Preconditioning promotes resilience but does not address extracted cell sample quality with respect to initial cell viability or regenerative capacity.

We have developed a bioprocessing technique to enhance the quality of adipose-derived stem cells (ASCs) for regenerative therapy. The specific aim of this study was to assess the feasibility of using nutrient deficient conditions to selectively enrich viable cells from extracted cell samples. Efficacy of the bioprocessing treatment was evaluated by measuring the metabolic activity of separated cell sample subpopulations and their capacity to differentiate along adipogenic, chondrogenic, and osteogenic mesenchymal stem cell lineages. We hypothesize that:

1) extracted cell samples are composed of a spectrum of cells exhibiting variable ranges of viability and regenerative capacity;

2) treatment-sensitive cells exhibit greater metabolic activity than treatment-resistant cells;

3) nutrient deficient conditions will not have a negative impact on the regenerative capacity of viable treatment sensitive cells.

The rationale behind this approach to enhancing extracted cell sample quality is multifaceted. During early stages of starvation, the cytoskeleton of a cell is remodeled and focal adhesions are compromised eventually leading to shedding of cells from adherent surfaces. The intracellular changes associated with starvation-induced autophagy and apoptosis are not yet fully understood. There continues to be debate over process dependent cytoskeletal integrity. For example, depolymerization of cytoskeleton is believed to occur during apoptosis but inhibited during autophagy to preserve transport functions within the cell. Autophagy is a catabolic process and an important cell survival mechanism capable of preserving basal cellular metabolic function in response to nutrient stress. It would stand to reason that autophagy would be a precursor to apoptosis in the context of promoting cellular survival. Shedding provides a nutrient-deprived cell an

opportunity to relocate to a nutrient-rich location. Accordingly, the premise of the novel bioprocessing technique is starvation-induced cell separation and coincidently enrichment of viable cells with regenerative capacity. Cells unable to respond to the inhospitable environment are left behind. Furthermore, the bioprocessing technique is rapid and compliant with translational research requirements for expedient, scalable sample processing.

During cell culture expansion, more efficient cells may outcompete less efficient cells for space and nutrients but this compensation requires a significant amount of time. By using adipose tissue as the cell source, a large volume of tissue may be processed in a short amount of time to yield higher quality cell samples. The process is dependent on an intrinsic cellular property and is therefore robust and reproducible. Finally, the treatment may prove more beneficial for improving transplant efficacy for a broader range of regenerative therapies than hypoxic or hyperthermic preconditioning. Preconditioning treatments require 1-5 days of cell culture exposure.

Materials and Methods

Cell Extraction and Culture Expansion

Human adipose tissue was obtained from patients undergoing total knee replacement surgery originally approved by the University of Arizona Investigational Review Board (Project # 01-0770-01). Portions of the infrapatellar fat pad were isolated for processing from the discarded tissue. Connective tissue, bone fragments, and blood vessels were aseptically removed from the tissue sample before mechanical and enzymatic disruption of the tissue and isolation of the stromal vascular fraction (SVF). The SVF was

a heterogeneous population of cells consisting of endothelial cells, fibroblasts, hematopoietic progenitor cells, and adult mesenchymal stem cells. It was extracted from the adipose tissue according to previously established methods. In brief, the adipose tissue was minced and intermittently rinsed with Delbucco's cation free phosphate buffered saline (DCF-PBS) until the tissue reached a slurry-like consistency. The tissue slurry was then combined with CIzyme AS collagenase solution (0.35 WU/mL) at a 1:1 ratio (v/v) and incubated for 2 hours at 37°C. Samples were periodically inverted at 30 minute intervals to enhance digestion. After 2 hours, cells freed from the extracellular matrix (ECM) were isolated by centrifuging at 1500 rpm for 8 minutes. The resulting cell pellet was then resuspended in Delbucco's Modified Eagle Medium (DMEM) supplemented with 10% fetal bovine serum (FBS) and 1% penicillin-streptomycin. The isolated cells were transferred to a tissue culture vessel for expansion. The cell samples were expanded in T-75 or T-182 culture vessels and incubated at 37°C and 5% CO_2. Cell cultures were provided fresh, complete media every 48 hours until reaching approximately 85% confluence. After reaching near confluence, cells were used for experimental studies, passaged, or stored for later use. Prior to storage, cell suspensions were counted using a hemocytometer and centrifuged to form a cell pellet. Next the supernatant was removed, and the cell pellet was resuspended in DMEM supplemented with 10% DMSO to yield a final concentration of $1x10^6$ cells/mL. Supplemented cell suspensions were then transferred to cryovials and stored in a -80°C freezer (for short-term storage) or in a -196°C Dewar (for long-term storage).

Stress-Induced Cell Separation

Cell cultures were exposed to nutrient-deficient conditions during their exponential growth phase after they were at approximately 85% confluence. Once the cell culture reached the appropriate level of confluence, cell growth media was removed from the culture vessel and the cell culture was rinsed with phosphate buffered saline (PBS) three times in order to remove residual media. After the final wash, fresh PBS was transferred to the cell culture vessel at a volume equal to the volume of growth media that had been removed. The culture vessel was then returned to an incubator and maintained at 37°C and 5% CO_2 for a period of 60 minutes. At 15 minute intervals, the cell culture was monitored using an inverted phase-contrast microscope to assess the impact of nutrient-deficient conditions. After 60 minutes, the culture vessel was removed from the incubator and given a single, abrupt tap with the palm of the hand to dislodge partially adherent cells from the culture vessel surface. At this point, the original cell culture was split into two distinct subpopulations consisting of treatment-sensitive cells (suspended in PBS) and treatment-resistant cells (attached to the culture vessel). For further expansion and characterization, treatment-sensitive cells were transferred to new culture vessels at a 1:3 ratio (original culture vessel:new culture vessels). The new culture vessels were then supplemented with complete growth medium at a ratio of 1:2 cell suspensions to growth medium. The appropriate volume of fresh growth medium was also added to the original culture vessel containing the treatment-resistant cells. After 12 hours, the diluted growth media previously added to the treatment-sensitive cell culture vessels was replaced with fresh, complete growth medium.

Treatment efficacy and reproducibility were assessed by manually counting treatment-sensitive cells with a hemocytometer. A cell sample extracted from adipose tissue was grown to near confluence within a T-75 culture vessel and then split among six T-75 culture vessels. Once the culture vessels reached approximately 85% confluence, three culture vessels were used to estimate the total number of cells present before treatment while the remaining three culture vessels were treated to obtain treatment-sensitive and treatment-resistant cell populations for counting. Treatment-sensitive and treatment-resistant cell culture subpopulations were obtained according to the method previously described. Samples were pelleted and resuspended in phenol-free DMEM supplemented with 10% FBS (for use in metabolic assay). Duplicate hemocytometer-derived counts were obtained for each sample. A hand tally counter was used to count the cells present over a cumulative 4 mm^2 region (on each of the 4 corners of the grid). Since cell counts obtained using hemocytometers for cell concentrations less than 1×10^5 cells/mL suffer from inaccuracy and variability, cell pellets suspected of having low cell numbers were suspended in smaller volumes prior to counting to increase cell suspension concentrations. Therefore, treatment-resistant cells (which appear to constitute less than half the total cell culture population) were resuspended in half the volume of media (0.5 mL) that was used for other samples.

Metabolic Activity

To assess the metabolic activity of the cell culture subpopulations, samples were exposed to complete growth media supplemented with resazurin sodium salt which is a blue non-fluorescent dye that is enzymatically reduced by metabolically active cells to resorufin – a pink and highly fluorescent compound. The resazurin solution was prepared

by dissolving 7.5 mg of resazurin sodium salt in 50 mL of phenol-free DMEM. Treatment-sensitive and treatment-resistant cells were obtained from the culture vessels previously used for determining treatment efficacy and reproducibility. After cell concentrations were determined by hemocytometer for the treatment-sensitive and treatment-resistant cell subpopulations, cells were transferred to one of two 6-well plates for use in the metabolism assay. Each well was seeded with 3.5×10^4 cells and supplemented with phenol-free DMEM to yield a total volume of 2 mL per well. Samples were incubated at 37°C with 5% CO_2 over the duration of the study. After 8 hours of incubation, samples were inspected to confirm cell adhesion to the culture well surfaces and 400 µL of resazurin solution was added to each of the six wells. After a subsequent 4 hour incubation period, 3 µL of media was extracted from each sample and transferred to methyl methacrylate cuvettes for fluorescent interrogation. The 3 µL media droplets were diluted in each cuvette with 3 mL of PBS to provide a sample with adequate volume for fluorescent measurement at a concentration low enough to avoid saturation of the spectrofluorometer. The fluorescence emission spectrum, ranging from 570 – 610 nm, was recorded for each sample interrogated with a 560 nm excitation wavelength. Samples were subsequently collected and fluorometrically evaluated after 4, 6, 8, 10, and 16 hours.

Induction of Multilineage Differentiation

Extracted cell samples were obtained from three separate donors to assess the regenerative capacity of the cell culture subpopulations. Samples were initially expanded in T-75 culture vessels and then transferred to T-182 culture vessels (1:2 split) for further growth. Large culture vessels were used for cell culture expansion to ensure sufficient cell concentrations could be harvested for differentiation experiments. For each sample, one

of the two T-182 culture vessels was treated according to the procedure outlined earlier for stress-induced cell separation. Accordingly, treatment-sensitive and treatment-resistant cell cultures were obtained for each extracted cell sample in addition to an untreated cell culture in the remaining T-182 culture vessel. Treatment-sensitive cells were transferred to T-182 culture vessels after the initial treatment. Treatment-sensitive and treatment-resistant cell cultures received follow-up treatments 24, 48, and 72 hours after the first treatment to enrich the subpopulation cell cultures. *StemPro* differentiation kits were used to induce adipogenesis, chondrogenesis, and osteogenesis of collected samples. Protocols supplied with the differentiation kits were followed after preliminary bioprocessing of the extracted cell samples.

For adipogenic differentiation studies, cells were seeded into 12-well plates at a concentration of 1×10^4 cells/cm^2. Treatment-sensitive and treatment-resistant cells obtained from each donor were evaluated in triplicate. The cells were incubated at 37°C and 5% CO_2 for 72 hours before media was replaced with complete adipogenic differentiation medium. Incubation was continued for 21 days and spent media was replaced every 72 hours. After 21 days, media was removed from the 12-well plates and the wells were rinsed once with PBS. Cells were fixed with 4% formaldehyde solution for 30 minutes, rinsed twice with deionized water, and stored in ethanol prior to histological staining. Fixed samples were stained with Oil Red O solution for 10 minutes and rinsed with distilled water to remove residual stain. Samples were visualized using phase-contrast microscopy.

For chondrogenic differentiation studies, micromass cultures were formed in 12-well plates with 5 µL droplets of cell solutions containing 1.6×10^7 cells/mL. Micromasses

were generated in triplicate for both treatment-sensitive and treatment-resistant cells derived from each of the extracted cell samples for a total of six samples. The micromass cultures were incubated for two hours to allow samples to coalesce. After 2 hours, complete chondrogenic differentiation medium was added to the samples and replaced every 72 hours for 21 days. After 21 days, media was removed from the 12-well plates and the wells were rinsed once with PBS. Cells were fixed with 4% formaldehyde solution for 30 minutes, rinsed twice with deionized water, and stored in ethanol prior to histological staining. The chondrogenic micromasses were stained with 1% Alcian Blue solution prepared in 0.1 N HCl for 30 minutes. Samples were rinsed three times with 0.1 N HCl and distilled water to neutralize the acidity. Samples were visualized using phase-contrast microscopy.

For osteogenic differentiation studies, cells were seeded into 12-well plates at a concentration of 5×10^3 cells/cm^2. Treatment-sensitive and treatment-resistant cells were evaluated in triplicate and plated in separate wells for a total of six samples. The cells were incubated at 37°C and 5% CO_2 for 72 hours before media was replaced with complete osteogenic differentiation medium. Cultures were fed every 72 hours for 21 days. After 21 days, media was removed from each of the 12-well plates and samples were rinsed once with PBS before being fixed with 4% formaldehyde solution for 30 minutes. Fixed samples were then rinsed twice with distilled water and stored in ethanol prior to histological staining. The osteogenic cell samples were stained with 2% Alizarin Red S solution for 3 minutes. Wells were rinsed with distilled water to remove residual stain solution and samples were visualized using phase-contrast microscopy.

Data Analysis

Measurements were averaged and standard deviations were calculated. Results were presented as averages ± standard deviations. All statistical comparisons in this study were performed using two-tailed, unpaired t-tests. P-values less than 0.05 were considered statistically significant.

Results

Bimodal Cellular Response to Nutrient Deprivation

Within 15 minutes of incubation, SVF cell cultures exposed to nutrient-deficient environmental conditions demonstrated sporadic morphological changes (Figure 7.1A). Only a small number of cells appeared to respond early in the treatment process. As time progressed, however, the proportion of cells responding to the nutrient-deficient conditions increased (Figure 7.1B). Prior to treatment, cells within the SVF cell cultures exhibited normal morphologies typified by spreading with distinct actin bundles and focal adhesions. Cells responding to the lack of nutrients within the environment underwent progressive cytoskeletal remodeling with a concomitant disruption of focal adhesions. These treatment-sensitive cells ultimately contracted into spherical shapes and some detached from the culture vessel surface. After 60 minutes, cells that did not detach automatically were easily released from the culture vessel surface with an abrupt tap of the culture vessel with the palm of the hand. More than half of the cells released from the culture vessel surface after treatment. Cells that remained adherent throughout the duration of the treatment exhibited limited or delayed morphological changes (Figure 7.1C).

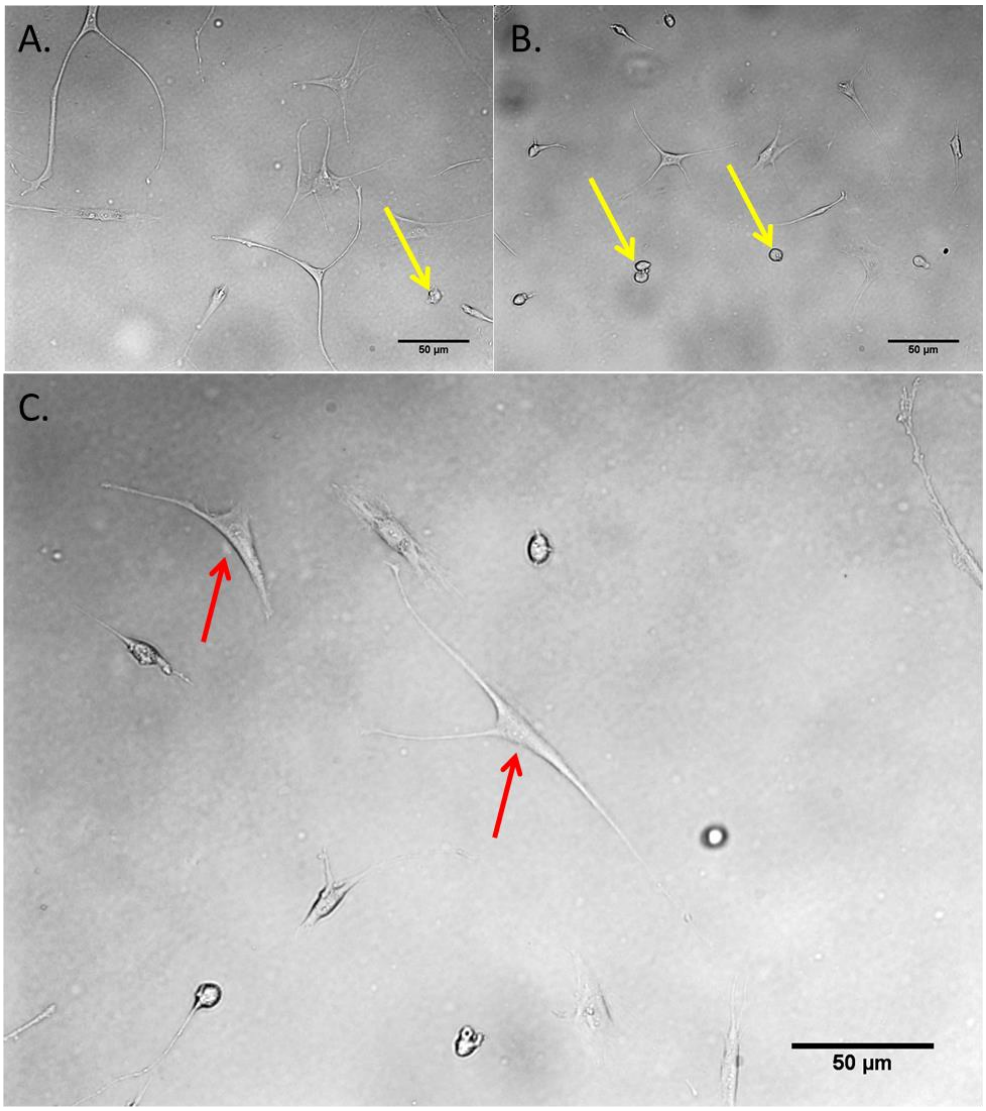

Figure 7.1. Images of a SVF cell culture progressing through stages of nutrient deprivation. (A) Image of cells after 15 minutes of treatment. Cells largely exhibit normal morphologies – sporadic cellular response observed in some cells (yellow arrow) as cells began to contract. (B) Image of cells after 30 minutes of treatment and an increased proportion of cells change (yellow arrows) and contract. (C) Image of cells after 55 minutes of treatment and some cells continue to exhibit little to no morphological response (red arrows). Scale bar in lower right corner of each image represents 50 µm.

Hemocytometer-derived cell counts obtained from three untreated cell cultures indicate that an average of $1.4 \times 10^6 \pm 1.4 \times 10^5$ cells are present within the 80% confluent T-75 culture vessels. The total cell counts for the derived treatment-sensitive and treatment-resistant cell culture subpopulations were $8.4 \times 10^5 \pm 6.7 \times 10^4$ cells and $1.2 \times 10^5 \pm 3.1 \times 10^4$ cells, respectively. According to these measurements, the treatment-

sensitive cell culture subpopulation accounted for 63.2 ± 4.8% of the total cell sample and the treatment-resistant cell culture subpopulation accounted for only 9.1 ± 2.2% (Figure 7.2). A total of 27.7 ± 7% of the cells did not fall into either of these populations. It is likely, the total cell counts for the treatment-resistant cells are lower than anticipated due to cell death during handling (trypsinization and centrifugation).

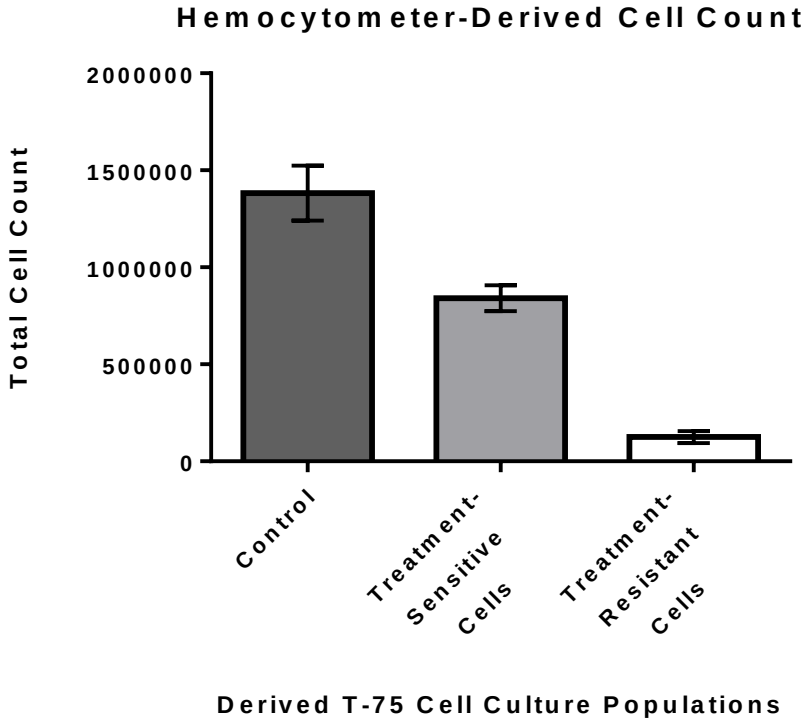

Figure 7.2. Cell culture subpopulations. The bar graph shows the average SVF cell counts and standard deviations for untreated cell cultures and cell culture subpopulations after stress-induced cell separation. Theoretically, the sum of the two cell culture subpopulations would be equivalent to the total cell count for untreated SVF cell cultures. The standard deviations for cell culture subpopulation cell counts were reasonably low suggesting accurate and reproducible results.

Just as treatment-sensitive and treatment-resistant cells exhibited irregular responses to nutrient deprivation, the cell culture subpopulations exhibited different morphologies and growth kinetics during subsequent expansion. Treatment-sensitive cells maintained normal cellular morphologies noted prior to treatment and continued to

proliferate in a normal fashion (Figure 7.3A). Treatment-resistant cells, however, expressed atypical morphologies characterized by highly branched cells with long, filamentous extensions and large, round cells with irregular and wavy membrane structure (Figures 7.3B and 3C). The treatment-resistant cells remained spaced apart with substantial gaps between cells. Nucleating islands of tightly packed cells appeared early after the first treatment of the SVF cell cultures but were eliminated with subsequent treatments. A total of 2-3 follow-up treatments of nutrient-deprivation were required to entirely eliminate nucleating cellular deposits.

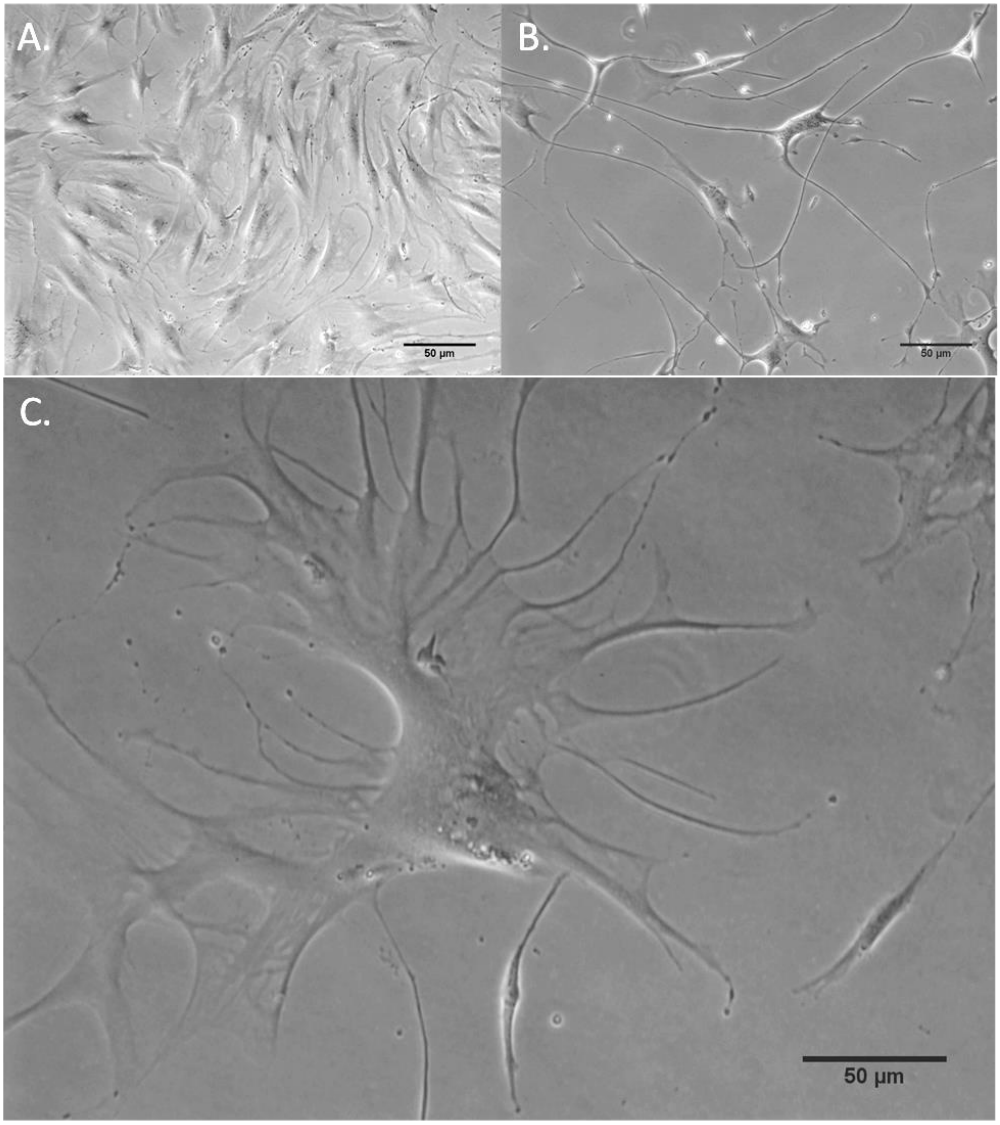

Figure 7.3. Characteristic SVF cell culture subpopulation morphologies. (A) Image of treatment-sensitive cell culture with cells exhibiting typical spacing and morphological expression as cells are well spread with distinct actin bundles and focal adhesions. (B and C) Image of treatment-resistant cells exhibiting atypical spacing and cell morphologies characterized by a high degree of branching with long filamentous extensions and sheet-like cells irregular membranes. Scale bar in lower right corner of each image represents 50 µm.

Metabolic Activity of SVF Subpopulations

Treatment-sensitive and treatment-resistant SVF cell culture subpopulations demonstrated a significant disparity in metabolic activity after four hours of exposure to

resazurin sodium salt solution (Figure 7.4). Treatment-sensitive cell samples reduced the resazurin dye more rapidly than the treatment-resistant cell samples. In Figure 7.4, a large increase in resazurin reduction was observed after 4 – 6 hours for treatment-sensitive cell samples. Treatment-resistant cells required 16 hours to enzymatically reduce enough resazurin dye to reach the relative fluorescence intensity achieved by the treatment-sensitive cell samples in 6 hours.

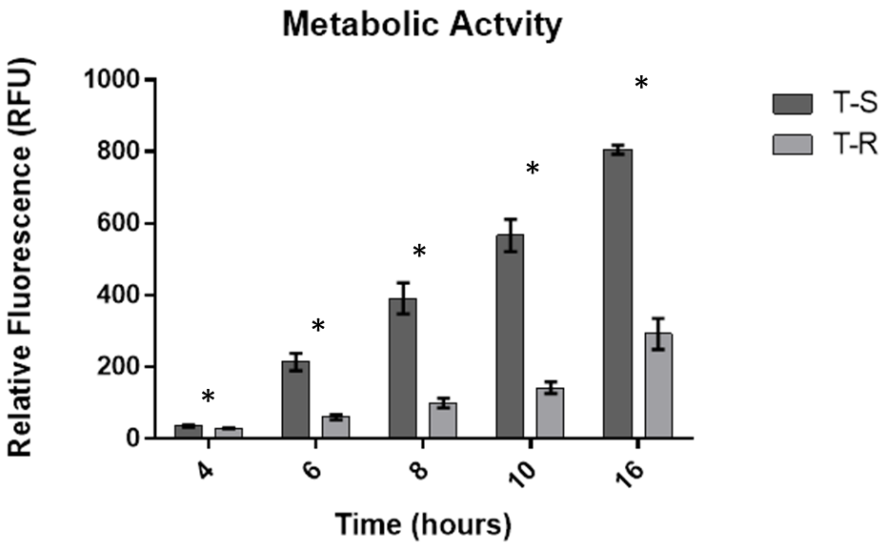

Figure 7.4. Metabolic activity of SVF cell culture subpopulations. Treatment-sensitive (T-S) cell samples more readily reduced resazurin to resorufin than the treatment-resistant (T-R) cell samples. *The difference between measurements were statistically significant between the two populations for all time points (P-values: 0.0411, 0.0004, 0.0004, 0.0001, < 0.0001).

Based on the changes in relative fluorescence between measurements (Figure 7.5), treatment-sensitive cells demonstrated a non-linear metabolic conversion of resazurin to resorufin after 6 hours of incubation. From 5 – 10 hours, the rate of metabolic conversion of the dye appeared to plateau for treatment-sensitive cell samples and exhibited roughly linear characteristics. Two treatment-sensitive samples returned to a non-linear state of dye conversion after 10 hours, but one sample continued to plateau. The treatment-

resistant cells, however, reduced the dye compound at a linear rate for 10 hours before experiencing a non-linear increase in conversion.

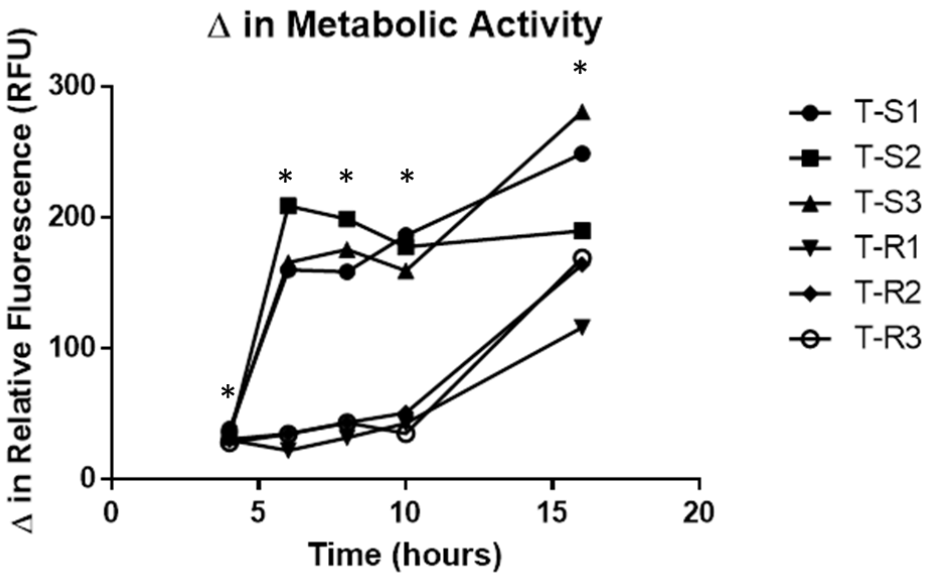

Figure 7.5. Changes in metabolic activity and the rate of resazurin solution reduction. Two treatment-sensitive cell samples demonstrated non-linear metabolic activity rates over the duration of the study (T-S1 and T-S3). These samples appeared to briefly plateau before continuing with an upward trend. One of the treatment-sensitive samples (T-S2) plateaued after 6 hours and demonstrated a sustained, linear metabolic activity rate. Treatment-resistant cell samples demonstrated linear metabolic activity rates during the first 10 hours of the study. After 10 hours, the metabolic activity rates of the treatment-resistant cell samples increased in a non-linear fashion. *Changes in metabolic activity were statistically significant for the averaged data sets obtained from both SVF cell culture subpopulations for each time point (P-values: 0.0411, 0.0008, 0.0004, 0.0001, 0.0461).

Capacity for Multilineage Differentiation

There was a stark contrast in the regenerative capacity of treatment-sensitive and treatment-resistant SVF cell culture subpopulations during adipogenic, chondrogenic, and osteogenic differentiation. After 6 days of sample incubation with differentiation media, treatment-resistant cell samples appeared to react unfavorably to growth factor stimulation. Cells could be seen floating in the media and cell fragments were dispersed across the cell culture wells. A portion of the seeded treatment-resistant cells remained adherent to the

culture well surface. However, after 9 days, all treatment-resistant cells had died. Within the first 6 days, the micromasses generated with treatment-resistant cells disaggregated and the cells eventually lysed.

Treatment-sensitive samples remained viable throughout the differentiation experiment and the micromasses maintained structural integrity (Figure 7.6). The treatment-sensitive cells readily differentiated along adipogenic, chondrogenic, and osteogenic cellular lineages. Unfortunately, one of the chondrogenic micromasses was physically lost during histological processing. Control samples grown in parallel with the SVF cell culture subpopulations remained viable over the duration of the experiment. Control samples (which were not exposed to differentiation growth medium) stained negatively for the presence of adipogenic, chondrogenic, and osteogenic differentiation indicators.

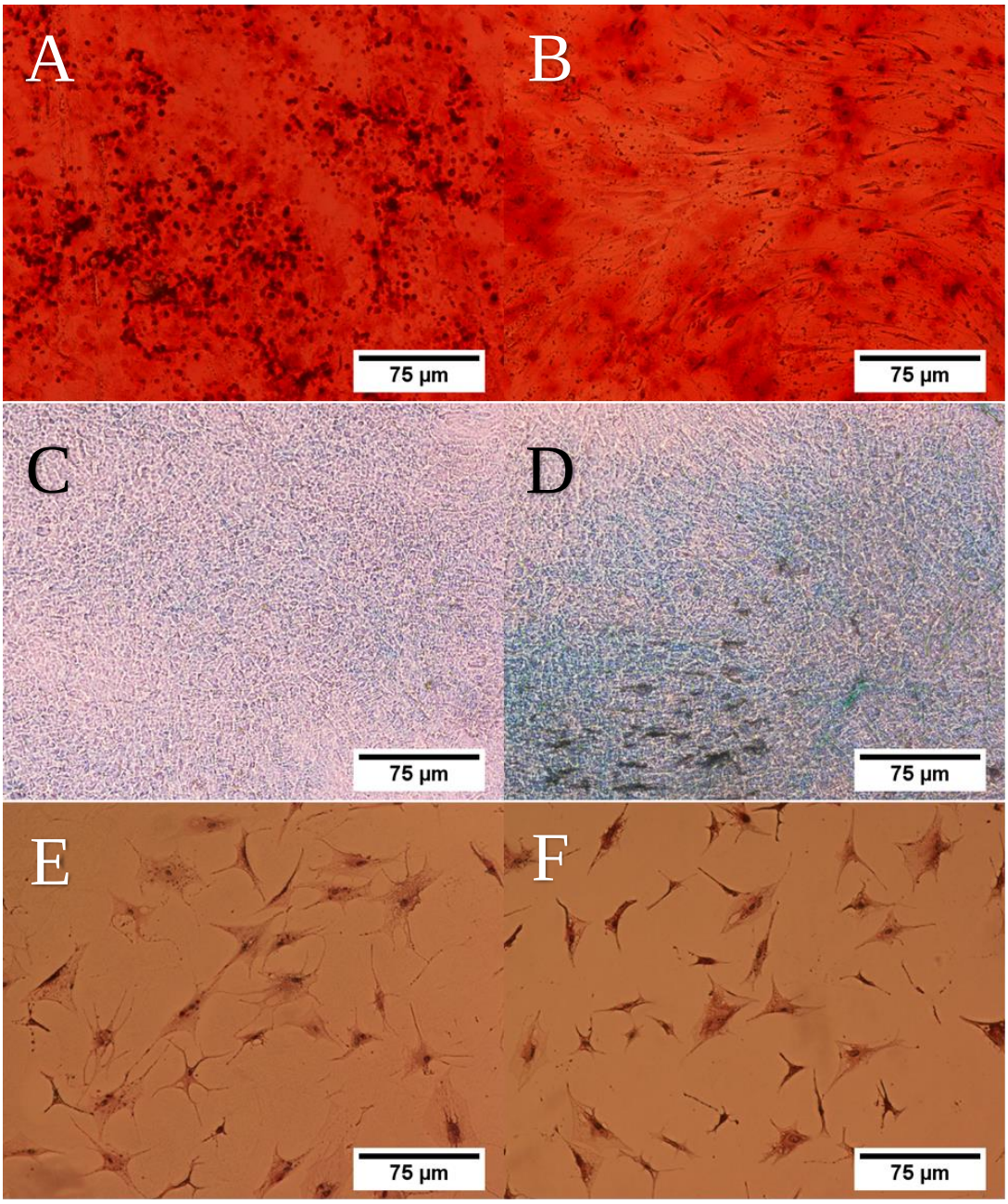

Figure 7.6. Adipogenic, chondrogenic, and osteogenic differentiation of treatment-sensitive cells. (A, B) Images show positive Alizarin Red staining of calcium deposits in treatment-sensitive cell samples exposed to osteogenic differentiation conditions. (C, D) Images show positive Alcian Blue staining of proteoglycans synthesized by treatment-sensitive cell samples exposed to chondrogenic differentiation conditions. (E, F) Images show positive Oil Red O staining of triglyceride deposits in treatment-sensitive cell samples exposed to adipogenic differentiation conditions. Scale bars are 75 µm long.

Discussion

The efficacy of cell-based regenerative therapy is contingent on the quality of the cell samples used for treatment. Low-quality cells used in any process will have a negative impact upon process efficiency and limit end-product properties. Three factors that may be used to assess cell quality include cell viability, regenerative capacity, and resilience. The viability of cells within an extracted cell sample is an important parameter because nonviable cells cannot contribute to product synthesis and pose a risk to viable cells should they lyse and release cytotoxic agents. Cell viability is insufficient for measuring extracted cell quality. Viable cells within a cell culture have variable capacities for regeneration and survival, independent of cell type. Deficiencies in any of the three quality indicators is detrimental to process efficiency and efficacy for cell-based technologies. The results from this study clearly demonstrate that our novel bioprocessing technique extends beyond selective enrichment of viable cells and provides an enhanced extracted cell sample.

One major obstacle to selective enrichment of viable cells extracted from tissue is the absence of a distinct cell-surface biomarker to identify viable or nonviable cells. Arrays of assays have been developed for quantifying cell viability based on dye-exclusion, nutrient consumption/waste production, and auto-fluorescent components of metabolic pathways. A large number of cell sorting technologies are also available that were designed for enriching cells including fluorescence-actuated cell sorting (FACS), magnetic-actuated cell sorting (MACS), size-exclusion (filtration), and target cell capture with functionalized substrates. Currently, cell viability is primarily used as a measure to assess the efficacy of cell sorting techniques. Current methods used to measure cell viability have limitations. Dye-exclusion assays, for example, depend on cell membrane integrity to identify viable

(intact) from nonviable (compromised) cells. These assays cannot identify senescent, quiescent, or dead cells with intact membranes. Assays that measure metabolic activity through nutrient consumption or waste product formation are inaccurate because less efficient cells still consume nutrients and produce waste. The proportion of the sample they make-up cannot be accurately measured because the samples also contain more active/efficient cells rapidly metabolizing nutrients or contaminates such as bacteria. These properties used for assessing viability are void of surface marker expression. As a result, current state-of-the art cell sorting technologies are unable to selectively isolate viable cells. In addition, these techniques are expensive, time-consuming, and have the potential to compromise biocompatibility impairing clinical utility.

Cell sorting technologies have been categorized as “active” or “passive”. Active cell sorting involves direct manipulation of cells within cell samples. Passive cell sorting involves relying on functional properties or innate qualities of cells to separate themselves. As noted earlier, the two methods have distinct advantages and limitations. Active cell sorting allows rapid sample processing while passive cell sorting is more time-consuming and less efficient. Active cell sorting can alter cells while passive cell sorting minimizes cell manipulation and expense preserving the biocompatible nature of the sample. In addition, passive cell sorting techniques include non-enzymatic cell extraction, and differential cell-adhesion preserving more of the useful cells.

The results of this study demonstrated that treatment-resistant and treatment-sensitive cell culture subpopulations exhibit distinct metabolic differences. The contribution of metabolic activity as a mechanism for viable cell enrichment was assessed

by examining cellular proliferation, morphology, susceptibility to nutrient deficient environments, and the oxidative-reduction of resazurin sodium salt.

Treatment-sensitive cell populations exhibited characteristics associated with heightened levels of metabolic activity while treatment-resistant cell populations displayed characteristics associated with low metabolic activity. Delineation of at least two distinct cell populations was first observed when different cellular responses were noted during extended cell culture exposure to nutrient deficient conditions. Once cells were separated, treatment-sensitive cell cultures continued to proliferate and exhibited typical cell morphologies. Treatment-resistant cell cultures proliferated slowly and displayed atypical cell morphologies associated with senescent cells. Additional evidence for the integral role of metabolic activity in the viable cell enrichment was obtained from the cell viability assay involving oxidative-reduction of resazurin sodium salt by metabolically active cells. The fluorescent measurements taken with respect to time indicate that the treatment-sensitive cells are more metabolically active than the treatment-resistant cells. Furthermore, the treatment-resistant cells were unable to survive the metabolic demands of growth factor induced cellular differentiation and protein synthesis.

Interestingly, the results obtained from the metabolic activity assay suggest that treatment-resistant cells experience an increased lag growth phase duration (of approximately 10 hours) before entering the logarithmic growth phase compared to the treatment-sensitive cells (Figure 7.5). This may be due to a difference in the characteristic metabolic activity level associated with the distinct cell sample subpopulations, or the difference may be attributed to the fact that treatment-resistant cells must be removed from their adherent state with trypsin. Trypsin is a cytotoxic reagent that will kill cells with

extended exposure [153]. Treatment-sensitive cells readily detach from the plastic culture vessel surface without trypsin and resume metabolic function more rapidly than the treatment-resistant cells. As a result, trypsin is not necessary for passaging SVF cells and the regenerative capacity of cells passaged without trypsin remains intact (Figure 7.6).

Significant outcomes of this study include: 1) validation of a reliable, selective process for enriching viable cells reliant on metabolic activity; 2) an alternative to using trypsin for passaging cells; 3) preservation of stem cell capacity for differentiation after application of the cell selection treatment. The bioprocessing technique for selectively enriching viable cells developed during this study bridges the gap between active and passive cell sorting techniques and consequently shares many of the same advantages without their limitations. The treatment actively sorts cells based on an innate, functional cellular property. Scalable, active cell sorting is necessary to meet the performance requirements for translational research. Large cell samples may be processed in a timely manner. The bioprocessing technique was reliable over a wide range of culture vessels from T-75 to T-182 flasks. The volume of cells processed simply depends on the culture surface area available. Higher volume samples can be processed using multiple culture vessels or specialized, high surface area culture vessels. This technique is not expensive, and therefore quite practical. The treatment is based on an innate, cellular property that is both reliable and robust. Functional cellular properties used for passive cell sorting are repeatable and effective because of these qualities, but require longer processing times.

CHAPTER 9: CONCLUSION

Project Summary

1. A significant fraction of cells (approximately 40%) within extracted cell samples are less metabolically active than the rest of the cell sample population.
    a. This fraction may be subject to change depending on donor age, cell extraction technique (and handling/manipulation), presence of underlying pathologies.
2. The less metabolically active cells exhibit diminished resilience to handling and growth factor stimulation.
3. The more metabolically active cells retain their regenerative capacity after treatment.
4. Metabolically active cells may be isolated from extracted cell samples without the use of trypsin in a passive cell sorting format.
5. The bioprocessing technique is scalable and may be applied to large volumes of cells in a timely process.
6. Cell samples treated with trypsin demonstrated an increased lag phase (approximately 10 hours) before entering exponential/logarithmic growth phase.
    a. Increased lag phase duration may contribute to impaired cell survival and compromise transplant efficacy.
7. The bioprocessing technique is reproducible with different cell types and donor species over a wide range of ages.
8. The two distinct cell sample subpopulations may be reliably separated to generate two cell system models for further research and investigation

Based on the experimental results from these preliminary studies, we have developed a novel bioprocessing technique that may be applied to cell-based regenerative therapies, diagnostics, and biopharmaceutical production. Further experiments are required to fully characterize the advantages and limitations of the bioprocessing technique and establish applications for the enriched cell populations.

Future Work

Over the last four decades, cell-based regenerative medicine has made significant progress toward treating numerous diseases. As this scientific and clinical field continues to evolve, new obstacles are encountered and old obstacles become better understood. These obstacles must be addressed in order for cell therapy strategies to become routine medical practice. Two obstacles that have limited treatment efficacy have been donor tissue availability and cell survival. Alternative cell sources, such as adipose tissue, have served to help alleviate concerns and promote a resurgence of interest in developing cell therapies. These sources still require further investigation and clinical trials to assess both safety and efficacy. Cell survival has been an issue since the inception of cell-based transplant therapy and has been described/characterized with diverse terminology from many studies as massive cell death, seeding efficiency, and acute-phase cell death. Regardless of phrasing, a fraction of the total number of cells transplanted die during the process or shortly thereafter. Factors that appear to affect this phenomenon include cell type, host response, tissue conditions (i.e. nutrient supply), mechanical loads, and the total number of cells transplanted. Interestingly, studies have shown that a decreasing fraction of cells survive transplant with increasing concentrations of transplanted cells. Current strategies for improving seeding efficiency include incorporation of cell scaffolds, enriching cells with desirable properties, preconditioning cell samples, and improving sample extraction and handling prior to transplant. These techniques have demonstrated marked improvement promoting cell survival but have yet to fully resolve the issue of seeding efficiency in a clinically relevant manner.

Over the course of these studies, we have developed a selective process for enhancing extracted cell sample quality by enriching metabolically active cells. Targeting cellular metabolism, we are able to isolate viable, resilient cells with a therapeutically relevant capacity for regeneration. The bioprocessing technique requires minimal sample manipulation, rapidly processes samples, is cost-effective, and scalable for processing large volumes of extracted cells. Furthermore, the process relies on a fundamental biological process and highly conserved processes integral to promoting cell survival. The bioprocessing technique, reliant upon these mechanisms, is therefore robust and highly reproducible – characteristics essential for process standardization and quality control. While the process has been largely treated in the context of cartilage repair, there are numerous alternative applications (repairing infarcted myocardium) and cell-based technologies.

A variety of cell-based technologies may benefit from integrating our novel bioprocessing technique with their current practices. These technologies include tissue engineering, diagnostics, and biopharmaceutical production. Although this research has been evaluated in the context of cartilage repair strategies, the cell treatment strategy has much broader implications for regenerative medicine including regeneration of alternative tissues and improved standardization of tissue engineering protocols. Cell therapy has been a lucrative option for treating myocardial infarctions, but this approach has been limited by poor cell survival. Preconditioning strategies have been effective for improving myocardial regeneration with cell-based therapies, but the process does not deplete undesirable cells. Applying our novel bioprocessing technique to eliminate dysfunctional and damaged cells from the sample may significantly improve treatment efficacy.

Translation of research from the laboratory to the clinical setting continues to remain a significant obstacle for tissue-engineered therapeutics. Engineering tissues with mechanical properties and functional characteristics equivalent to native tissues has proven difficult and limits clinical applicability. Protocols that do not control for extracted cell sample quality prior to tissue cultivation are subject to increased variability and limited tissue properties. Applying the bioprocessing technique to samples prior to cell culture will help establish consistent experimental conditions, reduce confounding factors, and potentially improve engineered tissue properties. Additionally, cells are used as diagnostics for screening drugs and assessing material biocompatibility in cytotoxicity assays. Cell samples may exhibit variable results depending on the fraction of dysfunctional cells present within the cell cultures. Enhanced cell culture quality would potentially improve biocompatibility measurements used early in expensive product and pharmaceutical design processes.

Lastly, the technique may be applied to batch reactors culturing adherent mammalian cells for synthesizing biopharmaceuticals (such as lubricin). Once again, the batch reactors with cell cultures composed of a large fractions of dysfunctional cells will synthesize products less efficiently and less effectively. Enhancing cultures prior to biopharmaceutical production will improve process efficiency, product yield, and product quality consistency.

Based on our experimental results, we have demonstrated an efficient process for enriching metabolically active cells in culture and subsequently enhancing overall sample quality. This process may have significant implications for regenerative medicine. The bioprocessing technique is cost-effective, rapid, highly reproducible, and requires minimal

sample manipulation. Cell cultures do not require exposure to trypsin (cytotoxic to cells) for handling and expansion procedures. In fact, treatment-sensitive cell culture subpopulations demonstrated greater metabolic activity after "transplant" (to new culture vessels) than the treatment-resistant cells which appeared to lag behind the sensitive cells by 10 hours. Those 10 hours may significantly impair the ability of the cells to adapt to the transplant environment and resist stressors.

Future work is necessary to characterize the advantages and limitations of the novel bioprocessing technique for regenerative therapies. Factors that require further investigation include cell type sensitivity, donor age related treatment dynamics, and animal model applicability. We have performed preliminary studies evaluating some of these topics. More research is necessary, however. Additional work may also be invested in improving the treatment protocol to improve efficiency and potentially isolate additional cell subpopulations. Parameters that may be varied include culture temperature, oxygen concentration (oxidative stress), and selective growth factors. While the treatment is already expedient, it should be feasible to cut processing time in half.

REFERENCES

[1] Gaither CC, Cavazos-Gaither AE, editors. Gaither's Dictionary of Scientific Quotations. New York, NY: Springer New York; 2008. p. 652-709.

[2] Schneider WH. Perspectives on Global Health: History of Blood Transfusion in Sub-Saharan Africa. Athens, OH, USA: Ohio University Press; 2013.

[3] McCullough J. Transfusion Medicine. Hoboken, GB: Wiley-Blackwell; 2011.

[4] Grindon AJ. Chapter 2 - Brief History of Blood Transfusion A2 - Abshire, Christopher D. Hillyer, Beth H. Shaz, James C. Zimring, Thomas C. Transfusion Medicine and Hemostasis. San Diego: Academic Press; 2009. p. 9-11.

[5] Myhre BA. The first recorded blood transfusions: 1656 to 1668. Transfusion. 1990; 30:358-62.

[6] Transfusion of Blood, Blood Components and Plasma Alternatives in Oligaemia. Mollison's Blood Transfusion in Clinical Medicine: John Wiley & Sons, Ltd; 2014. p. 22-52.

[7] Goodnough LT, Shander A, Brecher ME. Transfusion medicine: looking to the future. Lancet (London, England). 2003; 361:161-9.

[8] McCullough J. The Blood Supply. Transfusion Medicine: Wiley-Blackwell; 2011. p. 13-30.

[9] Kuehnert MJ, Basavaraju SV. 306 - Transfusion- and Transplantation-Transmitted Infections A2 - Blaser, John E. BennettRaphael DolinMartin J. Mandell, Douglas, and Bennett's Principles and Practice of Infectious Diseases (Eighth Edition). Philadelphia: 2015. p. 3351-60.e2.

[10] McCullough J. Complications of Transfusion. Transfusion Medicine: Wiley-Blackwell; 2011. p. 378-413.

[11] Practical Transfusion Medicine. Somerset, GB: Wiley-Blackwell; 2013.

[12] Marcelis JH. Bacterial Contamination of Blood and Blood Products an Underestimated Problem. In: Sibinga CTS, Dodd RY, editors. Transmissible Diseases and Blood Transfusion: Proceedings of the Twenty-Sixth International Symposium on Blood Transfusion, Groningen, NL, Organized by the Sanquin Division Blood Bank Noord Nederland. Boston, MA: Springer US; 2002. p. 51-6.

[13] Kortbeek LM, Pinelli E. Parasites Transmitted by Blood Transfusion. In: Sibinga CTS, Dodd RY, editors. Transmissible Diseases and Blood Transfusion: Proceedings of the Twenty-Sixth International Symposium on Blood Transfusion, Groningen, NL, Organized

by the Sanquin Division Blood Bank Noord Nederland. Boston, MA: Springer US; 2002. p. 57-71.

[14] Farmer SL, Isbister J, Leahy MF. History of blood transfusion and patient blood management. Transfusion-Free Medicine and Surgery: John Wiley & Sons, Ltd; 2014. p. 1-18.

[15] Maramica I, Shulman IA. Transfusion therapy—Balancing the risks and benefits. Transfusion-Free Medicine and Surgery: John Wiley & Sons, Ltd; 2014. p. 28-60.

[16] Hillyer KL. Chapter 6 - Apheresis Blood Component Collections A2 - Abshire, Christopher D. HillyerBeth H. ShazJames C. ZimringThomas C. Transfusion Medicine and Hemostasis. San Diego: Academic Press; 2009. p. 33-5.

[17] Greene CE, Hillyer CD. Chapter 9 - Component Preparation and Manufacturing A2 - Abshire, Christopher D. HillyerBeth H. ShazJames C. ZimringThomas C. Transfusion Medicine and Hemostasis. San Diego: Academic Press; 2009. p. 45-50.

[18] Kauvar DS, Lefering R, Wade CE. Impact of hemorrhage on trauma outcome: an overview of epidemiology, clinical presentations, and therapeutic considerations. The Journal of trauma. 2006; 60:S3-11.

[19] Kaur P, Basu S, Kaur G, Kaur R. Transfusion protocol in trauma. Journal of Emergencies, Trauma and Shock. 2011; 4:103-8.

[20] Crookston KP, Wilkinson SL, Simon TL. Recruitment and Screening of Donors and the Collection, Processing, and Testing of Blood. Rossi's Principles of Transfusion Medicine: Wiley-Blackwell; 2009. p. 973-92.

[21] Hillyer KL. Chapter 10 - Serologic Testing of Donor Products A2 - Abshire, Christopher D. HillyerBeth H. ShazJames C. ZimringThomas C. Transfusion Medicine and Hemostasis. San Diego: Academic Press; 2009. p. 51-4.

[22] Hillyer KL. Chapter 11 - Overview of Infectious Disease Testing A2 - Abshire, Christopher D. HillyerBeth H. ShazJames C. ZimringThomas C. Transfusion Medicine and Hemostasis. San Diego: Academic Press; 2009. p. 55-9.

[23] Shaz BH. Chapter 17 - Bacterial Detection Methods A2 - Abshire, Christopher D. HillyerBeth H. ShazJames C. ZimringThomas C. Transfusion Medicine and Hemostasis. San Diego: Academic Press; 2009. p. 83-6.

[24] Shaz BH. Chapter 19 - Pretransfusion Testing A2 - Abshire, Christopher D. HillyerBeth H. ShazJames C. ZimringThomas C. Transfusion Medicine and Hemostasis. San Diego: Academic Press; 2009. p. 93-101.

[25] Tedder R, Stanworth SJ, Goldman M. Blood Donation Testing and the Safety of the Blood Supply. Practical Transfusion Medicine: John Wiley & Sons, Ltd; 2013. p. 201-8.

[26] Choudhury N. Transfusion transmitted infections: How many more? Asian Journal of Transfusion Science. 2010; 4:71-2.

[27] Mbanya D. Use of quality rapid diagnostic testing for safe blood transfusion in resource-limited settings. Clinical microbiology and infection: the official publication of the European Society of Clinical Microbiology and Infectious Diseases. 2013; 19:416-21.

[28] Jean-Pierre Allain EV, Ayob Y, Allain J-P, Elizabeth Vinelli,, Ayob. Y. Blood safety in developing countries. Transfusion Microbiology: Cambridge University Press; 2008.

[29] Hassall O, Bates I, Maitland K. 20 - Blood Transfusion in Resource-limited Settings A2 - Ryan, Alan J. MagillDavid R HillTom SolomonEdward T. Hunter's Tropical Medicine and Emerging Infectious Disease (Ninth Edition). London: W.B. Saunders; 2013. p. 162-7.

[30] Lee HH, Allain JP. Improving blood safety in resource-poor settings. Vox Sanguinis. 2004; 87:176-9.

[31] Allain JP, Stramer SL, Carneiro-Proietti AB, Martins ML, Lopes da Silva SN, Ribeiro M, et al. Transfusion-transmitted infectious diseases. Biologicals: journal of the International Association of Biological Standardization. 2009; 37:71-7.

[32] Gabriel AS, Fabio Z, Francisco P, David B-B. Risk for Transfusion-Transmitted Infectious Diseases in Central and South America. Emerging Infectious Disease journal. 1998; 4:5.

[33] Bihl F, Castelli D, Marincola F, Dodd RY, Brander C. Transfusion-transmitted infections. Journal of Translational Medicine. 2007; 5:1-11.

[34] Infectious Agents Transmitted by Transfusion. Mollison's Blood Transfusion in Clinical Medicine: Blackwell Science Ltd; 2005. p. 701-73.

[35] Kitchen AD, Barbara JAJ. Current Information on the Infectious Risks of Allogeneic Blood Transfusion. Alternatives to Blood Transfusion in Transfusion Medicine: Wiley-Blackwell; 2010. p. 21-30.

[36] Tobler LH, Busch MP. History of posttransfusion hepatitis. Clinical Chemistry. 1997; 43:1487-93.

[37] Park YA, Brecher ME. Bacterial Contamination of Blood Products. Rossi's Principles of Transfusion Medicine: Wiley-Blackwell; 2009. p. 773-90.

[38] Eder AF, Kennedy JM, Dy BA, Notari EP, Weiss JW, Fang CT, et al. Bacterial screening of apheresis platelets and the residual risk of septic transfusion reactions: the American Red Cross experience (2004-2006). Transfusion. 2007; 47:1134-42.

[39] Damgaard C, Magnussen K, Enevold C, Nilsson M, Tolker-Nielsen T, Holmstrup P, et al. Viable Bacteria Associated with Red Blood Cells and Plasma in Freshly Drawn Blood Donations. PLoS ONE. 2015; 10:e0120826.

[40] Al-Kobaisi MF. Jawetz, Melnick & Adelberg's Medical Microbiology: 24(th) Edition. Sultan Qaboos University Medical Journal. 2007; 7:273-5.

[41] Azikiwe CCA, Ifezulike CC, Siminialayi IM, Amazu LU, Enye JC, Nwakwunite OE. A comparative laboratory diagnosis of malaria: microscopy versus rapid diagnostic test kits. Asian Pacific Journal of Tropical Biomedicine. 2012; 2:307-10.

[42] Runa F, Yasmin M, Hoq MM, Begum J, Rahman ASMM, Ahsan CR. Molecular versus conventional methods: Clinical evaluation of different methods for the diagnosis of tuberculosis in Bangladesh. Journal of Microbiology, Immunology and Infection. 2011; 44:101-5.

[43] Baron EJ. Conventional versus Molecular Methods for Pathogen Detection and the Role of Clinical Microbiology in Infection Control. Journal of Clinical Microbiology. 2011; 49:S43-S.

[44] Murray PR, Rosenthal KS, Pfaller MA. Medical microbiology. 2013.

[45] Roberts D, Allain J-P, Kitchen AD, Field S, Bates I. Blood Transfusion in a Global Context. Practical Transfusion Medicine: Wiley-Blackwell; 2009. p. 251-61.

[46] Pruett CR, Vermeulen M, Zacharias P, Ingram C, Tayou Tagny C, Bloch EM. The Use of Rapid Diagnostic Tests for Transfusion Infectious Screening in Africa: A Literature Review. Transfusion Medicine Reviews. 2015; 29:35-44.

[47] Brandt D, Figard S. Chapter 5.4 - Immunoassay Development in the In Vitro Diagnostic Industry A2 - Wild, David. The Immunoassay Handbook (Fourth Edition). Oxford: Elsevier; 2013. p. 417-23.

[48] Nichols JH. Chapter 6.3 - Point-of-Care Testing A2 - Wild, David. The Immunoassay Handbook (Fourth Edition). Oxford: Elsevier; 2013. p. 455-63.

[49] Wild D, Sheehan C, Binder S. Chapter 7.1 - Introduction to Immunoassay Product Technology in Clinical Diagnostic Testing. The Immunoassay Handbook (Fourth Edition). Oxford: Elsevier; 2013. p. 509-15.

[50] Wild D. Chapter 1.2 - Immunoassay for Beginners. The Immunoassay Handbook (Fourth Edition). Oxford: Elsevier; 2013. p. 7-10.

[51] Mbanya D. Use of quality rapid diagnostic testing for safe blood transfusion in resource-limited settings. Clinical Microbiology and Infection. 2013; 19:416-21.

[52] Fisher DG, Hess KL, Erlyana E, Reynolds GL, Cummins CA, Alonzo TA. Comparison of Rapid Point-of-Care Tests for Detection of Antibodies to Hepatitis C Virus. Open Forum Infectious Diseases. 2015; 2:ofv101.

[53] Binder S, Isler JA. Chapter 2.8 - Detection of Antibodies Relevant to Infectious Disease A2 - Wild, David. The Immunoassay Handbook (Fourth Edition). Oxford: Elsevier; 2013. p. 149-55.

[54] O'Farrell B. Chapter 2.4 - Lateral Flow Immunoassay Systems: Evolution from the Current State of the Art to the Next Generation of Highly Sensitive, Quantitative Rapid Assays A2 - Wild, David. The Immunoassay Handbook (Fourth Edition). Oxford: Elsevier; 2013. p. 89-107.

[55] Rattle S, Hofmann O, Price CP, Kricka LJ, Wild D. Chapter 2.10 - Lab-on-a-Chip, Micro- and Nanoscale Immunoassay Systems, and Microarrays. The Immunoassay Handbook (Fourth Edition). Oxford: Elsevier; 2013. p. 175-202.

[56] Reed J, Gimzewski JK. Chapter 2.11 - Immunological Biosensors A2 - Wild, David. The Immunoassay Handbook (Fourth Edition). Oxford: Elsevier; 2013. p. 203-7.

[57] Wild D, Kusnezow W. Chapter 3.3 - Separation Systems. The Immunoassay Handbook (Fourth Edition). Oxford: Elsevier; 2013. p. 287-99.

[58] Weeks I, Kricka LJ, Wild D. Chapter 3.2 - Signal Generation and Detection Systems (Excluding Homogeneous Assays). The Immunoassay Handbook (Fourth Edition). Oxford: Elsevier; 2013. p. 267-85.

[59] Liddell E. Chapter 3.1 - Antibodies A2 - Wild, David. The Immunoassay Handbook (Fourth Edition). Oxford: Elsevier; 2013. p. 245-65.

[60] Dent AH. Chapter 3.4 - Conjugation Methods A2 - Wild, David. The Immunoassay Handbook (Fourth Edition). Oxford: Elsevier; 2013. p. 301-13.

[61] Slater HC, Ross A, Ouedraogo AL, White LJ, Nguon C, Walker PGT, et al. Assessing the impact of next-generation rapid diagnostic tests on Plasmodium falciparum malaria elimination strategies. Nature. 2015; 528:S94-S101.

[62] Murphy WG, Katz LM, Flanagan P. Regulatory Aspects of Blood Transfusion. Practical Transfusion Medicine: John Wiley & Sons, Ltd; 2013. p. 169-80.

[63] Clinical Microbiology Procedures Handbook. 3rd ed. Washington, DC: American Society for Microbiology; 2010.

[64] L. S. Powers and C. R. Loyd, "Method and apparatus for detecting the presence of microbes with frequency modulated multi-wavelength intrinsic fluorescence," US Patent 7824883B2, Nov. 2, 2010

[65] C. Estes *et al.*, "Reagentless detection of microorganisms by intrinsic flourescence," in *Biosensors and Bioelectronics,* vol 18, no. 5-6, pp. 511-519, May 2002 & May 2003

[66] A. Duncan and L. Powers, "Low noise amplification for optical arrays," in *Proc. 23rd Annu. Int. Conf. IEEE Eng. Med. Biol. Mag.,* Istanbul, Turkey, Oct. 25-28, 2001.

[67] C. Lloyd *et al*., "Microbioengineering: microbe capture and detection," in *Proc. 23rd Annu. Int. Conf. IEEE Eng. Med. Biol. Mag.,* Istanbul, Turkey, Oct. 25-28, 2001.

[68] L. S. Powers, W. R. Ellis, C. R. Loyd, "Method for the rapid taxonomic identification of pathogenic microorganisms and their toxic proteins," US Patent 20060257929, Nov. 14, 2005

[69] Brandt D, Figard S. Chapter 5.4 - Immunoassay Development in the In Vitro Diagnostic Industry A2 - Wild, David. The Immunoassay Handbook (Fourth Edition). Oxford: Elsevier; 2013. p. 417-23.

[70] O'Farrell B. Chapter 2.4 - Lateral Flow Immunoassay Systems: Evolution from the Current State of the Art to the Next Generation of Highly Sensitive, Quantitative Rapid Assays A2 - Wild, David. The Immunoassay Handbook (Fourth Edition). Oxford: Elsevier; 2013. p. 89-107.

[71] Reed J, Gimzewski JK. Chapter 2.11 - Immunological Biosensors A2 - Wild, David. The Immunoassay Handbook (Fourth Edition). Oxford: Elsevier; 2013. p. 203-7.

[72] Wilde C, Out D, Johnson S, Granger DA. Chapter 6.1 - Sample Collection, Including Participant Preparation and Sample Handling. The Immunoassay Handbook (Fourth Edition). Oxford: Elsevier; 2013. p. 427-40.

[73] Kanter L. Accidental needle stick prevention: an important, costly, unsafe policy revisited. Annals of Allergy, Asthma & Immunology. 2006; 97:7-9.

[74] Eckstein EC, Tilles AW, Millero Iii FJ. Conditions for the occurrence of large near-wall excesses of small particles during blood flow. Microvascular Research. 1988; 36:31-9.

[75] Zielichowska A, Daczewska M, Saczko J, Michel O, Kulbacka J. Applications of calcium electroporation to effective apoptosis induction in fibrosarcoma cells and stimulation of normal muscle cells. Bioelectrochemistry. 2016; 109:70-8.

[76] Dermol J, Miklavčič D. Predicting electroporation of cells in an inhomogeneous electric field based on mathematical modeling and experimental CHO-cell permeabilization to propidium iodide determination. Bioelectrochemistry. 2014; 100:52-61.

[77] Mason H-Y, Lloyd C, Dice M, Sinclair R, Ellis Jr W, Powers L. Taxonomic identification of microorganisms by capture and intrinsic fluorescence detection. Biosensors and Bioelectronics. 2003; 18:521-7.

[78] Djeddi SR, Masoudi A, Ghadimi P. Numerical Simulation of Flow around Diamond-Shaped Obstacles at Low to Moderate Reynolds Numbers. American Journal of Applied Mathematics and Statistics. 2013; 1:11-20.

[79] Naddaf M, Alkhawwam A. Characterization of superhydrophobic a-C:F thin film deposited on porous silicon via laser ablation of a PTFE target. Diamond and Related Materials. 2016; 64:57-63.

[80] Yang H, Zhao TS, Cheng P. Gas–liquid two-phase flow patterns in a miniature square channel with a gas permeable sidewall. International Journal of Heat and Mass Transfer. 2004; 47:5725-39.

[81] Saisorn S, Wongwises S. The effects of channel diameter on flow pattern, void fraction and pressure drop of two-phase air–water flow in circular micro-channels. Experimental Thermal and Fluid Science. 2010; 34:454-62.

[82] Araújo JDP, Miranda JM, Campos JBLM. Flow of two consecutive Taylor bubbles through a vertical column of stagnant liquid—A CFD study about the influence of the leading bubble on the hydrodynamics of the trailing one. Chemical Engineering Science. 2013; 97:16-33.

[83] Abdulkadir M, Hernandez-Perez V, Lo S, Lowndes IS, Azzopardi BJ. Comparison of experimental and Computational Fluid Dynamics (CFD) studies of slug flow in a vertical riser. Experimental Thermal and Fluid Science. 2015; 68:468-83.

[84] Elperin T, Fominykh A. Two models of fluid flow and mass transfer at the trailing edge of a gas slug. International Journal of Heat and Mass Transfer. 1995; 38:3341-7.

[85] Lima LEM, Rosa ES. Comparative analysis of wall shear stress models to the drift-flux model applied to slug flow regime. Journal of Petroleum Science and Engineering. 2014; 122:371-83.

[86] Wang Y, Yan C, Sun L, Yan C. Characteristics of slug flow in a vertical narrow rectangular channel. Experimental Thermal and Fluid Science. 2014; 53:1-16.

[87] Araújo JDP, Miranda JM, Campos JBLM. Simulation of slug flow systems under laminar regime: Hydrodynamics with individual and a pair of consecutive Taylor bubbles. Journal of Petroleum Science and Engineering. 2013; 111:1-14.

[88] Hansra NK, Shinkai K. Cutaneous community-acquired and hospital-acquired methicillin-resistant Staphylococcus aureus. Dermatologic Therapy. 2011; 24:263-72.

[89] Test Method Standard MIL-STD-810G. United States Department of Defense. Methods 501.5, 502.5, 506.5, 507.5, 510.5, 514.6, 516.6 Annex A: Maryland, USA, 2008

[90] Goodship V, Middleton B, Cherrington R. Design and Manufacture of Plastic Components for Multifunctionality. US: William Andrew; 2015.

[91] Fink JK. Polymerization and Manufacture of Polyoxymethylene. Polyoxymethylene Handbook: John Wiley & Sons, Inc.; 2014. p. 21-51.

[92] Raimo M. Structure and Morphology of Polyoxymethylene. Polyoxymethylene Handbook: John Wiley & Sons, Inc.; 2014. p. 163-91.

[93] Fink JK. Physical Properties of Polyoxymethylene. Polyoxymethylene Handbook: John Wiley & Sons, Inc.; 2014. p. 227-40.

[94] Kennedy P, Zheng R. Flow Analysis of Injection Molds (2nd Edition). Hanser Publishers.

[95] Kazmer DO. Injection Mold Design Engineering. Hanser Publishers.

[96] Tempelman E, Shercliff H, van Eyben BN. Chapter 8 - Injection Molding of Thermoplastics. Manufacturing and Design. Boston: Butterworth-Heinemann; 2014. p. 121-56.

[97] Guo J. Solid State Welding Processes in Manufacturing Welding process Manufacturing, solid state welding processes in. In: Nee CAY, editor. Handbook of Manufacturing Engineering and Technology. London: Springer London; 2015. p. 569-92.

[98] Bruder U. Chapter 24 - Assembly Methods for Thermoplastics. User's Guide to Plastic: Hanser; 2015. p. 159-64.

[99] Troughton MJ. Handbook of Plastics Joining - A Practical Guide (2nd Edition). William Andrew Publishing. New York, USA. 2008.

[100] Hicok KC, Hedrick MH. Automated Isolation and Processing of Adipose-Derived Stem and Regenerative Cells #. T Adipose-Derived Stem Cells2011. p. 87-105.

[101] Mailey B, Hosseini A, Baker J, Young A, Alfonso Z, Hicok K, et al. Adipose-Derived Stem Cells: Methods for Isolation and Applications for Clinical Use. T Stem Cells and Tissue Repair. p. 161-81.

[102] Schäffler A, Büchler C. Concise Review: Adipose Tissue-Derived Stromal Cells—Basic and Clinical Implications for Novel Cell-Based Therapies. STEM CELLS. 2007; 25:818-27.

[103] Tubo R. 2 - Fundamentals of Cell-Based Therapies. In: Nerem AALATM, editor. Principles of Regenerative Medicine. San Diego: Academic Press; 2008. p. 16-26.

[104] Ratcliffe E, Thomas RJ, Williams DJ. Current understanding and challenges in bioprocessing of stem cell-based therapies for regenerative medicine. British Medical Bulletin. 2011; 100:137-55.

[105] Wong VW, Sorkin M, Gurtner GC. Enabling stem cell therapies for tissue repair: Current and future challenges. Biotechnology Advances. 2013; 31:744-51.

[106] Robey TE, Saiget MK, Reinecke H, Murry CE. Systems approaches to preventing transplanted cell death in cardiac repair. J Mol Cell Cardiol. 2008; 45:567-81.

[107] Robey TE, Saiget MK, Reinecke H, Murry CE. Systems Approaches to Preventing Transplanted Cell Death in Cardiac Repair. Journal of molecular and cellular cardiology. 2008; 45:567-81.

[108] Haider H, Ashraf M. Preconditioning and Stem Cell Survival. J of Cardiovasc Trans Res. 2010; 3:89-102.

[109] Francis KR, Wei L. Human embryonic stem cell neural differentiation and enhanced cell survival promoted by hypoxic preconditioning. Cell Death and Dis. 0000; 1:e22.

[110] Khan IM, Gilbert SJ, Singhrao SK, Duance VC, Archer CW. Cartilage integration: evaluation of the reasons for failure of integration during cartilage repair. A review. European cells & materials. 2008; 16:26-39.

[111] Archer CW, Redman S, Khan I, Bishop J, Richardson K. Enhancing tissue integration in cartilage repair procedures. Journal of Anatomy. 2006; 209:481-93.

[112] Hill CE, Hurtado A, Blits B, Bahr BA, Wood PM, Bartlett Bunge M, et al. Early necrosis and apoptosis of Schwann cells transplanted into the injured rat spinal cord. The European journal of neuroscience. 2007; 26:1433-45.

[113] Suzuki K, Murtuza B, Beauchamp JR, Brand NJ, Barton PJR, Varela-Carver A, et al. Role of Interleukin-1β in Acute Inflammation and Graft Death After Cell Transplantation to the Heart. Circulation. 2004; 110:II-219-II-24.

[114] Aguado BA, Mulyasasmita W, Su J, Lampe KJ, Heilshorn SC. Improving Viability of Stem Cells During Syringe Needle Flow Through the Design of Hydrogel Cell Carriers. Tissue Engineering Part A. 2012; 18:806-15.

[115] Stephan MT, Irvine DJ. Enhancing Cell therapies from the Outside In: Cell Surface Engineering Using Synthetic Nanomaterials. Nano today. 2011; 6:309-25.

[116] Mastri M, Lin H, Lee T. Enhancing the efficacy of mesenchymal stem cell therapy. World Journal of Stem Cells. 2014; 6:82-93.

[117] Mirsaidi A, Kleinhans KN, Rimann M, Tiaden AN, Stauber M, Rudolph KL, et al. Telomere length, telomerase activity and osteogenic differentiation are maintained in adipose-derived stromal cells from senile osteoporotic SAMP6 mice. Journal of Tissue Engineering and Regenerative Medicine. 2012; 6:378-90.

[118] Perin EC, Silva GV, Henry TD, Cabreira-Hansen MG, Moore WH, Coulter SA, et al. A randomized study of transendocardial injection of autologous bone marrow mononuclear cells and cell function analysis in ischemic heart failure (FOCUS-HF). American Heart Journal.161:1078-87.e3.

[119] Piacibello W, Gammaitoni L, Pignochino Y. Proliferative senescence in hematopoietic stem cells during ex-vivo expansion. Folia histochemica et cytobiologica / Polish Academy of Sciences, Polish Histochemical and Cytochemical Society. 2005; 43:197-202.

[120] Troell R. Adipose-Derived Stem and Regenerative Cells: Harvesting, Processing, and Administration. In: Shiffman MA, Di Giuseppe A, Bassetto F, editors. Stem Cells in Aesthetic Procedures: Springer Berlin Heidelberg; 2014. p. 249-92.

[121] Fernandes TG, Diogo MM, Cabral JMS. Woodhead Publishing Series in Biomedicine: Stem Cell Bioprocessing: for Cellular Therapy, Diagnostics and Drug Development. Jordon Hill, GBR: Woodhead Publishing; 2013.

[122] Haider HK, Ashraf M. Strategies to promote donor cell survival: combining preconditioning approach with stem cell transplantation. Journal of molecular and cellular cardiology. 2008; 45:554-66.

[123] Athanasiou KA, Darling EM, Hu JC, DuRaine GD, Reddi AH. Articular Cartilage. 1 ed. Hoboken: CRC Press; 2013.

[124] Sophia Fox AJ, Bedi A, Rodeo SA. The Basic Science of Articular Cartilage: Structure, Composition, and Function. Sports Health. 2009; 1:461-8.

[125] Flik K, Verma N, Cole B, Bach B, Jr. Articular Cartilage. In: Williams R, III, editor. Cartilage Repair Strategies: Humana Press; 2007. p. 1-12.

[126] Netti P, Ambrosio L. Articular Cartilage. In: Barbucci R, editor. Integrated Biomaterials Science: Springer US; 2002. p. 381-402.

[127] Poole CA. Review. Articular cartilage chondrons: form, function and failure. Journal of Anatomy. 1997; 191:1-13.

[128] Wilson W, van Burken C, van Donkelaar C, Buma P, van Rietbergen B, Huiskes R. Causes of mechanically induced collagen damage in articular cartilage. Journal of Orthopaedic Research. 2006; 24:220-8.

[129] Ateshian GA, Wang H. A theoretical solution for the frictionless rolling contact of cylindrical biphasic articular cartilage layers. Journal of biomechanics. 1995; 28:1341-55.

[130] Bonnevie ED, Baro VJ, Wang L, Burris DL. Fluid Load Support during Localized Indentation of Cartilage with a Spherical Probe. Journal of biomechanics. 2012; 45:1036-41.

[131] Williams R, III, Brophy R. Decision Making in Cartilage Repair Procedures. In: Williams R, III, editor. Cartilage Repair Strategies: Humana Press; 2007. p. 37-53.

[132] Steinert AF, Ghivizzani SC, Rethwilm A, Tuan RS, Evans CH, Nöth U. Major biological obstacles for persistent cell-based regeneration of articular cartilage. Arthritis Research & Therapy. 2007; 9:213-.

[133] Harris JD, Brophy RH, Siston RA, Flanigan DC. Treatment of chondral defects in the athlete's knee. Arthroscopy: the journal of arthroscopic & related surgery: official publication of the Arthroscopy Association of North America and the International Arthroscopy Association. 2010; 26:841-52.

[134] Harris JD, Brophy RH, Siston RA, Flanigan DC. Treatment of Chondral Defects in the Athlete's Knee. Arthroscopy: The Journal of Arthroscopic & Related Surgery. 2010; 26:841-52.

[135] Magnussen R, Dunn W, Carey J, Spindler K. Treatment of Focal Articular Cartilage Defects in the Knee. Clin Orthop Relat Res. 2008; 466:952-62.

[136] Hipp J, Atala A. Sources of Stem Cells for Regenerative Medicine. Stem Cell Rev. 2008; 4:3-11.

[137] Minteer D, Marra K, Rubin JP. Adipose-Derived Mesenchymal Stem Cells: Biology and Potential Applications. In: Weyand B, Dominici M, Hass R, Jacobs R, Kasper C, editors. Mesenchymal Stem Cells - Basics and Clinical Application I: Springer Berlin Heidelberg; 2013. p. 59-71.

[138] Gimble JM, Katz AJ, Bunnell BA. Adipose-Derived Stem Cells for Regenerative Medicine. Circulation Research. 2007; 100:1249-60.

[139] Mizuno H, Tobita M, Orbay H, Uysal AC, Lu F. Adipose-Derived Stem Cells as a Novel Tool for Future Regenerative Medicine. In: Hayat MA, editor. Stem Cells and Cancer Stem Cells, Volume 12: Springer Netherlands; 2014. p. 165-74.

[140] Bourin P, Bunnell BA, Casteilla L, Dominici M, Katz AJ, March KL, et al. Stromal cells from the adipose tissue-derived stromal vascular fraction and culture expanded adipose tissue-derived stromal/stem cells: a joint statement of the International Federation for Adipose Therapeutics and Science (IFATS) and the International Society for Cellular Therapy (ISCT). Cytotherapy. 2013; 15:641-8.

[141] Boquest AC, Shahdadfar A, Brinchmann JE, Collas P. Isolation of Stromal Stem Cells From Human Adipose Tissue. 2005. p. 35-46.

[142] Hicok K, Hedrick M. Stem Cells and the Art of Mesenchymal Maintenance. In: Bronner F, Farach-Carson M, Mikos A, editors. Engineering of Functional Skeletal Tissues: Springer London; 2007. p. 1-16.

[143] Anderson JA, Little D, Toth AP, Moorman CT, Tucker BS, Ciccotti MG, et al. Stem Cell Therapies for Knee Cartilage Repair: The Current Status of Preclinical and Clinical Studies. The American Journal of Sports Medicine. 2014; 42:2253-61.

[144] Roelofs AJ, Rocke JPJ, De Bari C. Cell-based approaches to joint surface repair: a research perspective. Osteoarthritis and Cartilage. 2013; 21:892-900.

[145] Punwar S, Khan WS. Mesenchymal Stem Cells and Articular Cartilage Repair: Clinical Studies and Future Direction. The Open Orthopaedics Journal. 2011; 5:296-301.

[146] Gratz KR, Wong BL, Bae WC, Sah RL. The Effects of Focal Articular Defects on Cartilage Contact Mechanics. Journal of orthopaedic research: official publication of the Orthopaedic Research Society. 2009; 27:584-92.

[147] Robinson N, Picken A, Coopman K. Low temperature cell pausing: an alternative short-term preservation method for use in cell therapies including stem cell applications. Biotechnol Lett. 2014; 36:201-9.

[148] Serra M, Correia C, Brito C, Alves P. Bioprocessing of Human Pluripotent Stem Cells for Cell Therapy Applications. In: Al-Rubeai M, Naciri M, editors. Stem Cells and Cell Therapy: Springer Netherlands; 2014. p. 71-95.

[149] Srijaya TC, Ramasamy TS, Kasim NHA. Advancing stem cell therapy from bench to bedside: lessons from drug therapies. Journal of Translational Medicine. 2014; 12:243.

[150] Diogo M, da Silva C, Cabral JS. Separation Technologies for Stem Cell Bioprocessing. In: Al-Rubeai M, Naciri M, editors. Stem Cells and Cell Therapy: Springer Netherlands; 2014. p. 157-81.

[151] Shields CW, Reyes CD, López GP. Microfluidic Cell Sorting: A Review of the Advances in the Separation of Cells from Debulking to Rare Cell Isolation. Lab on a chip. 2015; 15:1230-49.

[152] Singh P, Williams DJ. Cell therapies: realizing the potential of this new dimension to medical therapeutics. Journal of Tissue Engineering and Regenerative Medicine. 2008; 2:307-19.

[153] Izadpanah R, Bunnell B. Gene Delivery to Mesenchymal Stem Cells. In: Prockop D, Bunnell B, Phinney D, editors. Mesenchymal Stem Cells: Humana Press; 2008. p. 153-67.